Resonant Gain Enhancement in Microstrip Antennas

by **Farshad Kaymaram**

A thesis Submitted to the Faculty of

Graduate Studies in partial fulfillment of the

Requirements for the degree of

Master of Science

University of Manitoba
Department of Electrical and Computer Engineering
Winnipeg, Manitoba

THE UNIVERSITY OF MANITOBA

FACULTY OF GRADUATE STUDIES

*****

COPYRIGHT PERMISSION

Resonant Gain Enhancement in Microstrip Antennas

BY

Farshad Kaymaram

A Thesis/Practicum submitted to the Faculty of Graduate Studies of The University of Manitoba in partial fulfillment of the requirement of the degree

Master Of Science

In memory of Mr. Sayedaliasghar Kazemmoossavi

dedicated to my parents, my first and entire life teachers,
principled and honorable humans,...
courteously and humbly

Table of Contents

ACKNOWLEDGEMENTS

The best, I start with name of the Lord of spirit and wisdom.

I wish to thank my advisor *Prof L. Shafai* for his wise advice and being a source of inspiration all the time. His manners and patience are also sincerely appreciated.

I would like to thank *Dr. Hassan M. Soliman* and *Dr. Vladimir Okhmatovski* for their valuable time, useful discussions, and comments as members of my examining committee.

I sincerely thank *Prof E. Bridges* and *Dr. S. Noghanian* for spending many hours to answer my questions. Special thanks to *Mr. B. Tabachnik* for his wonderful cooperation and helping me with the fabrications and experimental measurements. Extended thanks to *Ms. S. Girardin* for her kind help. I would also like to thank *Mr. S.I.R. Latif, M. Kandik, Dr. B. Kordi, A. Foroozesh, Dr. S. Oh, and Dr. S.K. Sharma* in this regard.

ABSTRACT

The microstrip antenna (MSA) is one of the most widely used microwave antennas possessing several advantages. However, it presents a low inherent directivity. It is overcome here by adding a dielectric layer above the patch. The directivity increases almost proportionally to the superstrate relative permittivity.

A parametric study of the effects of different layers, i.e. the air gap and the dielectric layers, on both radiation and input characteristics of the microstrip antennas are carried out. Single- (SSC) and multiple-superstrate (MSC) cases are investigated along with a modified configuration of adding a parasitic patch to the superstrate. If a proper superstrate thickness and dielectric constant are present, the desired directivity can be realized by SSC. Otherwise, multiple-superstrate and the modified single-superstrate-patch configurations must be used. It is shown that, by using MSC, large antenna directivity can be obtained with even moderate superstrate dielectric constants. The modified single-superstrate-patch configuration can be employed when the superstrate thickness is much smaller than the required quarter wave-length. An antenna prototype for each of the configurations of single-superstrate, double-superstrate, and the modified single-superstrate configurations are fabricated and tested in the Antenna Laboratory of the University of Manitoba in order to verify the simulated results. Within fabrication tolerances, the agreement with simulations has been satisfactory.

List of Figures

List of Tables

CHAPTER 1

Introduction

Microstrip antennas have become one of the most popular antennas, for the past three decades. They offer many desirable advantages, and still receive attention from researchers in both universities and industry. However, they also suffer from two major shortcomings of narrow bandwidth and low directivity. Investigations in recent years have addressed mostly the improvement of the bandwidth. This thesis addresses the enhancement of their gain. Below, the objectives and organization of the thesis are presented.

1.1. Purpose of this Thesis

Microstrip antennas for high directivity are usually designed in array forms, which require a complex feed. The resonant gain enhancement method investigated in this thesis is capable of increasing directivity significantly without the need for an array. The large directivity is obtained simply by adding a superstrate dielectric layer over the patch. It can be used as a single element, or in an array, where it allows the use of fewer elements and provides space for additional devices. It also reduces the feed network complexity and loss [22]. The main goals of this study are to explore the full capabilities of this technique using different configurations consisting of:

- A single-superstrate configuration
- A multiple-superstrate configuration

- A modified single-superstrate configuration

The characteristics of these configurations are investigated and compared with each other. The effect of tolerances on their performance is also studied.

1.2. Organization of the Thesis

This thesis is divided into six chapters. Chapter one states the purpose and discusses organization of the thesis. The second chapter introduces the development of the resonant gain enhancement method and related concepts, in chronological order. The resonant gain enhancement is shown first for any antenna on ground plane, where the multiple- reflection phenomenon occurs between the ground plane and dielectric layer. In its simplest form, the antenna with ground plane is assumed to be an electric current element, which is covered by the dielectric plate suspended in the air. The directivity varies proportionally with the permittivity of the dielectric layer under the resonant conditions for the thickness and height of the dielectric plate [5]. The resonant conditions for the embedded Herzian dipole and its corresponding asymptotic formulas for directivity and bandwidth were derived by using T-lines analogy and reciprocity theorem [6]. It will be shown later that these formulas are useful even for microstrip patch antennas. Under resonant conditions, a resonance is created in the layered structure of the antenna analogous to the resonant transmission lines, which results in high directivity. Adaptation of this technique to the microstrip patch antennas due to its growing popularity was carried out by Lin et al. [14]. The analytical methods for this purpose are also introduced in chapter two, out of them; the variational

methods and the moment method are the most successful. A short history of the short back-fire antennas is also explained, since they use multiple-reflection phenomenon as well.

Chapter three provides an extensive study for the single-superstrate configuration. It studies the effects of the superstrate parameters, i.e. *permittivity, thickness and height* on different characteristics of the microstrip patch antenna. It consists of the superstrate parameters effects on the input impedance and directivity, the substrate effect on the directivity, and the joint effects of superstrate and substrate on the input impedance. The section entitled "Tolerance analysis" illustrates how sensitive the directivity is with respect to the superstrate parameters, regarding the resonant gain. Compensation for the directivity loss is also explored in this section. It is demonstrated that the superstrate spacing from ground can compensate for the directivity loss due to the superstrate thickness deviations. For a 25% superstrate thickness deviation, the directivity discrepancy was only about two to three percent after compensation.

Chapter four is devoted to the multiple-superstrate configuration. Contrary to the single-superstrate configuration, large resonant directivities can be obtained with moderate superstrate dielectric constants. The structure of this chapter is almost similar to the preceding one. Moreover, the double-superstrate and triple-superstrate configurations are compared to the single-superstrate configuration with similar directivity. It studies the superstrate parameters' effects on the directivity and input impedance. The section titled "Tolerance analysis" illustrates how sensitive the directivity is with respect to the superstrate parameters. Also, different superstrate

layers are compared with each other. The radiation characteristics of the double-superstrate configuration in the frequency-domain and spatial-domain are demonstrated. Measured results of the fabricated antenna with double-superstrate configuration are compared with simulated results, in order to validate the simulation. The measured directivity of the fabricated antenna is 15.8dBi, with an impedance bandwidth of 7% at 13.64GHz.

A modified version of the single-superstrate configuration is proposed in chapter five. A parasitic patch is added underneath the superstrate. The relation between the parasitic patch parameters, i.e. *radius and height* with the directivity and input impedance are discussed. The radiation characteristics of the modified single-superstrate configuration in the frequency-domain and spatial-domain are investigated. Measured results of the fabricated antenna, with the modified single-superstrate configuration, are presented in order to validate the simulation results. The measured directivity of the fabricated antenna is 15.61dBi with impedance bandwidth of 7.3% at 4.8GHz. The modified single-superstrate configuration will be useful in cases, where the dielectric superstrates, with desired thickness is not available. For instance, at low frequencies the superstrate thickness becomes excessively large, and difficult to implement. The proposed modified design presents a practical alternative. The thesis ends with concluding remarks and a note for future research scopes.

In the appendix, under the title of "Terminology", the definition for the terms; *Gain, Directivity, and Directivity-bandwidth* are presented, since their terminology in the literature is either inconsistent or unclear.

CHAPTER 2

Background Theory

Introduction: A method which improves the gain significantly, in particular for printed antennas, involves the addition of a superstrate, *i.e.* a dielectric cover layer, above the patch. It has been shown that a very large directivity, and therefore gain, may be realized by choosing the layer's thicknesses properly. Similar to the short backfire antenna, which achieves high gain by utilizing the multiple-reflection phenomenon between a large and small reflecting (conducting) plane, the dielectric superstrate enhances the gain in the microstrip patch antennas by using the multiple-reflection phenomenon, but between the ground plane and superstrate dielectric layer with relative permittivity of $\varepsilon_r >> 1$ [1-4]. In principle, other antennas like a dipole, patch or traveling wave antennas, can be used in a similar manner to enhance the gain [5]. This method of gain enhancement has been referred to as the resonant gain method, since the geometry functions like a leaky resonator. Resonance conditions and asymptotic formulas for the directivity and its variation with frequency have been derived by Jackson and Alexopoulos [6]. They have shown that the directivity varies proportionally to the superstrate relative permittivity ε_r. However, its bandwidth varies inversely with ε_r.

In this chapter, the development of this method is presented in chronological order, and the background theory is introduced alongside. The short backfire antennas will be reviewed first, since the gain enhancement of the dielectric covered and short

backfire antennas is rooted in the same idea, i.e. the multiple reflection technique. The short backfire antennas, however, are relatively simpler and came into existence earlier, in 1960's.

2.1. Short Backfire Antenna

In this section the backfire and short backfire antennas will be reviewed briefly, in order to provide a greater insight into the basic nature of multiple-reflection phenomenon. The principle of backfire antennas was first conceived by Ehrenspeck in 1960 [7]. It provides a means for significantly increasing the directivity of the end-fire antenna without increasing its length. The backfire antenna is a modified version of the ordinary end-fire slow wave antenna, which may be, for example, a Yagi antenna, a helical antenna, or a dielectric rod antenna. According to the Hansen-Woodyard condition, the maximum directivity obtainable for such end-fire antennas is directly proportional to the length of the surface wave structure traversed by the wave [8].

The backfire antenna, as proposed by Ehrenspeck consists of an end-fire surface wave structure terminated with a large conducting plate, usually called the surface wave reflector. It is placed perpendicular to the axis of the endfire structure *Fig.2.1.* The large conducting plate acts as a mirror which turns the surface wave backwards, thus forcing the wave to traverse the physical length of the antenna structure twice. This means that the backfire antenna acts as an end-fire antenna of double physical length. The Backfire principle provides a means for significantly increasing the directivity of an end-fire antenna without increasing its length. Typical gain increases

of 6 to 8 dB over a conventional end-fire Yagi of equal length can be obtained by application of the backfire principle.

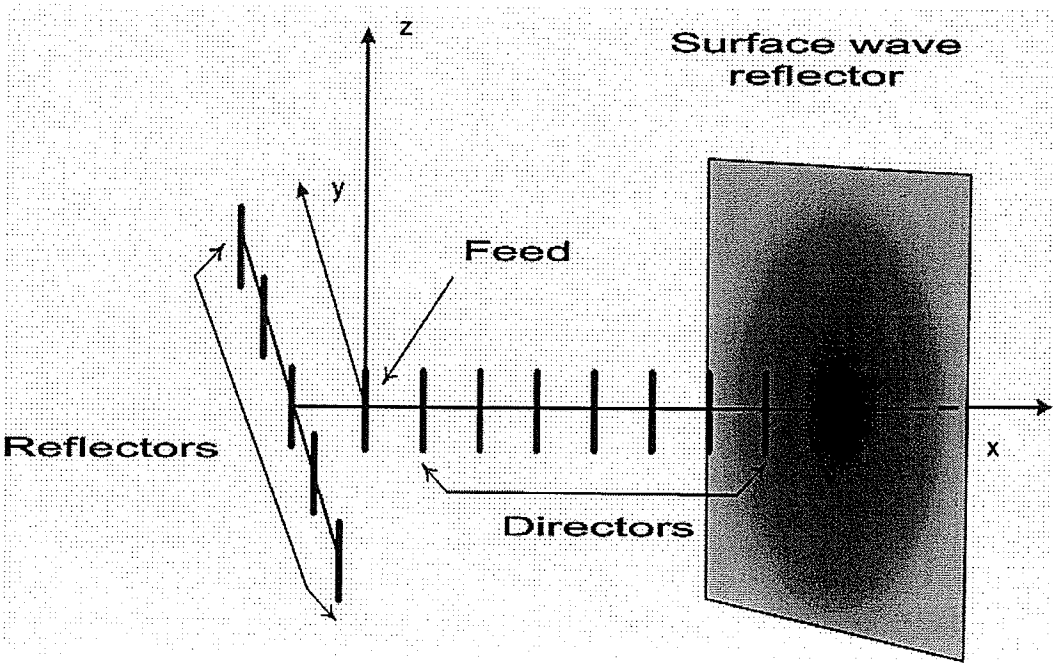

Fig.2.1. Geometry of Yagi backfire antenna [8]

Ehrenspeck later reported that a shorter structure about $0.5\lambda_0$ in length also functioned as a useful antenna [9], and named it "short back-fire antenna". *Fig.2.2* shows a cross-section through the short backfire antenna [10]. It has a gain that is typically in the range of 14-17dBi. It consists of a cylindrical cavity of diameter D and a conducting rim of height H, *Fig.2.2*. The cavity is excited by a single linear dipole feed of length L, placed at a height dh, above the base of the cavity. A small conducting disc subreflector of diameter d is placed above the dipole feed at a height h above the base of the cavity.

The optimum operating mode for the backfire antenna is characterized by multiple reflections of electromagnetic waves between the two plane reflectors, with a standing-wave field distribution along the antenna axis. This condition requires that the reflectors be separated by $n\lambda_0/2$ (n is an integer), such that the tangential E fields vanish at their surface. The stored energy in the near-zone field is concentrated in the region between reflectors along the antenna axis, and is radiated off through the aperture plane passing through subreflector. A short backfire antenna with a reflector separation of $0.5\lambda_0$ is the shortest possible configuration of this type.

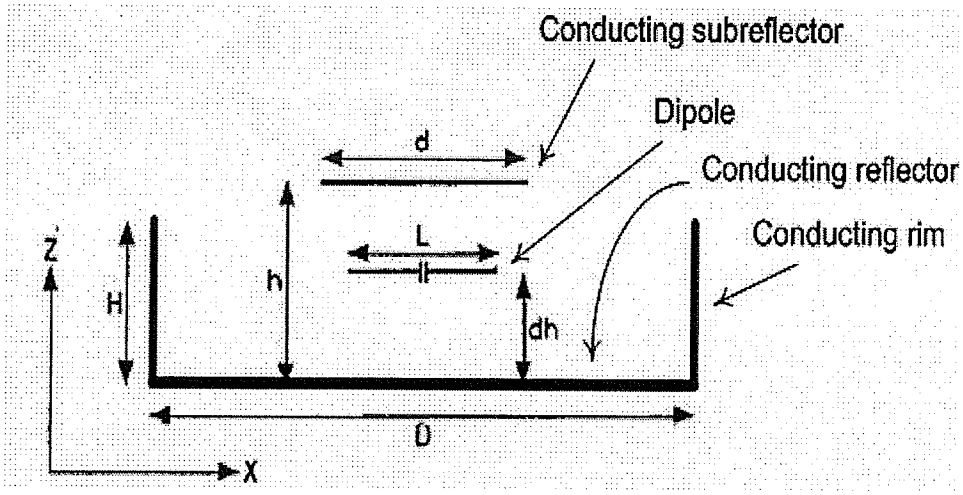

Fig.2.2. Cross-section of short backfire antenna [10]

It is evident that the short backfire antenna is essentially a leaky cavity structure for which the excitation is provided by the primary dipole source. The aperture field distribution is therefore well approximated by the transverse distribution of the cavity resonator. With a height of about $0.5\lambda_0$ (rim height) as opposed to several wavelengths

in end-fire antennas, it is a low profile alternative to horn antennas. With different cavity profiles, they have been recently studied by Gray and Shafai [11].

2.2. Dielectric Covered Antenna with a Ground plane

One of the early researches done on antennas covered by dielectric layers was performed by Y. Sugio et al. at the Setsunan University, Osaka, Japan in 1981 [3]. They described the resonant gain enhancement of the dielectric covered antennas with a ground plane. As short backfire antennas achieve high gain by utilizing multiple reflection phenomenon between a large and small reflecting (conducting) planes, these antennas also utilize multiple reflection phenomenon between a ground plane and the dielectric plate for the gain enhancement. In principle, any antenna, for example, a dipole, patch or traveling wave antennas, can be used as their feed [5]. Sugio et al. showed that the radiation beam becomes sharper as the relative permittivity ε_r of the dielectric plate becomes large. The directivity, and hence the gain at broadside becomes maximum and are multiplied by about ε_r provided the thickness of the dielectric and its spacing from the ground plane reflector equal one quarter and one half wavelength, respectively, i.e.[5]:

$$t\sqrt{\varepsilon_r}/\lambda = 1/4 \qquad (2.1)$$

$$h/\lambda = 1/2. \qquad (2.2)$$

Sugio et al. used a variational method to analyze the gain enhancement and input characteristics. They investigated both infinite and finite dielectric loaded antennas, which were fed by a waveguide aperture, current element or a coaxial excited patch

antenna [12]. Using the transmission line (T-line) analogy, Jackson and Alexopoulos analyzed the resonant gain enhancement for the printed circuit antennas by a simple model [6]. They developed the resonance conditions, which maximize the antenna gain. They also derived asymptotic formulas for the gain, beamwidth, and bandwidth. Their work is reviewed in the next section.

2.3. Resonant Gain Enhancement Analysis by T-Lines Analogy

Jackson and Alexopoulos [6] studied a substrate-superstrate printed antenna, i.e. Herzian dipole embedded in a grounded substrate, which allows for large antenna gain. They derived asymptotic formulas for gain, beamwidth, and bandwidth by using the transmission line analogy and reciprocity theorem. These analytic results provide a greater insight into the basic nature of the resonant gain, though the embedded Herzian dipole case and the corresponding model are simpler. The basic printed antenna geometry under consideration is shown in *Fig.2.3*. The Herzian electric dipole is embedded within a grounded substrate of thickness B having relative permittivity and permeability ε_1, μ_1. On top of the substrate is the superstrate layer of thickness t with relative permittivity and permeability ε_2, μ_2. Above the superstrate is free space, with total permittivity and permeability ε_0, μ_0.

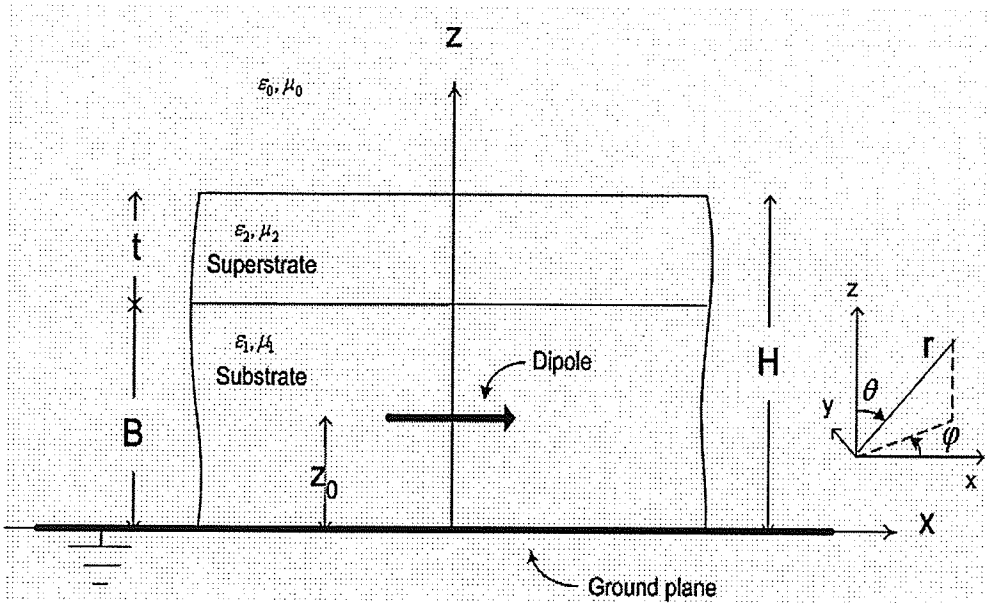

Fig.2.3. Superstrate-substrate geometry [6]

A convenient way to analyze the radiation from this antenna structure is by the transmission line analogy. In this method, E_x field is determined at the original dipole location due to a Herzian dipole source in either a_θ or a_Φ direction, when the dipole source is far from the origin ($k_0R >> 1$), at specified angles θ and φ, in the specified coordinates. By reciprocity, this must be the E_θ or E_Φ field at (R, θ, φ) due to the original dipole at $z=z_0$. The E_x field near the layered structured due to this reciprocity source is essentially a plane wave, and hence can be accounted for by modeling each layer as a transmission line, having a characteristic impedance and propagation constant which depend on the angle θ, Fig.2.4. The E_θ field corresponds to an E field from the reciprocity source, which is in the plane of incidence, while the E_Φ field corresponds to an incident E field normal to the plane of incidence. Each case is

handled differently by the transmission line analogy. The radiated field is obtained to be [6];

$$E_\theta = -\cos\varphi\left(\frac{j\omega\mu_0}{4\pi R}\right)e^{-jk_0R}G(\theta) \qquad (2.3)$$

$$E_\phi = -\sin\varphi\left(\frac{j\omega\mu_0}{4\pi R}\right)e^{-jk_0R}F(\theta) \qquad (2.4)$$

The functions $F(\theta)$ and $G(\theta)$ depend only on θ and represent the voltage (corresponding to E_t, the component of the E field normal to z-direction), at $z=z_0$ in the transmission line analogy, due to an incident wave of unit strength. The characteristic impedance (Z_{ci}) for each layer, i = 0, 1, or 2, used in the transmission line analogy are shown in *Fig.2.4*.

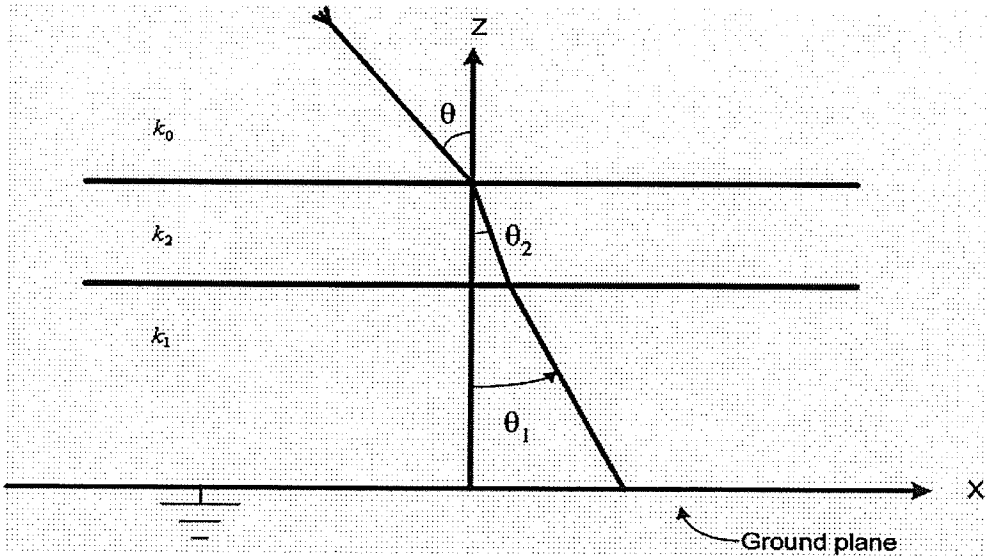

(a)

For $F(\theta)$: $Zc_0 = \eta_0 \sec\theta$, $Zc_1 = \eta_0\mu_1 / n_1(\theta)$, $Zc_2 = \eta_0\mu_2 / n_2(\theta)$

For $G(\theta)$: $Zc_0 = \eta_0 \cos\theta$, $Zc_1 = \eta_0 n_1(\theta)/\varepsilon_1$, $Zc_2 = \eta_0 n_2(\theta)/\varepsilon_2$

(b)

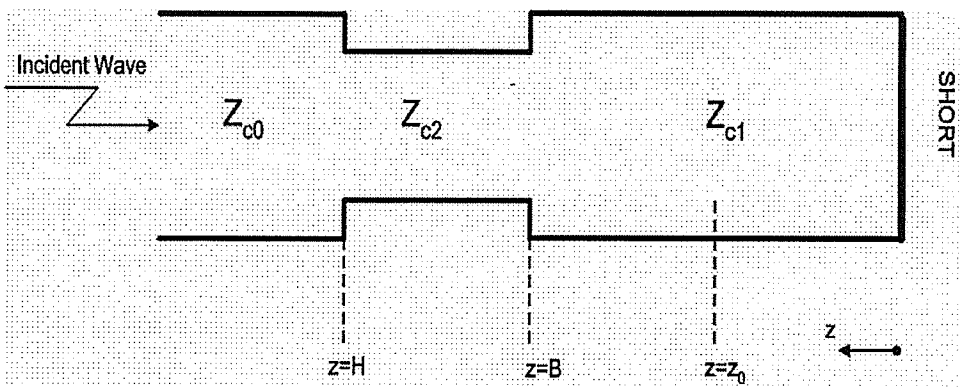

(c)

Fig.2.4. (a) Plane wave incident on layered structure from reciprocity source, (b)Characteristic impedances for analogous transmission line model, and (c) Transmission line equivalent circuit [6]

By solving the analogous transmission line model, $G(\theta)$ and $F(\theta)$ for E_θ *and* $E\varphi$ components can be obtained, respectively as follows [6]:

$$G(\theta) = 2\frac{T}{Q + jP}\cos\theta \qquad (2.5)$$

$$F(\theta) = 2\frac{T}{M + jN} \qquad (2.6)$$

where

$$T = \sin[\beta_1 z_0]\sec[\beta_1 B]\sec[\beta_2 t] \qquad (2.7)$$

$$Q = \tan[\beta_1 B] + \frac{\varepsilon_1}{\varepsilon_2}\frac{n_1(\theta)}{n_2(\theta)}\tan[\beta_2 t] \qquad (2.8)$$

$$P = -\frac{\varepsilon_1}{n_1(\theta)}\cos\theta\left[1-\frac{\varepsilon_2}{\varepsilon_1}\frac{n_1(\theta)}{n_2(\theta)}\tan[\beta_1 B]\tan[\beta_2 t]\right] \tag{2.9}$$

$$M = \tan[\beta_1 B]+\frac{\mu_2}{\mu_1}\frac{n_1(\theta)}{n_2(\theta)}\tan[\beta_2 t] \tag{2.10}$$

$$N = -\frac{n_1(\theta)}{\mu_1}\sec\theta\left[1-\frac{\mu_1}{\mu_2}\frac{n_2(\theta)}{n_1(\theta)}\tan[\beta_1 B]\tan[\beta_2 t]\right] \tag{2.11}$$

with

$$\beta_1 = k_0 n_1(\theta) \tag{2.12}$$

$$\beta_2 = k_0 n_2(\theta) \tag{2.13}$$

and

$$n_1(\theta) = n_1\cos\theta_1 = \sqrt{n_1^2-\sin^2\theta} \tag{2.14}$$

$$n_2(\theta) = n_2\cos\theta_2 = \sqrt{n_2^2-\sin^2\theta} \tag{2.15}$$

In general, the gain of the antenna can be evaluated exactly by a numerical integration. However, Jackson and Alexopoulos have derived a simple formula for the gain asymptotically, under the high gain resonance conditions.

2.3.1. Resonance conditions and asymptotic formulas

In order for the equivalent circuit to be resonant, the following conditions for the length of each section of the transmission lines should be met [13].

$$\frac{n_1 B}{\lambda_0} = \frac{m}{2}, \qquad m = 1,2,... \tag{2.16}$$

$$\frac{n_1 z_0}{\lambda_0} = \frac{2n-1}{4}, \qquad n = 1,2,... \tag{2.17}$$

$$\frac{n_2 t}{\lambda_0} = \frac{2p-1}{4}, \qquad p = 1,2,... \tag{2.18}$$

Under these conditions, when the superstrate permittivity becomes large *($\varepsilon_2 >> 1$)*, a very high gain pattern is produced at the broadside *($\theta = 0$)*. The method requires physically thick layers at low frequencies, which may be a potential disadvantage for some applications. Taking m, n, p=1 to obtain the thinnest layers possible, it is observed that the dipole is in the middle of substrate for the resonance condition.

For the given antenna configuration, Jackson and Alexopoulos have reported the gain, -3dB beamwidth, and -3dB bandwidth as follows [6]:

$$gain \approx 8\frac{n_1 B}{\lambda_0}\left(\frac{\varepsilon_2}{n_1 \varepsilon_1 \mu_2}\right) \tag{2.19}$$

$$\theta_h \approx \left[\pi \frac{n_1 B}{\lambda_0}\frac{\varepsilon_2}{\varepsilon_1}\frac{1}{n_1 \mu_2}\right]^{-1/2} \tag{2.20}$$

$$f_w = \frac{f_2 - f_1}{f_0} \approx \frac{3.58}{2\pi}\frac{\lambda_0}{n_1 B}\frac{\varepsilon_1}{\varepsilon_2}\frac{\mu_2}{n_1} \tag{2.21}$$

where f_1 and f_2 are the half-power frequencies. As can be observed from *(2.21)* and *(2.19)*, the bandwidth is inversely proportional to the gain, which means the gain bandwidth product of this antenna is constant.

2.4. Applying Resonant-Gain Enhancement to MSP Antenna

Although the microstrip antennas have enjoyed a growing popularity since 1970's, and it had been shown that an improvement in the directivity, and therefore the gain, can be obtained by adding a dielectric cover layer in front of any antenna with a ground plane, it was not applied to the microstrip patch antennas till late 1980's. The classical resonance conditions with a substrate thickness of a half wavelength were not applicable to microstrip patch antennas, which causes degradation of the radiation characteristics. Lin et al. adapted this technique for applying to the microstrip patch antenna, due to its growing popularity at that time [14]. In addition, it is interesting to obtain the gain enhancement in the microstrip antennas based on their original configurations not only for the single element microstrip antenna applications, but also for their arrays. Lin et al. proposed a modified technique which is convenient for the microstrip antenna array applications. As it can be seen from Fig. 2.5, the radiating element, rather than being located in the middle of the substrate is placed on the substrate, i.e. as in the original case, covered by a superstrate at a proper height. They proved the gain enhancement of this new configuration by a series of experiments for several microstrip antenna arrays over X- to Ku frequency bands.

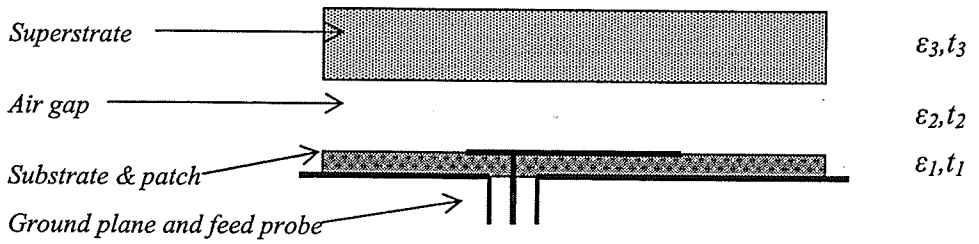

Fig.2.5. Modified Superstrate-substrate geometry for MSP antennas [14]

2.5. Analysis of dielectric covered Microstrip Patch Antennas

The superstrate effects on the antenna input characteristics have been investigated earlier than their effects on the other characteristics of the microstrip antennas. The superstrate as a radome was already used in order to protect the antenna from environmental hazards. It may be also naturally formed, e.g. the ice layer, during the flight or severe weather conditions. Sugio et al. [5] studied the gain enhancement mechanism of dielectric covered antennas with a ground plane by the saddle point method and the geometrical ray theory. They showed that the radiation beam becomes sharp as the permittivity of the dielectric plate becomes large, provided that the superstrate thickness and its spacing are selected properly. Later, they used a technique based on the variational methods, to study the gain enhancement and the input characteristic of the dielectric layer loaded antennas, assuming that the dielectric layer and ground plane are infinite transversally. They also analyzed the antennas loaded by a finite dielectric layer, based on the solution of the former case, i.e. infinite dielectric layer, by using Fourier analysis [12]. Generally, the problem of finite structures is

difficult to handle analytically. On the other hand, investigating the property for finite structures which is the practical case is important. A major breakthrough in this regard was made by using integral equation methods, such as the moment method. Formulations of boundary value problem using surface integral equations for the combination of both conducting and dielectric bodies of revolution were used by Kishk and Shafai [16] to calculate the electromagnetic scattering due to a plane wave incidence. They investigated the performance of an electric dipole located between a finite ground plane and a dielectric disc [16].

In order to calculate the radiation properties of a rectangular microstrip patch antenna covered by a dielectric layer, Qasim and Zhong [17]. used the spectral domain immittance (SDI) matrix approach. Using SDI method, they obtained the patch current distribution, and also derived a set of formulas for the radiation pattern. They found that the gain enhancement is possible by optimizing the thickness of cover layer and its spacing. Their method, based on the moment method, is merely suitable for the rectangular patch antennas covered by a single dielectric layer.

Radiation pattern calculations by using moment method for the microstrip patch antennas in stratified dielectric media for more complex structures have been also reported by Shen et al. [18]. Their method has also been used to study the resonant gain enhancements for the microstrip antennas. Vandenbosch et al. developed a mixed-potential form of the electric field integral equation (EFIE), so named because it involves both vector and scalar potentials. This form is preferable to several other possible variants of the EFIE because it requires only the determination of potential spectral Green's functions, whose inverse Fourier transformation gives rise to

Sommerfeld integrals, converging faster. It also results in spatial Green's functions less singular than their derivatives, which are needed in other forms of the EFIE. The Ansoft Designer simulator, which has been used in this work, is also based on the mixed-potential electric field integral equations. In the next section, its specifications and the settings used in this work are discussed.

2.6. Ansoft Designer Simulator [23]

In Ansoft Designer, the surface of the geometric model is automatically divided into triangles and rectangles (meshing). Ansoft Designer employs the mixed-potential integral equation (MPIE) method. The method of moments (MoM) is applied to the MPIE to solve for $\boldsymbol{J}$, the current distribution on the surface mesh. Then the S-parameters and the radiated fields are calculated from $\boldsymbol{J}$. By defining a non-adaptive solution setup, Ansoft Designer can be instructed to add narrow rectangles along the edges of the model. These rectangles efficiently capture electromagnetic effects close to the model edges, resulting in faster solution times and/or higher accuracy. Ansoft Designer determines the length of the rectangles (the longer edges, which lie parallel to the model edge) by making them smaller than a fraction of the guided wavelength at the specified frequency. The width of the rectangles is determined by the ratio of the rectangles' length to the width. The ratio value should be between 0.02 and 0.2 to prevent extremely narrow rectangles and extremely wide triangles [23].

In order to obtain more accurate results, edge meshing is used. Edge mesh length ratio of 0.1 was selected. The real parameters of materials are considered in modeling, including permittivity and permeability, dielectric loss tangent, and bulk conductivity for conductors. The confidence in simulated results has been taken from the directivity convergence to within the second decimal place of accuracy for different meshing frequency.

2.7. Summary and Conclusion

In this chapter, the development of the resonant gain method was introduced in a chronological order. The related ideas from the backfire and short backfire antennas were also reviewed. The main idea in the resonant gain method is in using the multiple-reflection phenomenon. The background theory was also introduced briefly. The devised asymptotic formulas for the resonant gain and the development of more rigorous numerical methods were reviewed. Finally, the Ansoft Designer simulator is introduced and the applied settings for this work are discussed.

CHAPTER 3

Single-superstrate Configuration

Introduction As it was seen in the preceding chapter, the gain of a single element microstrip patch antenna can be improved significantly by using a superstrate with the proper thickness and height. In this chapter the single-superstrate configuration will be investigated extensively. First the superstrate effects on input impedance will be discussed, and then the superstrate effects on the directivity of microstrip patch antenna will be investigated. The effects of substrate (in the presence of superstrate) on both input impedance and directivity will be studied next. Then the tolerance analysis will be discussed, since the resonant gain is essentially narrowband, so the relevant parameters should exhibit sufficient accuracy. There are also some tolerances for available dielectric materials in the market and fabrication deviations are inevitable. Next, the radiation characteristics in the frequency- and spatial domain will be studied. Finally, the measured results of the fabricated antenna prototype are demonstrated, in order to validate the simulated results.

3.1. Superstrate Effects on Input Response

One of the main characteristics of any antenna is its input characteristics. So the effects on the microstrip patch antenna input impedance by adding superstrate is considered, first. There are three basic parameters for the superstrate; the thickness, the

dielectric constant and the height above the substrate. The effects of each of these parameters will be demonstrated separately. To study the effects of superstrate parameters on the input response, a coaxial-fed rectangular microstrip patch antenna is considered. At the frequency of *10 GHz*, the original patch is matched with a *50 Ohm* probe feed. Its parameters are listed in *Table 3.1.*

Table 3.1. The specifications of the selected microstrip patch Antenna for the study of superstrate effects

Layer	***Material***	***Geometry***
Patch	*Copper*	*Rectangular, 9.1×12 mm*
Substrate	$\varepsilon_{r=2.2}$	*Thickness=1.575 mm*
Ground Plane	*Copper*	*Infinite*
Feed	*Coaxial Probe*	X_f*=-2.8 mm,* Y_f*=0 mm (location from the center of patch)*

3.1.1. Superstrate Thickness Effects on Input Resistance

Different superstrate thicknesses are selected, while the superstrate relative permittivity is kept fixed at the value of ε_3=*9.2*. Superstrates with thicknesses *(t_3)* of *3.175mm (0.32λ_3), 2.540mm (0.25λ_3), 1.905mm (0.19λ_3),* and *1.524mm (0.15λ_3)* are assumed to be above the patch at the height of t_{2r} (the optimum air gap height for each t_3), *Fig.3.1.*

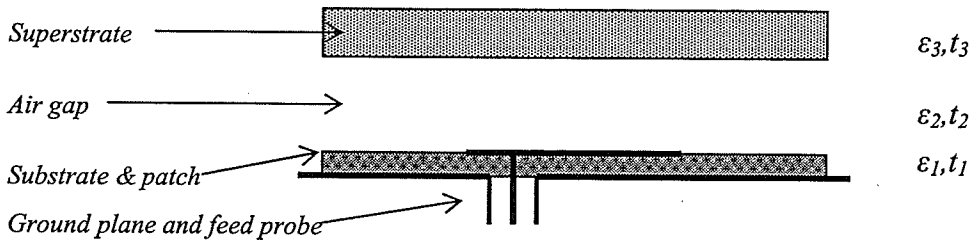

Fig.3.1. The single-superstrate microstrip Patch Antenna configuration

As it will be shown in *section 3.2*, for every superstrate thickness (t_3), there is an optimum air gap height (t_{2r}), required for obtaining the optimum directivity. The variation of input resistance, i.e. $Re\{Z_{in}\}$, with frequency are calculated for different superstrate thicknesses and shown in *Fig.3.2*. Here, $t_2=\infty$, $t_3=0$ means that there is no superstrate above the patch, *i.e.* the case of original microstrip patch antenna. The resonant frequency (f_r) is defined as the frequency at which the input resistance, $Re\{Z_{in}\}$ reaches its maximum value. The value of maximum input resistance is called the resonant resistance; R_r. *Fig.3.2* shows that the resonant frequency of the original patch is *9.4GHz*. When the superstrate is added in the thicknesses of *0.15, 0.19, 0.25, and 0.32* of λ_3, where the $\lambda_3 = \lambda_0 / \sqrt{\varepsilon_3}$, the following effects are observed:

- The resonant frequency decreases from *9.4GHz* to about *9.2GHz*,
- The R_r increases from *119 Ohms* to *287 Ohms*,
- The impedance bandwidth decreases from *6.4%* to *1.9%*.

As seen in *Fig.3.2,* the frequency shift is about *2.1%* and almost invariant to this range of superstrate thickness changes.

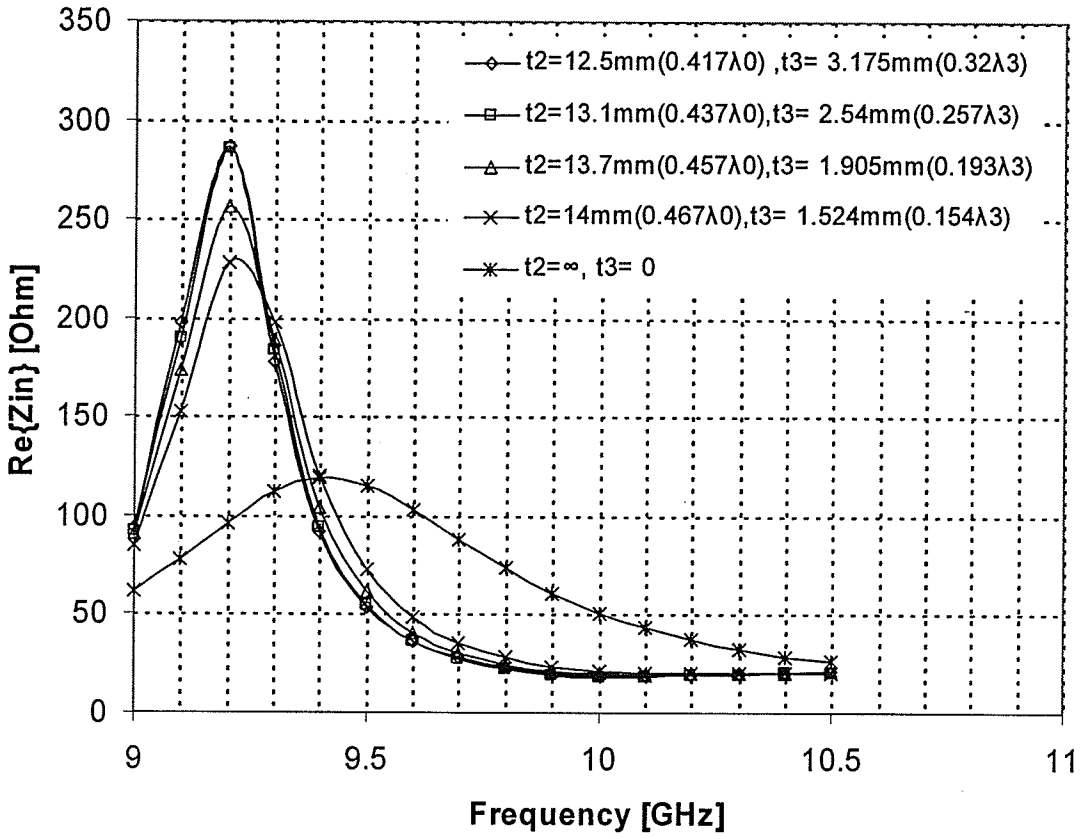

Fig.3.2. Effects of the superstrate thickness on the input resistance of microstrip patch antenna and its variations with frequency (ε_3=9.2, the other parameters are listed in Table3.1)

It can be seen in *Fig.3.2* that, the superstrate also narrows the impedance bandwidth. The impedance bandwidth is defined as [18]:

$$\frac{\Delta f_{0.69Rr}}{f_r} = \frac{(f_2 - f_1)|_{Rin=0.69Rr}}{f_r} \qquad (3.1)$$

where f_1 and f_2 are the frequencies at which the input resistance, *Re{Zin}*, equals $0.69R_r$. The bandwidth decreases to about *2%*, but the bandwidth of the original patch was *6.4%*.

The impedance resonant frequency f_r, the corresponding resistance R_r and impedance bandwidths for different superstrate thicknesses are listed in *Table 3.2*. In conclusion, it should be noted that, as the superstrate becomes one quarter wavelength in thickness ($t_3=0.25\lambda_3$), the bandwidth becomes minimum, while the directivity is maximum, as will be shown in section 3.2. Therefore, by changing the superstrate thickness, the impedance bandwidth can be traded off with the directivity.

Table3.2. Comparison of the microstrip patch antenna input resistance characteristics for different superstrate thicknesses ($\varepsilon_3=9.2$, $f_0=10GHz$, the other parameters are listed in Table3.1)

t2 [mm]	t_3 [mm]	Rr [Ohm]	fr [GHz]	Δf [GHz]	BW [GHz]
12.5(0.416 λ_0)	3.175(0.32 λ_3)	287	9.2	-0.24	0.17(1.9%)
13.1(0.436 λ_0)	2.54(0.25 λ_3)	285	9.2	-0.21	0.18(2.0%)
13.7(0.456 λ_0)	1.905(0.19 λ_3)	256	9.2	-0.185	0.2(2.2%)
14(0.47 λ_0)	1.524(0.15 λ_3)	228	9.2	-0.18	0.24(2.6%)
Without superstrate		119	9.4	-	0.6(6.4%)

3.1.2. Superstrate Dielectric Constant Effects on Input Resistance

The effects of different superstrate dielectric constants on the input resistance are investigated in this section, while the superstrate thickness and the air gap height are kept fixed at $\lambda_3/4$ and t_{2r}, respectively. Therefore, this study only assumes the case of the maximum gain. The variations of the input resistance, $Re\{Z_{in}\}$, with frequency are calculated for different superstrate relative permittivities and shown in *Fig.3.3*. Here, the relative permittivity of unity means that there is no superstrate above the patch, *i.e.* the

case of original microstrip patch antenna. When the microstrip patch antenna is covered by the superstrates with relative permittivities of *9.2, 6.0, 4.5, and 3.27*, respectively, the following effects are observed:

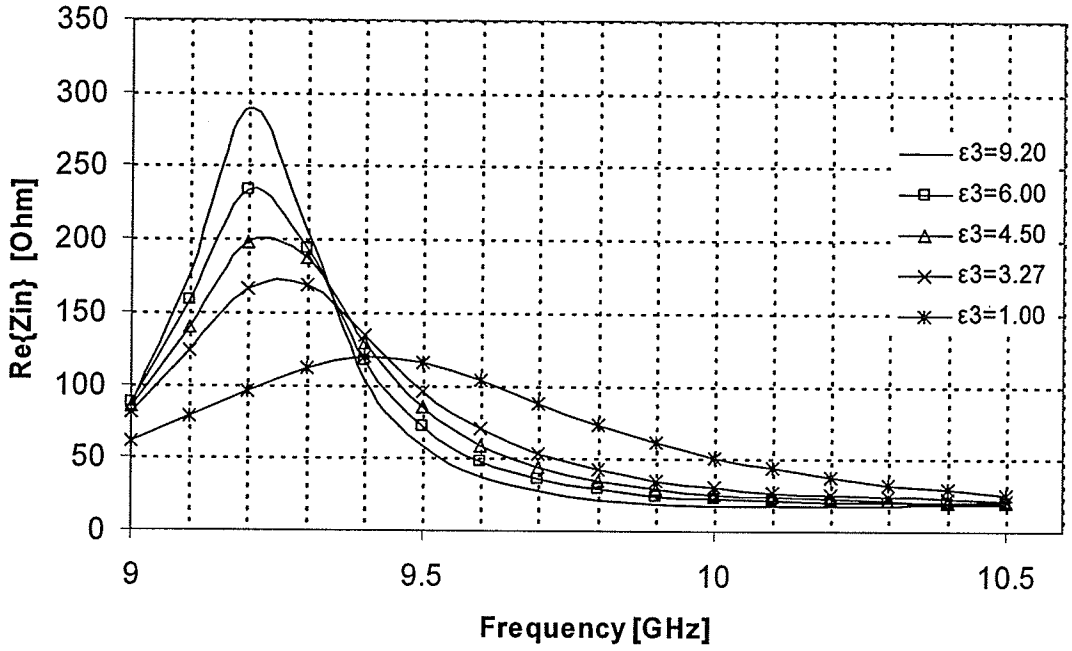

Fig.3.3. Effects of the superstrate dielectric constant on the microstrip patch antenna input resistance, and its variations with frequency (t_{2r}=13.1mm (0.436 λ_0), $t_3=\lambda_3/4$, f_0=10GHz, the other parameters are listed in Table3.1)

- The resonant frequency decreases from *9.4GHz* to about *9.2GHz*,
- The R_r increases from *119 Ohms* to *289 Ohms*,
- The impedance bandwidth decreases from *6.4% to 2.0%.*

By changing the superstrate dielectric constant, the observed effects are nearly the same as when the superstrate thickness was changed. Therefore, as the superstrate dielectric constant becomes larger, the impedance bandwidth decreases, but the gain increases as it will be shown in *section 3.2*. Therefore, by changing the superstrate

dielectric constant, the impedance bandwidth can also trade off the gain. The impedance resonant frequencies *(f_r)* and the corresponding resistance *(R_r)* and impedance bandwidth *(BW)* for different superstrate thicknesses are listed in *Table 3.3*.

Table 3.3 Comparison of the microstrip patch antenna input resistance characteristics for different superstrate dielectric constants (t_{2r}=13.1mm (0.436 λ_0), $t_3=\lambda_3/4$, f_0=10GHz, the other parameters are listed in Table3.1)

t_3 [mm]	ε_3	Rr [Ohm]	fr [GHz]	Δf [GHz]	BW [GHz]
2.5(0.25λ_0)	9.2	289	9.2	-0.36	0.18(2.0%)
3.1(0.25λ_0)	6.0	233	9.2	-0.29	0.23(2.5%)
3.5(0.25λ_0)	4.5	198	9.2	-0.23	0.29(3.1%)
4.1(0.25λ_0)	3.27	169	9.25	-0.18	0.36(3.9%)
Without superstrate		119	9.4	-	(6.4%)

3-1-3. Superstrate Height Effects

To complete the study of the superstrate effects on the input resistance, the superstrate height above the patch *(t_2)* is changed while the two other parameters are kept fixed at ε_3=9.2 and t_3=2.54mm, respectively. As it will be shown, the relation between input impedance and the superstrate parameters becomes clear. The air gap height *(t_2)* is given values of *13, 12, 11, 10, 8, 6, and 4 mm*. The input resistance, *Re{Z_{in}}* is calculated and shown in *Fig.3.4*. It is observed that as the superstrate becomes closer to the patch, the resonant frequency *(f_r)* moves toward higher values, that is a positive frequency shift occurs. In conclusion, the effects of each parameter can be summarized as follows:

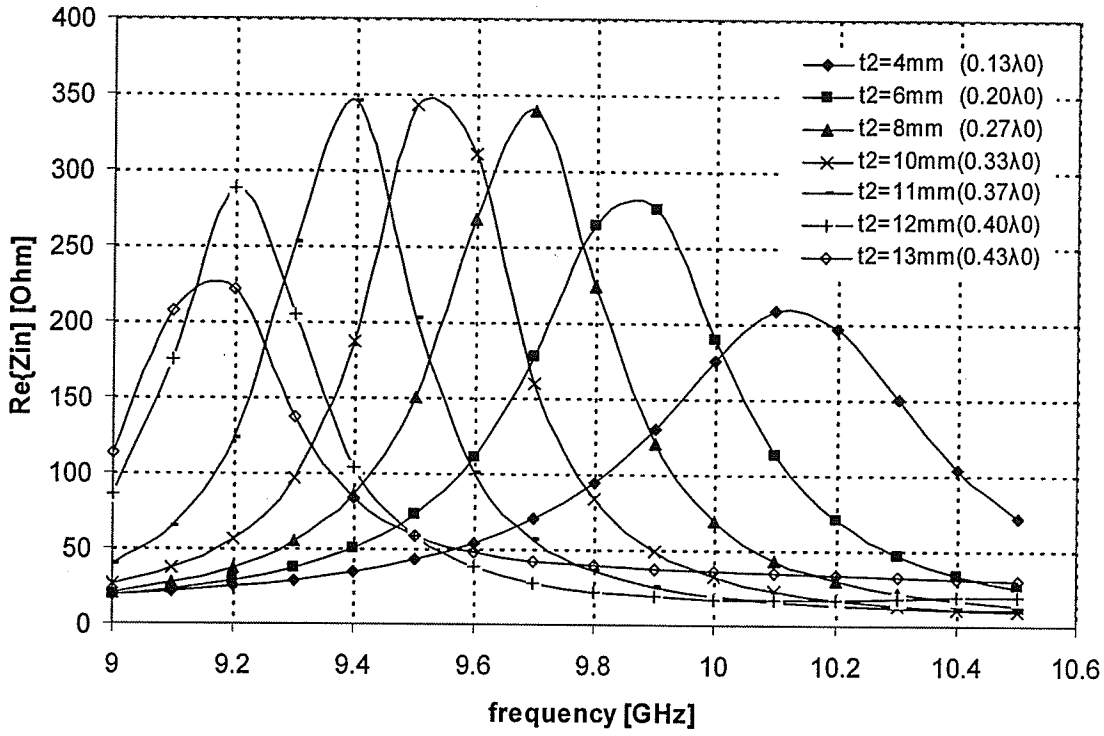

Fig.3.4. Effects of the superstrate height on the microstrip patch antenna input resistance, and its variations with frequency,(ε_3=9.2, t_3=2.5mm (λ_3/4), , f_0 =10GHz, the other parameters are listed in Table 3.1)

As the superstrate becomes thicker, or its dielectric constant increases, the resonant frequency shifts to the lower frequencies, the resonant resistance increases, and the impedance bandwidth decreases. On the other hand, as the superstrate becomes closer to the substrate, the resonant frequency shifts to the higher frequencies.

3.1.4. Superstrate Effects on Imaginary part of Z_{in}

The variation of the input reactance $Im\{Z_{in}\}$ with frequency are calculated for different superstrate thicknesses, dielectric constants, and heights, in the same way as

was done for the input resistance, $Re\{Z_{in}\}$. *Fig.3.5.a-c* plots the variations of the input reactance, $Im\{Z_{in}\}$, with respect to frequency, for different superstrate thicknesses, relative permittivities, and heights.

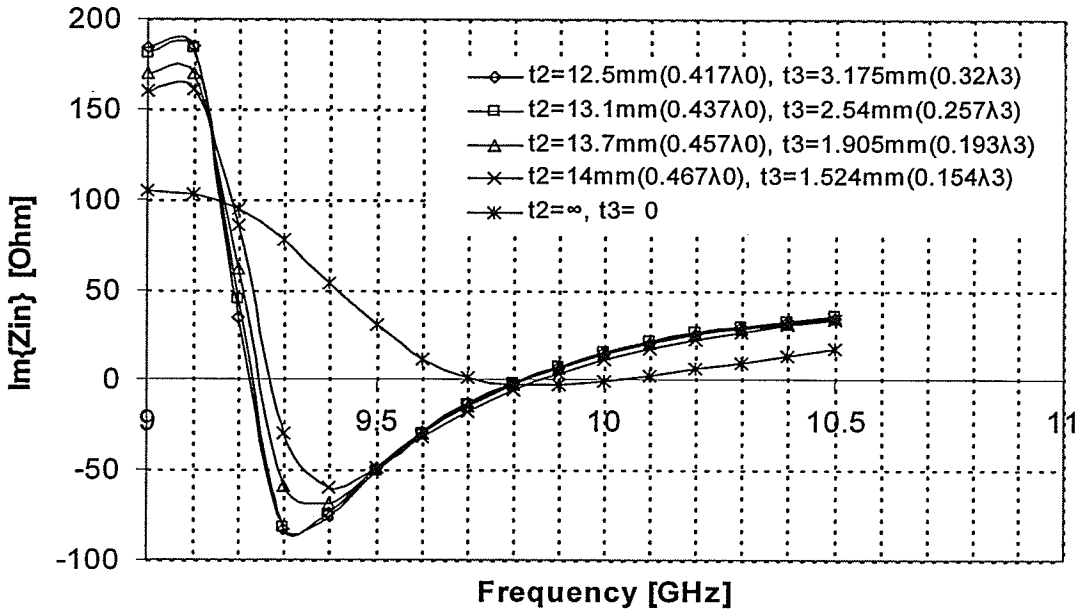

(a)

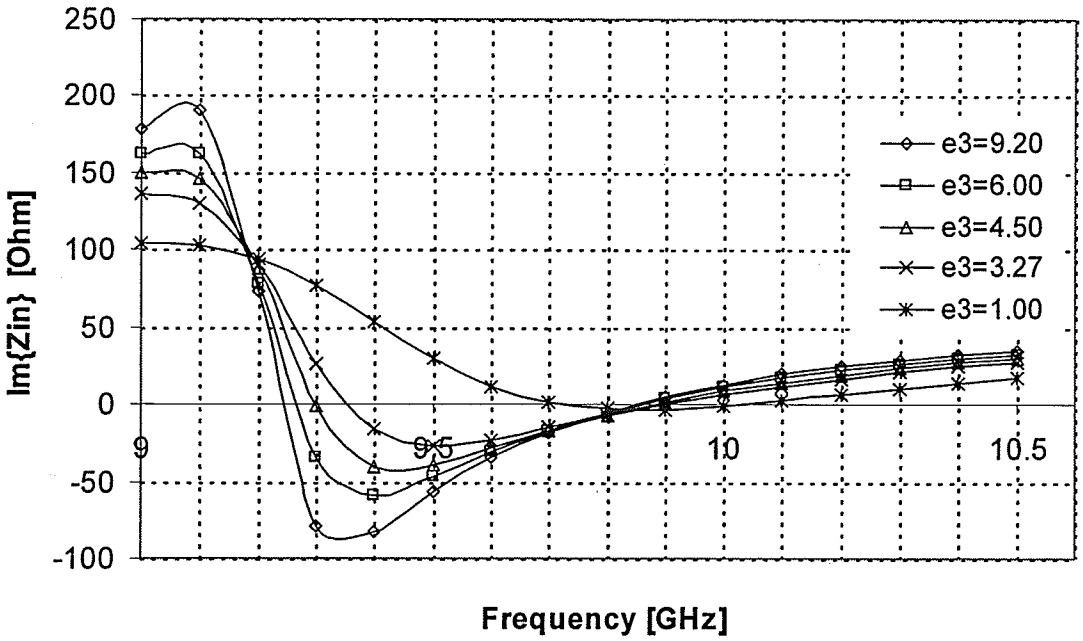

(b)

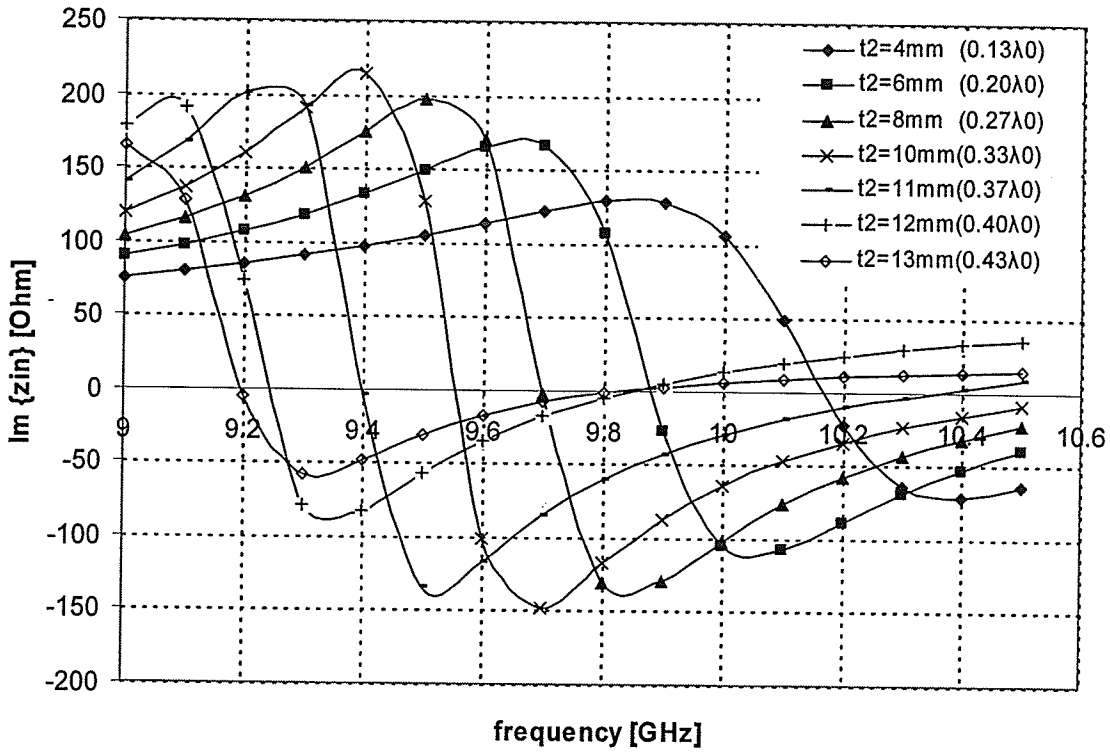

(c)

Fig3.5. Effects of the superstrate on the microstrip patch antenna input reactance, and its variations with frequency for different superstrate parameters (a) thickness, (b) dielectric constant (c) height (f_0=10GHz, the parameters are the same as those of Figures 3.2,3.3,3.4, respectively)

As it is clear from *Fig.3.5a-c*, the effects observed for the input reactance, *Im{Zin}* are quite similar to the effects for the input resistance, $Re\{Z_{in}\}$.

3.2. Superstrate Effects on Directivity

The effects of the superstrate parameters on the directivity of microstrip patch antennas are considered in this section. The effects of the superstrate thickness and dielectric constant will be demonstrated separately in subsequent sections. It will be shown that the directivity varies with respect to the air gap height, and for each

superstrate thickness and dielectric constant, the directivity can be optimized by the air gap height above the patch.

3.2.1. Superstrate Thickness Effects on Directivity

At the frequency of *10 GHz*, four different superstrates with the thicknesses *(t_3)* of *3.175mm ($0.32\lambda_3$), 2.540mm ($0.25\lambda_3$), 1.905mm ($0.19\lambda_3$), and 1.524mm ($0.15\lambda_3$)* are used, and the directivity in the *z-direction* (the broadside case, *$\theta=0°$)* versus the distance t_2 (air gap height) are calculated, respectively. The dielectric constants are kept fixed at *9.2* for each case. The results are shown in *Fig.3.6.* It can be seen that for each superstrate thickness, the directivity first increases with the height t_2, then reaches its maximum value *Dmax* at a resonant distance t_{2r}, and then decreases. So for each t_3, there are a corresponding t_{2r}, and a corresponding *Dmax*. These values are listed in *Table 3.4,* where $\lambda_i=\lambda_0/\ \varepsilon_{ri}^{1/2}$ and λ_0 is the wavelength in free space. Generally, the larger t_3 is, the smaller t_{2r} is, so we can conclude that t_3 can be offset by t_2. This will be discussed in more details in *section 3.4.*

It can be seen from *Fig.3.6* that in order to obtain the highest directivity, the best value of t_3 is $\lambda_3/4$ (quarter wavelength in superstrate medium). The directivity of the original microstrip patch antenna is *7.24dBi.* By adding a dielectric plate with the relative permittivity of *9.2* and the thickness of one quarter wavelength above it and adjusting the distance t_2, a directivity of *15.45dBi* is obtained with a net increment of *8.2dB.*

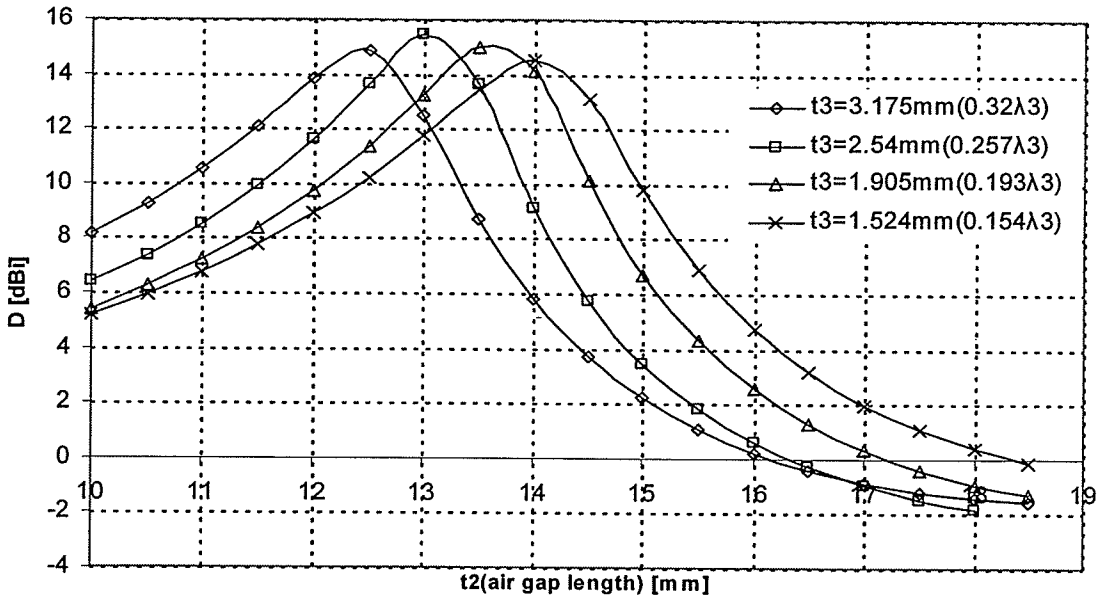

Fig.3.6 Effects of the superstrate thickness on microstrip patch antenna directivity, and its variations with superstrate height (ε_3=9.2, f_0=10GHz, the other parameters are listed in Table 3.1)

Table 3.4. Comparison of microstrip patch antenna directivity for various superstrate thicknesses (ε_3=9.2, f_0=10GHz, the other parameters are listed in Table 3.1)

t_{2r} [mm]	t3[mm]	Dmax [dBi]
12.5(0.416λ_0)	3.175(0.32λ_3)	14.85
13.1(0.436λ_0)	2.54(0.25λ_3)	15.45
13.7(0.456λ_0)	1.905(0.19λ_3)	15.00
14.0(0.47λ_0)	1.524(0.15λ_3)	14.52

3.2.2. Superstrate Dielectric Constant Effects on Directivity

To observe the effect of the superstrate dielectric constant on the directivity, the variations of the directivity with respect to air gap height is computed for different values of superstrate dielectric constants. Superstrates with relative permittivities *(ε_3)* of *9.2, 6.0, 4.5, and 3.27* are selected, respectively. At the frequency of *10 GHz* the directivity is calculated in the *z-direction* (broadside case, *θ=0°*). The calculated results are shown in *Fig.3.7* and *Table3.5*. It is clear from *Fig.3.7* that t_{2r} is almost constant for different superstrate dielectric constants, and the peak value of directivity is only changed. It should be noted that the superstrate thickness is one quarter wavelength. That resembles the classic resonant condition, *section 2.3.1*. In *Table 3.5*, it is seen that the directivity also varies almost proportionally with the superstrate dielectric constant as predicted by the asymptotic gain formula *(3.2)* derived by *Jackson and Alexopoulos [6]*. For validating this similarity, the asymptotic gain formula result will be compared with the exact calculation given by the simulation for the above cases.

The asymptotic formula for gain *(3.2)* has been derived in the *z-direction* under resonant condition for a Herzian dipole embedded at the middle of the substrate, while superstrate relative permittivity ε2>>1 as;

$$Gain = 8\frac{n_1 B}{\lambda_0}\left(\frac{\varepsilon_2}{n_1 \varepsilon_1 \mu_2}\right) \qquad (3.2)$$

where

$n_1 = \sqrt{\varepsilon_1 \mu_1}$ (Substrate refractive index)

B= substrate thickness

λ_0 = *free space wavelength*

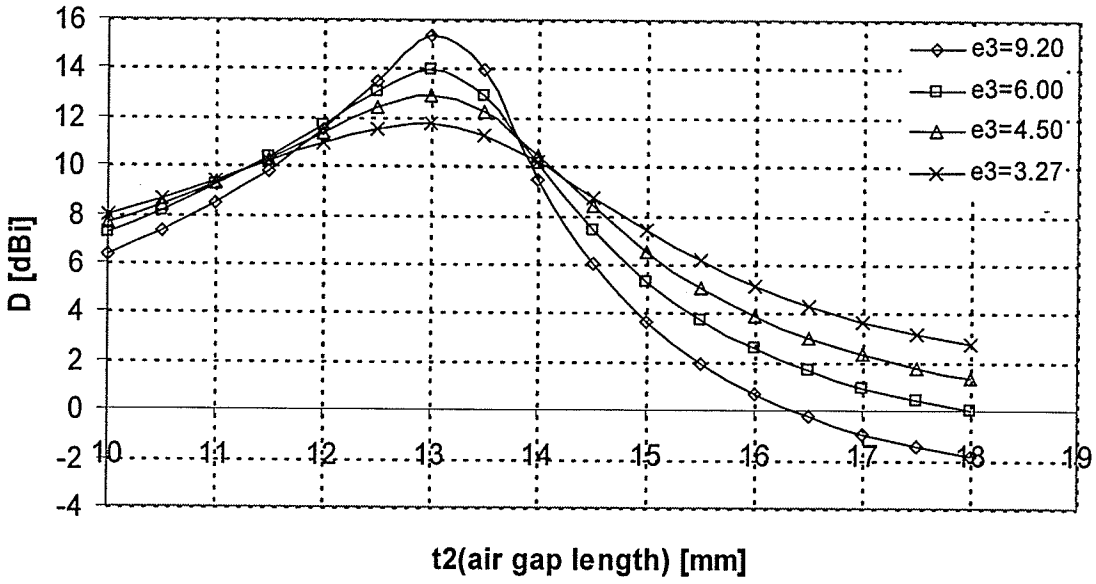

Fig.3.7 Effects of the superstrate dielectric constant on microstrip patch antenna directivity variations with superstrate height ($t_3=\lambda_3/4$, $f_0=10GHz$, the other parameters are listed in Table 3.1)

Table 3.5 Comparison of the microstrip patch antenna directivity for various superstrate dielectric constants (t2r=13.1mm(0.436 λ_0), $f_0=10GHz$, the other parameters are listed in Table 3.1)

t_3 [mm]	ε_3	Dmax [dBi]
2.5(0.25 λ_3)	9.20	15.3785
3.1(0.25 λ_3)	6.00	13.94823
3.5(0.25 λ_3)	4.50	12.90201
4.1(0.25 λ_3)	3.27	11.71733

ε_1, ε_2, μ_1, *and* μ_2 are permittivity and permeability of substrate and superstrate respectively. In order to validate that, at the frequency of *10 GHz*, different superstrate relative permittivities (ε_3) of *3.27, 4.50, 6.00*, and *9.20* are considered. The gain is calculated in the *z-direction* ($\theta=0^o$) by both methods. The calculated results are listed in *Table 3.6.*

Table 3.6 Comparison of the Asymptotic gain formula result with simulated gain result (t2r=13.1mm (0.436 λ_0),$t_3=\lambda_3/4$, f_0=10GHz, the other parameters are listed in Table 3.1)

ε_3	**Simulated gain [dBi]**	**Asymptotic gain[dBi]**	**Error [%]**
3.27	*11.72*	*11.16*	*−4.78%*
4.50	*12.9*	*12.55*	*−2.71%*
6.00	*13.95*	*13.8*	*−1.08%*
9.20	*15.38*	*15.65*	*+1.76%*

As it can be seen from the *Table 3.6*, the difference between the results becomes smaller by increasing the superstrate relative permittivity, as expected *[6]*. Jackson and Alexopoulos have shown that the asymptotic formula approaches the exact gain calculation as the superstrate dielectric constant becomes larger, but it always gives a smaller value for gain, *Fig.3.8.*

The only difference is that for the case of $\varepsilon_3=9.2$, the asymptotic formula gain is greater than the simulated gain. This can be justified as follows. The asymptotic formula derivation is based on a configuration consisting of only two layers (substrate-

superstrate). But the simulation result is based on a configuration consisting of three layers (substrate-air gap-superstrate). As a matter of fact, the substrate thickness had been ignored and the asymptotic calculation was done by assuming $\varepsilon_1 = 1$ (free space permittivity). However, an effective value for ε_1 should have been defined, in order to take into account both substrate and air gap layers. Then, the ε_1 would be larger, so asymptotic formula gain would become smaller.

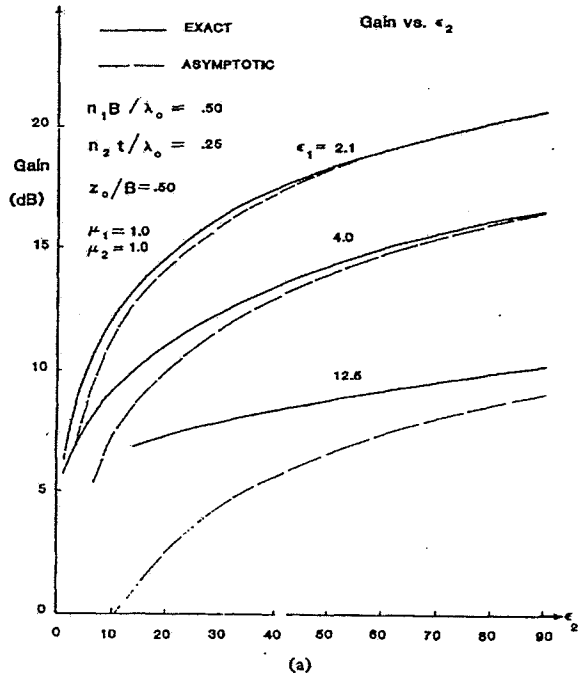

Fig.3.8. Comparison of asymptotic gain formula result with exact calculated gain [6]

3.3. Substrate Effects

The study of substrate effects has been done into two parts; *a)* the effect of the substrate thickness on the directivity, and *b)* the effect of substrate thickness on the input impedance.

3-3-1. Substrate Thickness Effect on Directivity

In reference [6], the simplest resonant conditions in a two layer substrate-superstrate configuration are described as, $t_1=\lambda_1/4$, $t_2=\lambda_2/4$, $t_3=\lambda_3/4$ for a Herzian dipole embedded in the middle of substrate. For a coaxially fed microstrip patch antenna, $\lambda_1/4$ is too large for t_1. Some difficulties such as abnormal radiation patterns, high surface wave, and high cross-polarization will be experienced [14]. This problem has been solved by making an air gap between the substrate and superstrate, while the substrate can be kept thin enough. In order to investigate the effects of the substrate thickness, a number of different substrate thicknesses (t_1) are considered, while the superstrate thickness is one quarter wavelength. At the frequency of *10 GHz*, for the superstrate relative permittivity of 9.2 and thickness of *2.54mm* and for substrate dielectric constant of *2.2*, with different substrate thicknesses of *0.254mm*($.0125\lambda_1$), *0.381mm*($.019\lambda_1$), *0.508mm*($.025\lambda_1$), *0.787mm*($.039\lambda_1$), *and 1.575mm*($.078\lambda_1$), respectively, the variations of the directivity with respect to the air gap height are calculated in the z-direction ($\theta=0^o$), and the results are shown in *Fig.3.9.*

It can be seen from *Fig.3.9*, that when the superstrate thickness t_3 is kept at the optimal value of $0.25\lambda_3$, for different substrate thicknesses (t_1), the optimum directivity can be obtained by adjusting the distance t_2. For each value of t_1, there exists a different resonant distance t_{2r}, but the optimum directivity are almost the same. The substrate thickness, optimum air gap height, and the corresponding directivity are summarized in *Table3.7.* Therefore, the substrate thickness t_1 can be offset by the air gap height t_2, in order to obtain the maximum directivity.

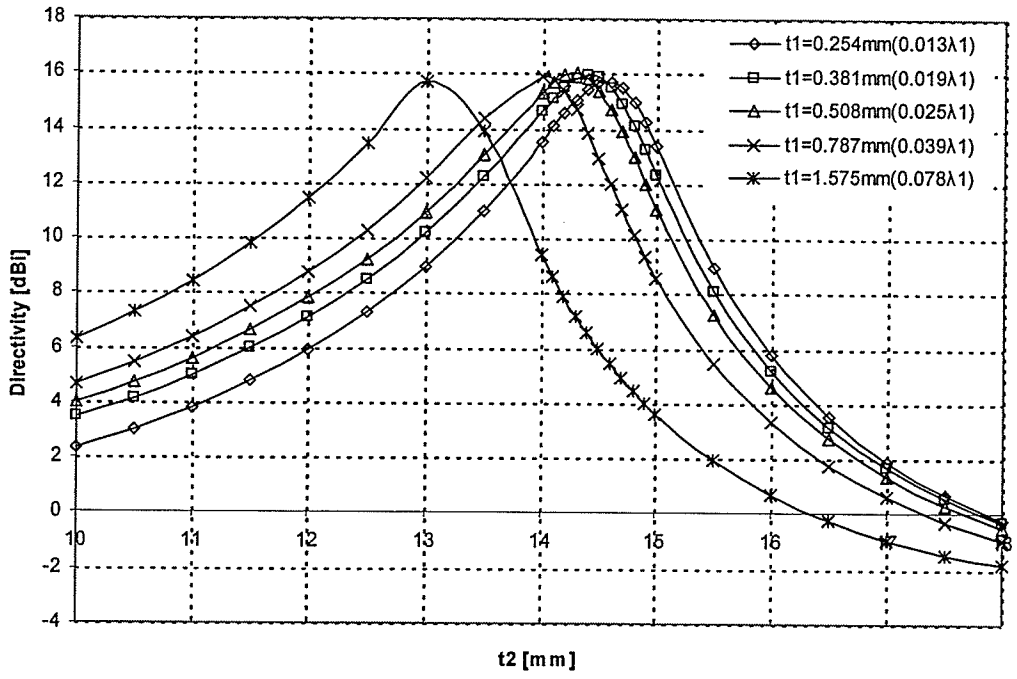

Fig.3.9 Effects of the substrate thickness on variations of the microstrip patch antenna directivity with respect to the superstrate height (ε_3=9.2, $t_3=\lambda_3/4$, f=10GHz, the other parameters are listed in Table 3.1)

Therefore, in order to obtain the optimum directivity, the substrate thickness is not a constraint, contrary to the classic resonant gain condition, but the combination of the substrate thickness *(t_1)* and the air gap height *(t_2)* are required to realize the resonance. Hence, it provides one more degree of freedom. From Table 3.7, it can be also observed that the peak value for the directivity is obtained for $t_1=0.025\lambda_1$.

3.3.2. Substrate Effect on Input Impedance

Related to the superstrate effects on the input impedance which have been provided in *section 3.1*, the investigation will be continued further in this section by considering the variations of thickness for both substrate and superstrate. It will be concluded that the

superstrate effect on the input impedance is stronger, as substrate thickness becomes larger.

Table3.7 Comparison of the microstrip patch antenna directivity for various substrate thicknesses (ε_3=9.2, $t_3=\lambda_3/4$, f_0=10GHz, the other parameters are listed in Table 3.1)

Substrate thickness (t_1) [mm]	***Air gap height (t2r) [mm]***	***Dmax [dBi]***
0.254(.0125λ_1)	*14.6(0.487 λ_0)*	*15.70*
0.381(.019λ_1)	*14.4(0.48 λ_0)*	*15.95*
0.508(.025λ_1)	*14.3(0.477 λ_0)*	*15.99*
0.787(.039λ_1)	*14.0(0.467 λ_0)*	*15.88*
1.575(.078λ_1)	*13.1(0.437 λ_0)*	*15.53*

At the frequency of *10 GHz*, for substrate dielectric constant of *2.2*, the microstrip patch antenna with different substrates thicknesses *(t_1)* of *0.787mm and 1.575mm* are matched with a *50 Ohm* coaxial feed. Their parameters are listed in *Table3.8*.

Table3.8. The selected specifications of the microstrip patch antennas for studying the Substrate Effects on the input impedance

t1 [mm]	***ε_1***	***L x W [mm]***	***Xf (feed location from the center of patch) [mm]***
0.787(.039λ_1)	*2.2*	*9.4×12*	*2.1*
1.575(.078λ_1)	*2.2*	*9.1×12*	*2.8*

The patch is covered by a superstrate with ε_3 =9.2 *and* t_3=2.54. The input impedance are calculated and compared with the former case (uncovered patch) for substrate thicknesses of *1.575 mm* ($.078\lambda_1$) *a*nd *0.787 mm* ($.039\lambda_1$). Their plots are overlaid in *Fig.3.10.* The values of R_r, the peak value of input resistance, the frequency shift, and the impedance bandwidth for each case are summarized in *Table 3.9* for comparison.

It can be seen from *Table 3.9* that, the input resistance, resonant frequency shift and the bandwidth of input impedance are affected more by the superstrate when the substrate is thicker.

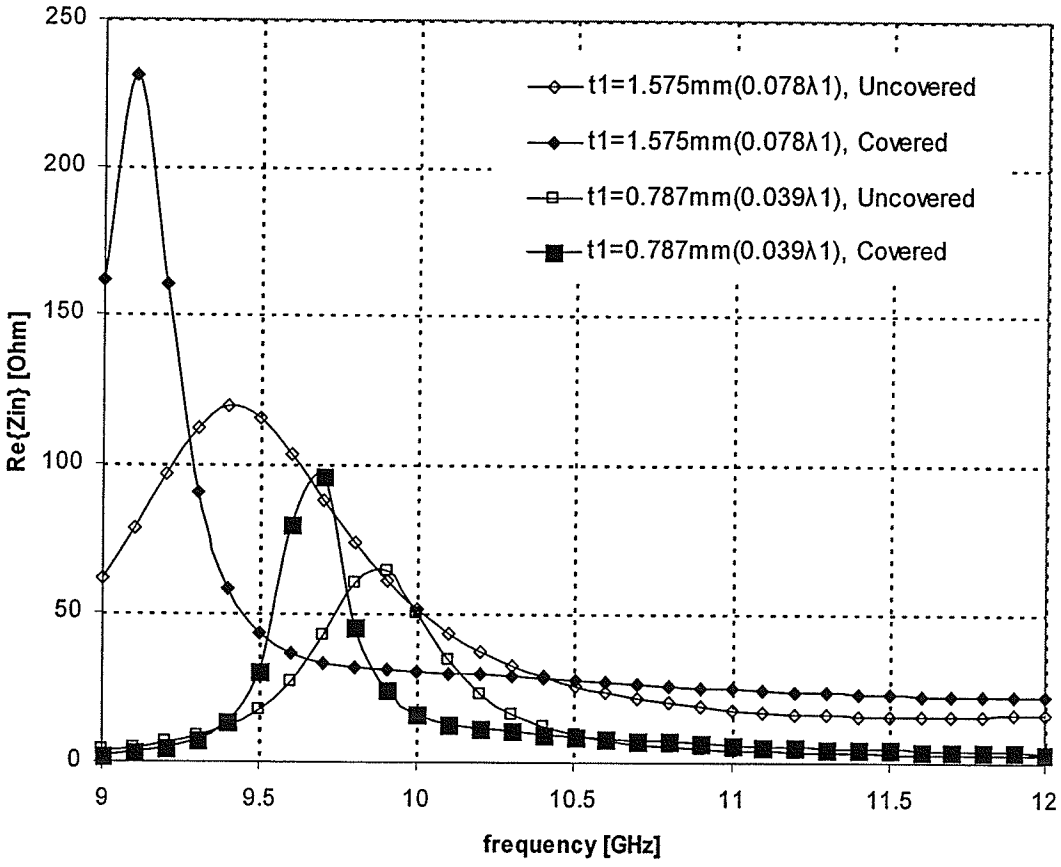

Fig.3.10. Effects of the substrate thickness on the microstrip patch antenna input resistance characteristics variations with frequency ($t_2=t_{2r}$, ε_3=9.2, $t_3=\lambda_3/4$, f_0=10GHz, the other parameters are listed in Table 3.8)

Table3.9 Input resonant resistance, resonant frequency, and impedance bandwidth of a microstrip patch antenna and its percentage changes after adding superstrate for two different substrate thicknesses ($t_2=t_{2r}$, $\varepsilon_3=9.2$, $t_3=\lambda_3/4$, $f_0=10GHz$, the other parameters are listed in Table 3.8)

t1 [mm]	R_r *[Ohm]*	ΔR_r*[%]*	f_r *[GHz]*	Δf_r*[%]*	*BW [GHz]*	ΔBW*[%]*
1.575	*118*	*96%*	*9.4*	*-3.2%*	*0.6*	*-67%*
0.787	*63*	*51%*	*9.9*	*-2%*	*0.3*	*-50%*

3.4. Tolerance Analysis

In this section, the acceptable tolerances of dielectric materials regarding the resonant gain are investigated. The dielectric material is usually the most expensive part of a microstrip patch antenna. That would be much more expensive in case of custom made dielectric, rather than conventional materials available in the market. When the dielectrics with desired specification are not available in the market, it could be replaced with another comparable material. Thus, knowing tolerances would be considerably helpful in this regard. Besides, there is always the issue of inaccuracies in fabrication which requires adjusting.

The deviations from design values could be due to the superstrate dielectric constant or thickness. The air gap height deviations also affect the directivity and are studied accordingly. It will be shown that the superstrate and air gap effects on the directivity are

rather similar. The air gap thickness can also compensate for the superstrate thickness deviation to an acceptable degree, which will be used later in this study.

The amount that the input impedance would be affected, from different superstrate loading when the microstrip patch antenna is already matched, will be investigated last. Knowing that, helps us in practice with designing the prototype and then, adjusting the parameters to obtain the optimum gain.

3.4.1. Superstrate Dielectric Constant Deviation

As it was discussed in section *3.2*, the directivity varies with superstrate dielectric constant almost proportionally *(3.2)*, so the directivity would be very sensitive to its deviations. When there is no dielectric with the desired permittivity, the desired directivity can be achieved by using another dielectric material with a higher dielectric constant. But the air gap thickness *(t_2)* needed to be offset from its optimum t_2 *(t_{2r})*. As it is clear in *Fig.3.7* (*section 3.2*), the optimum directivity in the case of a superstrate, with a relative permittivity of *3.27*, can be also obtained with a higher dielectric constant superstrate, *e.g.* a relative permittivity of *4.5, 6, or 9.2*, but properly adjusting t_2 is required.

3.4.2. Superstrate thickness deviation

As it was discussed in *Section 3.2*, the quarter wavelength thickness of the superstrate is the strict constraint for obtaining the maximum directivity. However, with other superstrate thicknesses, the maximum directivity can be obtained by adjusting the air gap height (t_2). In order to compare the effects of the superstrate thickness and the air gap

height deviations on the directivity, the directivity is calculated with respect to each of these deviations while the other one is kept fixed. The antenna parameters selected for this study, are listed in *Table 3.10.*

Table 3.10 The selected specification of the single-superstrate microstrip patch antenna for tolerance analysis of the superstrates parameters (f_0=10GHz)

Layer	***Material***	***Geometry***
Superstrate	ε_r=9.2	*Thickness=2.5 mm*
Air gap	*Air*	*Height=13.1 mm*
Patch	*Copper*	*Rectangular 9.1×12 mm*
Substrate	ε_r=2.2	*Thickness=1.575 mm*
Ground Plane	*Copper*	*Infinite*
Feed	*Coaxial Probe*	X_f=-2.8 mm, Y_f=0 mm *(location from the center of patch)*

The directivity discrepancies from the optimum value are calculated for both cases. The plots are shown in *Fig.3.11.*

It was expected that the superstrate thickness deviation affects the directivity more , as compared with the air gap height deviation, due to the greater superstrate dielectric constant $\varepsilon_3 >> 1$. This is due to the fact that, the same deviation of the superstrate thickness would be larger in terms of electrical length than that of the air gap height deviation. Despite that, their effects are almost similar, and even for positive deviations

(in right half plane) the air gap thickness deviation affects directivity more, as it can be seen from *Fig. 3.11*.

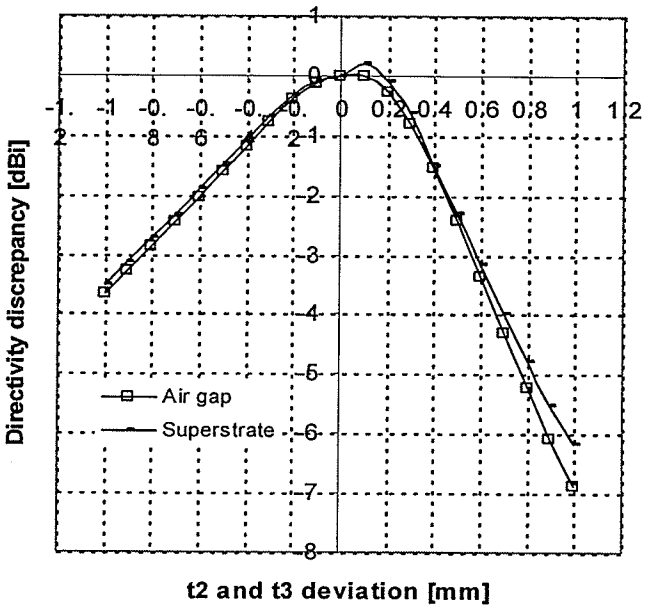

Fig. 3.11 Directivity variation versus the superstrate thickness and air gap height deviations (f_0= 10GHz, the other parameters are listed in Table3.10)

To verify this further, another configuration with even a higher superstrate dielectric constant is considered. This time, the superstrate relative permittivity of *25* is selected. Similar to the previous case of superstrate with a relative permittivity ε_3=*9.2*, the directivity is calculated with respect to the superstrate thickness or the air gap height deviations, while the other one is kept fixed. The antenna parameters selected for this purpose are listed in *Table 3.11*.

The directivity discrepancies from its optimum value are shown in *Fig.3.12*. These results show good agreement with the previous results and prove the hypothesis that the

superstrate thickness and air gap height deviations have almost similar impact on the directivity.

Table 3.11 The selected specification of the single-superstrate microstrip patch antenna for tolerance analysis of the superstrates parameters (f_0=10GHz)

Layer	***Material***	***Geometry***
Superstrate	ε_r=25	*Thickness=1.5 mm*
Air gap	*air*	*Height=13.3 mm*
Patch	*Copper*	*Rectangular, 9.1×12 mm*
Substrate	ε_r=2.2	*Thickness=1.575 mm*
Ground Plane	*Copper*	*Infinite*
Feed	*Coaxial Probe*	X_f=-2.8 mm, Y_f=0 mm *(location from the center of patch)*

As it can be seen from *Fig. 3.12*, even if a much higher value for the superstrate dielectric constant is considered, the effect of the air gap height deviation is almost the same as that of the superstrate. This was mentioned earlier that, the air gap height can compensate for the superstrate thickness deviation to some acceptable extent. Considering *Fig. 3.11 and 3.12*, it can be concluded that the superstrate thickness and the air gap height deviations might cancel each other, when their values are similar but opposite in the type of effect. This effect is investigated next, and will be used later in this study.

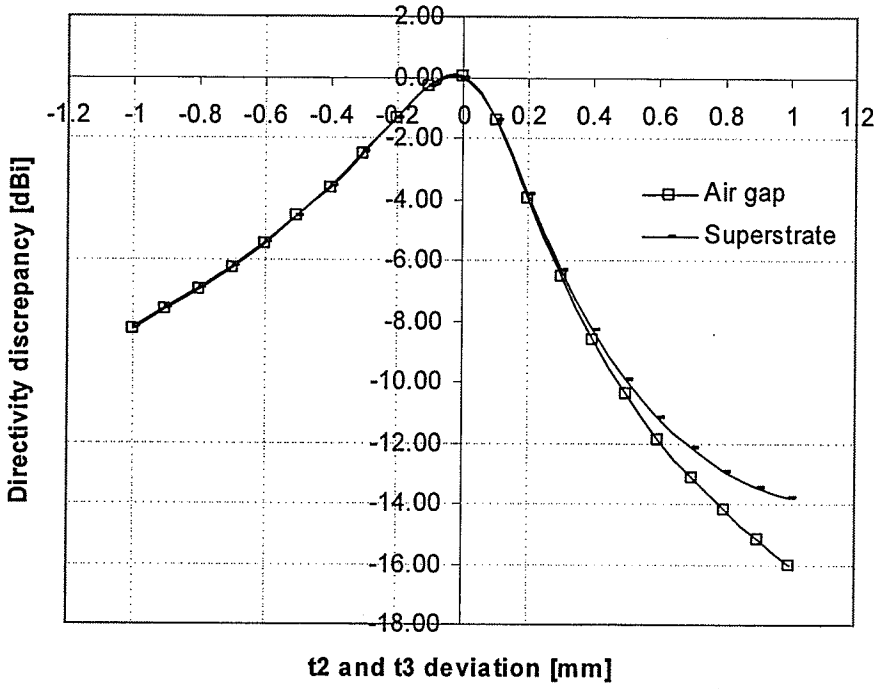

Fig. 3.12 Directivity variation versus the superstrate thickness and air gap height deviations (f_0= 10GHz, the other parameters are listed in Table3.10)

At the frequency of *10GHz*, for the microstrip patch antenna with the parameters as listed in *Table 3.11*, the superstrate thickness deviation is selected in a range of $\pm 1mm$ $(\pm 0.40\lambda_3/4)$, and the air gap height deviation with the opposite sign, that is $t_2 + t_3 =$ *constant*, the directivity discrepancies are calculated and shown in *Fig.3.13*. The maximum difference from the optimum directivity is listed in *Table 3.12*.

As it can be seen in *Table 3.12*, the maximum change in the directivity is less than *10%* for 40% superstrate thickness variations from the designed value and by comparing *Fig. 3.11 with Fig.3.12*, the same result is expected for the case of $\varepsilon_3=25$. It should be noted that, the compensation feature is considered only as an initial assumption which could be helpful, particularly in the design and test of the antenna.

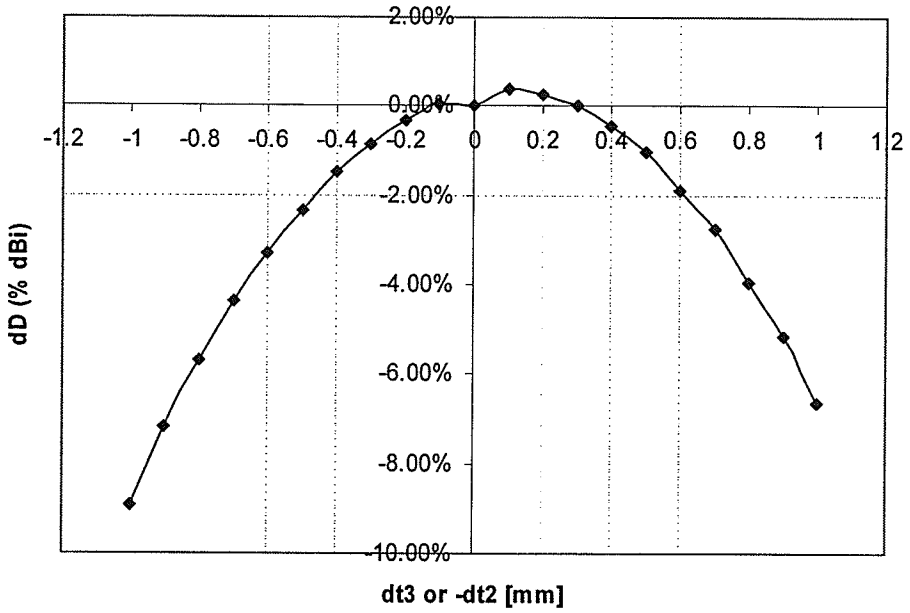

Fig.3.13. Directivity discrepancies due to the superstrate thickness deviation with air gap compensation (f_0= 10GHz, the other parameters are listed in Table3.10)

Table 3.12 Directivity discrepancy due to 40% superstrate thickness deviation, with air gap compensation (f_0= 10GHz, the other parameters are listed in Table3.10)

Deviation	***D [dBi]***	***ΔD[%]***
$dt_3=+0.40\lambda_3/4=-dt_2$	*14.4*	*-7 %*
$dt_3=-0.40\lambda_3/4=-dt_2$	*14.1*	*-9 %*

3.4.3. *Sensitivity of the Impedance-matching to Directivity center frequency*

For the sake of simplicity, the frequency where the maximum directivity can be obtained is called "directivity center frequency" f_0. In this section the sensitivity of input impedance to the directivity center frequency will be investigated. It will be shown that, over a reasonable frequency range, the effect due to changes in directivity center frequency on the input response is negligible. The directivity center frequency can be calculated by *(3.3)* as follows, which is also valid for the microstrip patch antenna case [14].

$$t_3 = \frac{\lambda_0}{4\sqrt{\varepsilon_3}} \qquad (3.3)$$

so;

$$f_{res} = \frac{c}{4t_3\sqrt{\varepsilon_3}} \qquad (3.4)$$

where c is the speed of light in free space.

If the antenna is not matched at frequency (f_{res}), the gain is different from the directivity, by as much as the the mismatch loss, as shown below:

$$Gain_{|dBi} = D_{|dBi} + L_{m|dB} \qquad (3.5)$$

where L_m is the mismatch loss. In order to investigate the correlation between the changes in input impedance and the changes in directivity center frequency (by changing the superstrate thickness), a microstrip patch antenna matched at *10GHz* is considered with the substrate thickness (t_1) of *1.575 mm*. Then, in the range of twenty percent around the

directivity center frequency, i.e. from *8* to *12 GHz,* in steps of *0.5GHz*, the optimum superstrate thicknesses *(t_{3r})* are calculated by (3.3) which are listed in *Table 3.13*.

Table 3.13 The required superstrate thicknesses and air gap heights for directivity center frequencies in the range of 8 to 12 GHz (the other parameters are listed in Table3.10)

directivity f_0 [GHz]	**t_{3r} [mm]**	**t_{2r} [mm]**
8.0	*3.1*	*12.5*
8.5	*2.9*	*12.7*
9.0	*2.8*	*12.8*
9.5	*2.6*	*13.0*
10	*2.5*	*13.1*
10.5	*2.4*	*13.2*
11.0	*2.3*	*13.3*
11.5	*2.2*	*13.4*
12.0	*2.1*	*13.5*

The corresponding t_{2r} values are calculated based on the compensation property (section 3.4.2), that is the deviation in t_3, which can be compensated by a deviation in t_2

of the opposite sign. The input resistance variations with respect to frequency are calculated and shown in *Fig.3.14*.

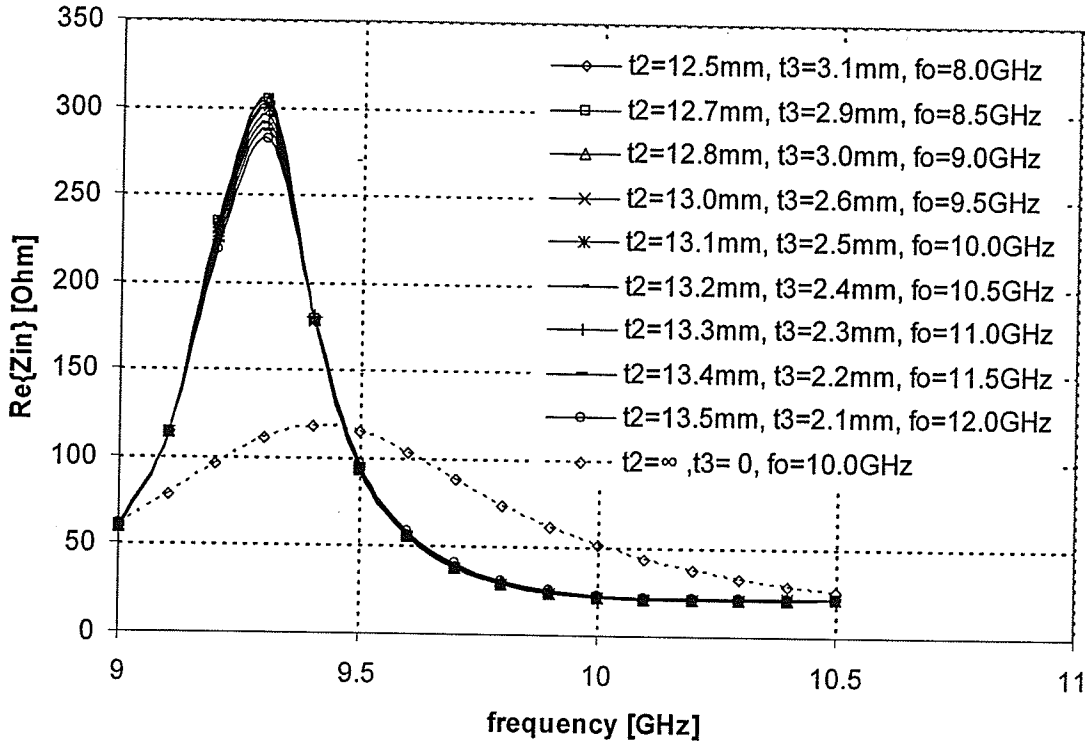

Fig. 3.14 The input resistance (Re{Zin}) variations with respect to frequency for various directivity center frequencies

As it can be seen from *Fig. 3.14*, the input resistance frequency response remains almost invariant. Therefore, the simulation results for the antenna impedance matching, i.e. the input impedance response still will be useful, even in the case where there is some deviation in the directivity center frequency due to the superstrate relative permittivity or thickness tolerances.

3.5. Radiation Characteristics

In this section, the radiation characteristics are studied. It includes the broadside directivity variations with frequency and directivity pattern in the two main planes *i.e. E-plane* and *H-plane*. In the first part, for obtaining the desired directivity, *i.e.* by selecting the proper superstrate dielectric constant, the directivity as a function of frequency will be shown for different superstrate thicknesses. It is shown that there are minor differences among the broadside directivity variations, with respect to frequency, for different superstrate thicknesses. Also the radiation pattern in the *E-plane* and *H-plane* are similar for different superstrate thicknesses. Finally, the radiation patterns at center frequency (f_0) and also at the half power frequencies (f_1, f_2) are plotted for comparison. It can be seen that, the side lobe level (*SLL*) is larger for the higher half power frequency (f_2), but the cross-polarization is smaller, in comparison with the lower half power frequency (f_1). In the second part, the directivity variations with frequency for different superstrate dielectric constants are shown and then their radiation patterns are compared. As it is expected, the directivity bandwidth decreases with increasing superstrate dielectric constant.

3.5.1. Superstrate Thickness Effects on Radiation Characteristic

Different thicknesses of *3.175mm* $(0.321\lambda_3)$, *2.54mm* $(0.257\lambda_3)$, *1.905mm* $(0.193\lambda_3)$, *and 1.524mm* $(0.154\lambda_3)$ are selected to investigate the broadside directivity variations with respect to frequency. The superstrate relative permittivity of *9.2* is selected for this purpose. The air gap height is also optimized to give the optimum directivity at *10 GHz*. The corresponding values for the air gap height are 12.5mm $(0.417\lambda_0)$, *13.1mm (*

0.437λ0), 13.7mm (0.457 λ0), and 14mm (0.467λ0), respectively. The broadside directivity variations with frequency, in the range of *7.5 to 12.5 GHz*, are calculated and shown in *Fig.3.15.* The directivity of the simple patch is also plotted, as a reference.

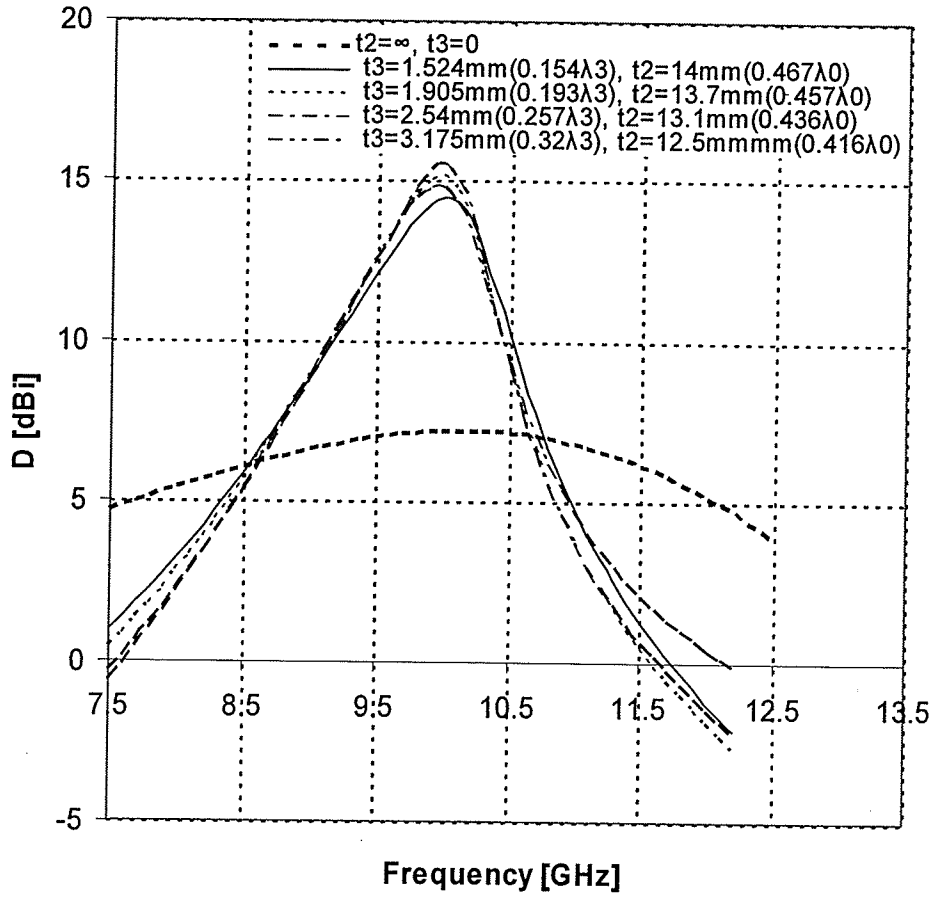

Fig. 3.15 Directivity variations with frequency for various superstrate thicknesses (ε_3=9.2, the other parameters are listed in Table 3.1)

As it can be seen from *Fig.3.15,* the directivity shows a remarkable increment. On the other hand the directivity bandwidth (-3dB bandwidth) decreases. In addition, the directivity variations with respect to frequency are almost similar for different superstrate

thicknesses. The maximum directivity and the corresponding directivity bandwidth for each case are also summarized in *Table 3.14*.

Table 3.14 Maximum directivity, directivity bandwidth, and their products for various superstrate thicknesses (ε_3=9.2, f=10GHz, the other parameters are listed in Table 3.1)

t_3[mm]	t_2[mm]	Dmax[dBi]	BW[GHz]	directivity × BW
without superstrate		*7.2*	*5.23 (52.3%)*	*274.5*
1.524(0.154 λ_3)	*14mm(0.467λ_0)*	*14.47*	*1.0 (10%)*	*279.9*
1.905(0.193 λ_3)	*13.7mm(0.457λ_0)*	*15.16*	*0.85 (8.5%)*	*278.9*
2.54(0.257 λ_3)	*13.1mm(0.437λ_0)*	*15.49*	*0.80 (8.0%)*	*283.2*
3.175(0.321 λ_3)	*12.5mm(0.417λ_0)*	*14.80*	*0.91(9.1%)*	*274.8*

As it can be seen from *Table 3.14*, the directivity for t_3/λ_3=0.257, i.e. complying with the classical resonant gain condition (2.18), is maximum and the directivity bandwidth is minimum. It is also verified that the directivity-bandwidth product is also constant, which is predicted by the asymptotic formulas for the gain and bandwidth *[6]*. The radiation pattern for different superstrate thicknesses at the center frequency (f_0=10GHz) are calculated and shown in *Fig. 3.16*.

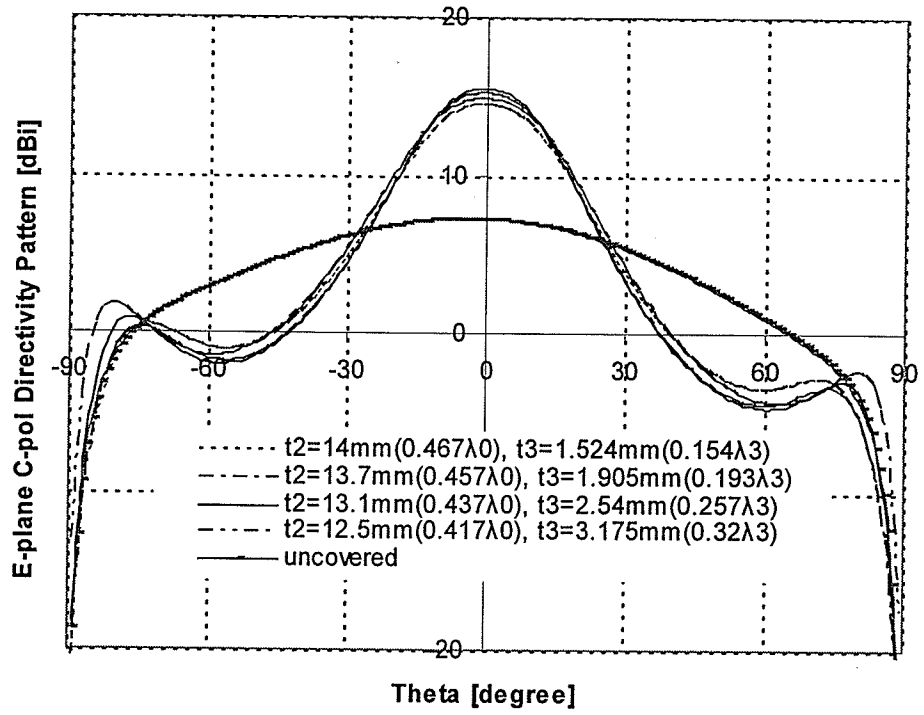
E-plane C-pol Directivity Pattern [dBi]
20
10
0
-90
-60
-30
0
30
60
90
t2=14mm(0.467λ0), t3=1.524mm(0.154λ3)
t2=13.7mm(0.457λ0), t3=1.905mm(0.193λ3)
t2=13.1mm(0.437λ0), t3=2.54mm(0.257λ3)
t2=12.5mm(0.417λ0), t3=3.175mm(0.32λ3)
uncovered
Theta [degree]

(a)

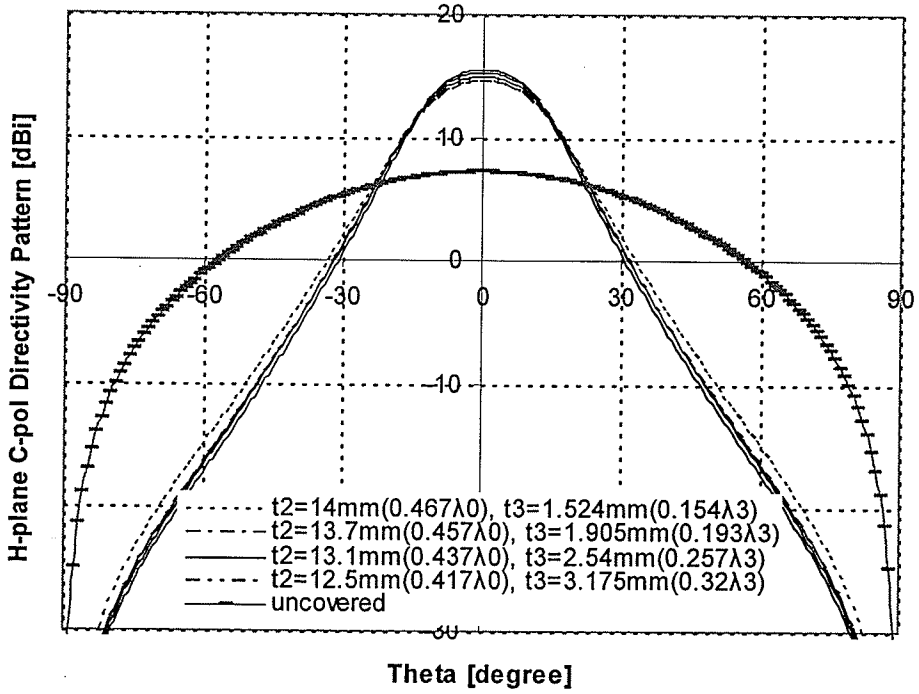
H-plane C-pol Directivity Pattern [dBi]
20
10
0
-10
-90
-60
-30
0
30
60
90
t2=14mm(0.467λ0), t3=1.524mm(0.154λ3)
t2=13.7mm(0.457λ0), t3=1.905mm(0.193λ3)
t2=13.1mm(0.437λ0), t3=2.54mm(0.257λ3)
t2=12.5mm(0.417λ0), t3=3.175mm(0.32λ3)
uncovered
Theta [degree]

(b)

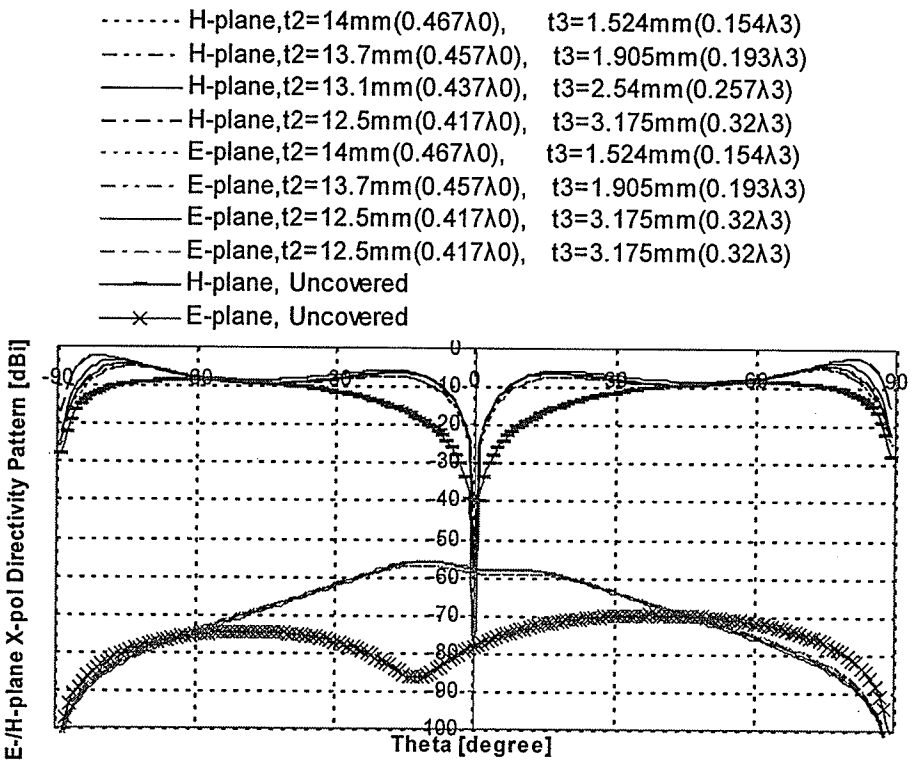

(c)

Fig.3.16 a) E_θ in E- plane, b) E_Φ in H – plane, and c) E_θ in H –plane and E_Φ in E- plane (ε_3=9.2, f_0=10GHz, the other parameters are listed in Table3.1)

The co-polarization components in the *E- and H-planes* are shown in *Fig.3.16(a) and (b)* ,respectively, and the cross-polarization components in *Fig.3.16 (c)*. As it can be seen in *Fig.3.16*, the radiation patterns and side lobe levels *(SLL)* are almost the same for different superstrate thicknesses. The cross-polarization component in the E-plane is negligible, which is much lower than -30dBi. The values of beamwidths and side lobe levels are listed in *Table 3.15*. As it is expected, the narrowest beamwidth belongs to the superstrate thickness of one quarter wavelength, i.e. $t_3/\lambda_3 \approx 0.25$).

Table3.15 Beamwidths and Side Lobe Levels for various superstrate thicknesses (f_0=10GHz, other parameters are kept the same as in Table3.1)

t_3[mm]	Dmax[dBi]	E-plane Beamwidth	H-plane Beamwidth	E-plane SLL [dB]
(without superstrate)	7.2	89°	76°	–
1.524(0.154 λ_3)	14.47	29°	28°	-14.02
1.905(0.193 λ_3)	15.16	28°	27°	-14.85
2.54(0.257 λ_3)	15.49	27°	25°	-14.59
3.175(0.321 λ_3)	14.80	30.5°	28°	-13.08

The radiation pattern for resonant superstrate thickness, $t_3/\lambda_3=0.25$ at the center frequency (f_0=10GHz) and half power frequencies (f_1=9.49GHz, and f_2=10.3GHz) are calculated and shown in *Fig. 3.17.*

At f_1 and f_2, where the broadside directivity falls *3dB*, the main beam becomes wider. For f_2, the beam is wider, due to a dip that occurs at broadside and also shows a better side lobe level, and also lower cross-polarization, as compared with the radiation pattern at f_1 or f_0.

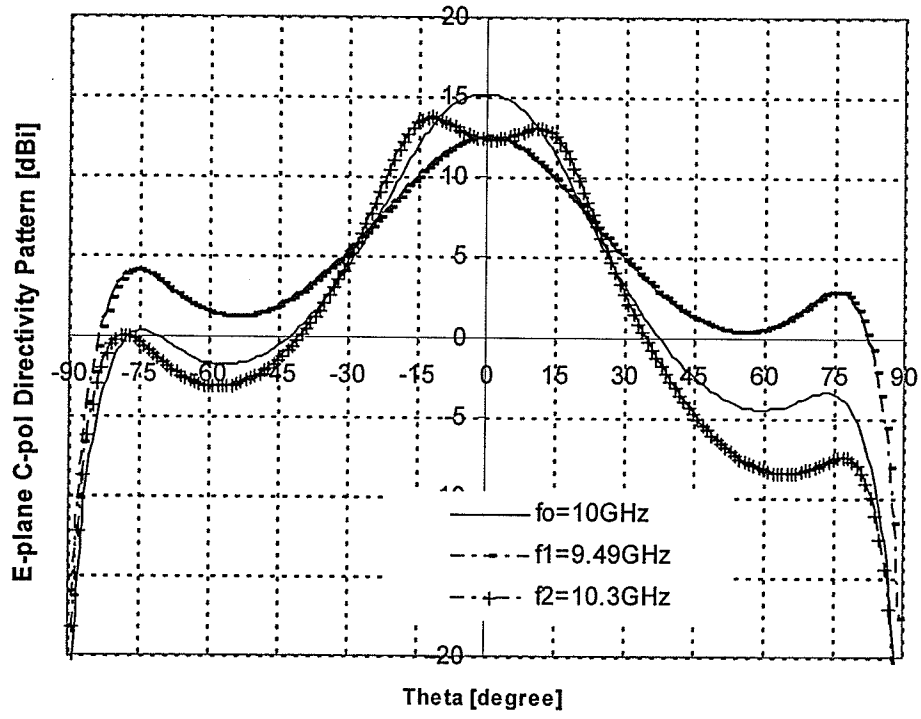
E-plane C-pol Directivity Pattern [dBi]
20
15
10
5
0
-5
-90
-75
-60
-45
-30
-15
0
15
30
45
60
75
90
fo=10GHz
f1=9.49GHz
f2=10.3GHz
Theta [degree]

(a)

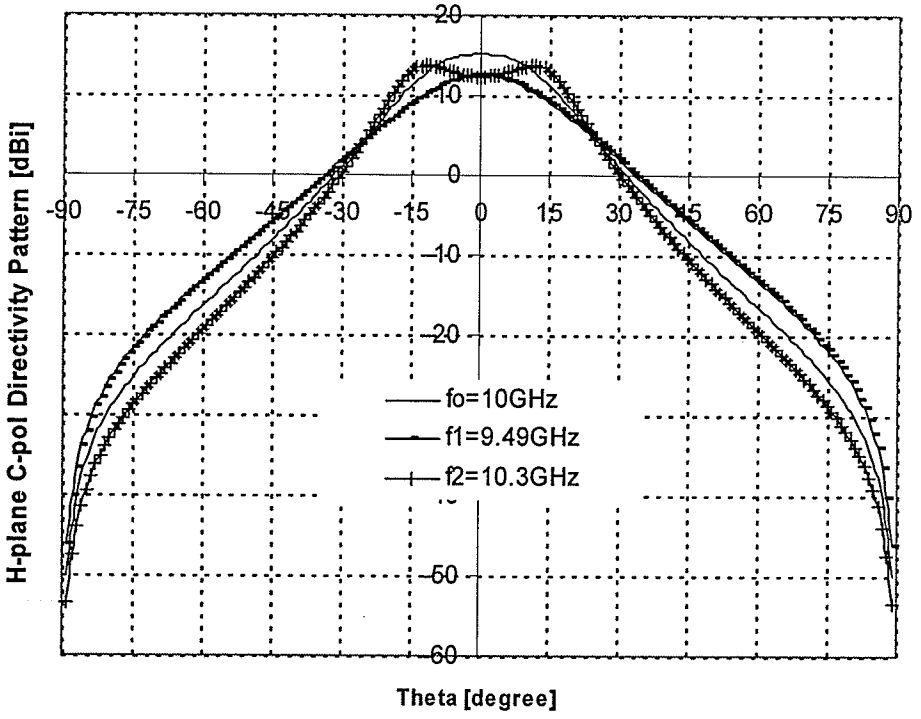
H-plane C-pol Directivity Pattern [dBi]
20
10
0
-10
-20
-60
-90
-75
-60
-45
-30
-15
0
15
30
45
60
75
90
fo=10GHz
f1=9.49GHz
f2=10.3GHz
Theta [degree]

(b)

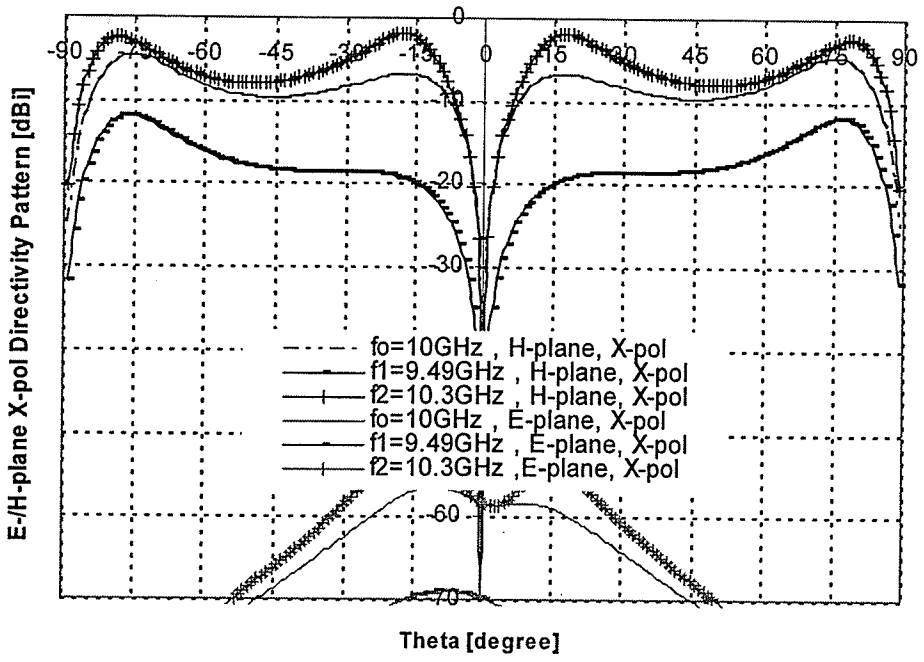

(c)

Fig.3.17 The radiation patterns for the center frequency, f_0=10GHz, and the half power frequencies, f_1=9.49GHz, and f_2=10.3GHz, a) E- plane C-pol, b) H – plane C-pol, and c) H – and E- plane X-pol, (The other parameters are listed in Table3.10)

3.5.2. Superstrate Dielectric constant Effects on Radiation Characteristic

Different superstrate relative permittivity of *9.2, 6.0, 4.5, and 3.27* are selected to investigate the broadside directivity variations with frequency for resonant superstrate thickness of $\lambda_3/4$. The air gap height has been also optimized to obtain the optimum directivity at f_0=*10 GHz.*

The broadside directivity variations with respect to frequency, in the range of *7.5 to 12.5 GHz,* are calculated and shown in *Fig.3.18.* The broadside directivity of the simple patch is also plotted as the reference.

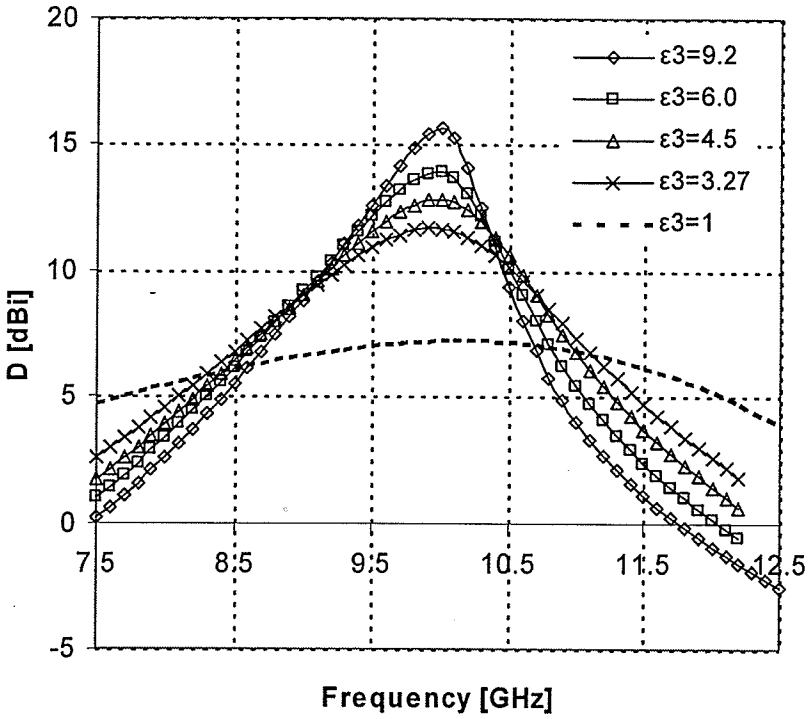

Fig.3.18. Directivity variations with frequency for various superstrate Dielectric constants (t_2=13.1mm(0.437λ_0), t_3=λ_3/4) the other parameters are listed in Table 3.1)

As it is seen from *Fig.3.18* the directivity increases with the superstrate dielectric constant; but the directivity-bandwidth decreases. The peak value of the directivity and the corresponding directivity-bandwidth for each case are summarized in *Table 3.16*. The directivity bandwidth trade-off can be observed from *Table 3.16*. It is verified that the directivity-bandwidth product is almost costant, which is predicted by the asymptotic formulas for the gain and bandwidth *[6]*. The results in *Table 3.16* show good agreement with the asymptotic formulas for the gain and bandwidth.

The radiation patterns for different superstrate dielectric constants at the directivity center frequency (f_0=10GHz) are calculated and shown in *Fig. 3.19*. The co-polarization components in the two main planes, E-plane and H-plane, are shown in *Fig.3.19(a) and (b)* respectively, and the cross-polarization components for the E- and H-planes in *(c)*. As

it can be seen from *Fig.3.19(c)*, the cross-polarization patterns are almost the same for different superstrate dielectric constants. The cross-polarization component in the E-plane is negligible, i.e. it is much lower than -30dBi. The values of beamwidths and side lobe levels are listed in *Table 3.17*. As it can be seen, the higher relative permittivity of the superstrate is, the higher directivity is, and the side lobe level is also higher.

Table 3.16 Directivity for various superstrate relative permittivities (t2=13.1mm(0.437λ_0), the other parameters are listed in Table 3.1)

ε_3	t_3 *[mm]*	*Dmax[dBi]*	*BW [GHz]*	**directivity × *BW***
Without superstrate		*7.2*	*52.3%*	*274.5*
9.2	*2.5 (0.25 λ_3)*	*15.66*	*7.8%*	*287.1*
6.0	*3.1(0.25 λ_3)*	*14.03*	*11.3%*	*285.8*
4.5	*3.5(0.25 λ_3)*	*12.98*	*14.3%*	*284*
3.27	*4.1(0.25 λ_3)*	*11.80*	*18.4%*	*278.5*

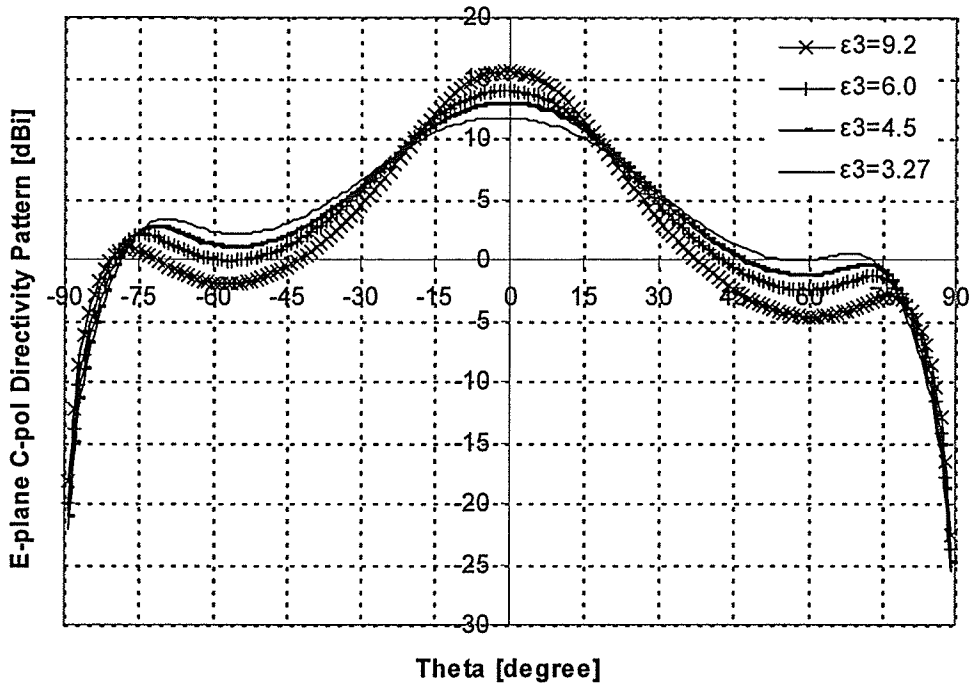
E-plane C-pol Directivity Pattern [dBi]
Theta [degree]
ε3=9.2
ε3=6.0
ε3=4.5
ε3=3.27
20
10
5
0
-5
-10
-15
-20
-25
-30
-90
-75
-60
-45
-30
-15
0
15
30
45
60
75
90

(a)

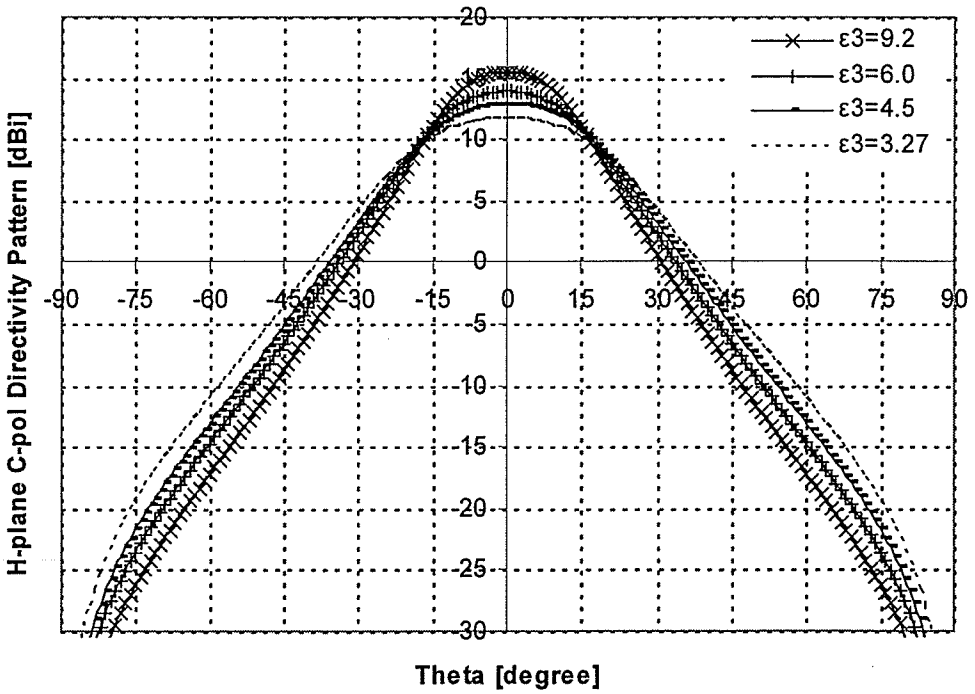
H-plane C-pol Directivity Pattern [dBi]
Theta [degree]
ε3=9.2
ε3=6.0
ε3=4.5
ε3=3.27
20
10
5
0
-5
-10
-15
-20
-25
-30
-90
-75
-60
-45
-30
-15
0
15
30
45
60
75
90

(b)

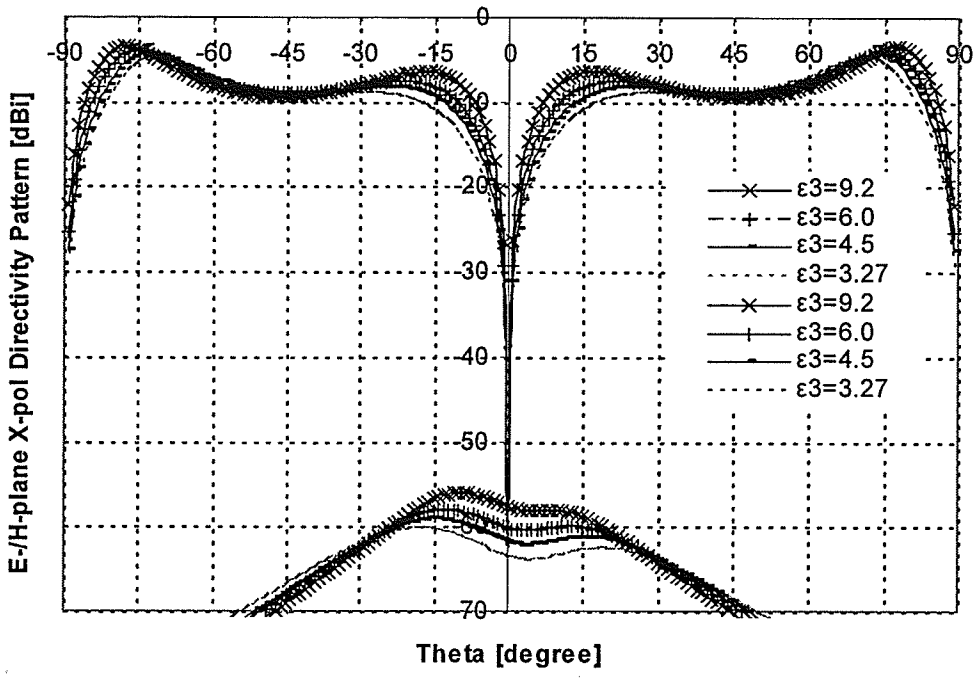

(c)

Fig.3.19. Radiation Pattern for various superstrate dielectric constants a) E-plane C-pol, b) H-plane C-pol, and c)E- and H-plane X-pol (t_2=13.1mm(0.437λ_0), t_3=λ_3/4, f_0=10GHz, the other parameters are listed in Table 3.1)

Table3.17 Beamwidths and Side Lobe Levels for various superstrate dielectric constants (t_2=13.1mm(0.437λ_0), t_3=λ_3/4, f_0=10GHz, the other parameters are listed in Table 3.1)

ε_3	Dmax[dBi]	E-planeBeamwidth	H-plane Beamwidth	E-plane SLL [dB]
uncovered	7.2	89°	76°	–
9.2	15.49	27°	25°	-14.59
6.0	13.90	32.5°	30°	-11.94
4.5	12.86	36.5°	34°	-10.19
3.27	11.68	42°	40°	-8.33

As it is expected, the narrowest beamwidth, i.e. *27° in the E-plane and 25° in the H-plane* belongs to the largest superstrate relative permittivity of $\varepsilon_3=9.2$. It should also be noticed that, as the directivity increases, the side lobe level also increases, i.e. the side lobe level of *-14.59dB* for $\varepsilon_3=9.2$, compared with the side lobe level of *-8.33dB* for $\varepsilon_3=3.27$.

3.6. Experimental Verifications

In order to confirm the simulation results, a microstrip patch antenna was designed to verify the input and the radiation characteristics of a single-superstrate configuration. The used substrate has a relative permittivity of *2.5*, thickness of *0.38 mm (0.015 inch)*, and loss tangent of $tan\delta=0.0022$, on a ground plane of *150mm* by *150mm*. The patch length and width are *11* by *15mm*, respectively, which is fed by a *50* Ω SMA probe, at *3*mm from the center of patch, along its length ($X_{feed}=-3mm$). The antenna specifications are summarized in *Table 3.18*. The superstrate with a relative permittivity of *9.8* and thickness of *3.175*mm (*0.125* inch) , and loss tangent of $tan\delta=0.002$ is placed above the patch at the height of *17.25*mm supported with plastic screws and nuts, to make the resonant gain at *8.35*GHz. It should be noted that the superstrate thickness is greater than one quarter wavelength ($t_3>\lambda_3/4$) , so it needs to be compensated by the air gap height, in order to have the maximum directivity. The superstrate thickness has not been taken equal to a quarter wavelength, i.e. the center frequency of 7.5GHz. Otherwise, less accurate results would be obtained, due to the measurement setup failure in accuracy around that frequency. The antenna was fabricated and tested in the Antenna Laboratory at the University of Manitoba.

Table.3.18 The parameters of the fabricated single-superstrate microstrip patch antenna

Layer	***Material***	***Geometry***
Superstrate	ε_r=9.8	*Thickness=3.175 mm (0.27λ_3)*
Air gap	*Air*	*Height=17.25 mm (0.48λ_0)*
Patch	*Copper*	*Rectangular 11×15 mm*
Substrate	ε_r=2.5	*Thickness=0.38 mm*
Ground Plane	*Copper*	*150×150mm*
Feed	*Coaxial Probe*	*X_f=-3 mm, Y_f=0 mm (location from the center of patch)*

The antenna return loss variations with respect to frequency was measured by ANRITSU ME 7808A Network Analyzer and is shown in *Fig.3.20*. The simulated return loss variations, with respect to frequency, were also computed by Ansoft Designer simulator, which is shown for comparison. It can be seen that the measured results agree well with the simulated results, though there are ripples in the measured results. They may be the result of, yet un-radiated, power of the guided waves diffractions from the finite superstrate and ground plane edges. The radiation characteristics of the fabricated single-superstrate microstrip patch antenna were measured in the anechoic chamber of the Antenna Laboratory at the University of Manitoba. The measurement set up for measuring far electric field is as follows. The fabricated antenna under the test, as a receiving antenna, is situated at the origin of the coordinates. The patterns of θ and φ components of the electric field (E_θ and $E\varphi$) are measured as a function of θ along φ=0° and 90° plane. These patterns are determined by rotating the antenna under the test, when illuminated by the plane wave from the Compact Antenna Range.

Its broadside gain variations with frequency are shown in Fig.3.21. As it can be seen from Fig.3.21, the measured results agree well with the simulated results. As expected the broadside gain rises slowly with frequency, reaching its peak at the resonant frequency and falls off much more rapidly for $f>f_0$ than for $f<f_0$. This is due to the fact that, for $f<f_0$, the pattern merely broadens as the gain drops. However, for $f>f_0$, the pattern broadens slightly and the chief effect is that the pattern is scanned so that the main beam peak is not at $\theta=0$, but rather a dip appears at the broadside [6].

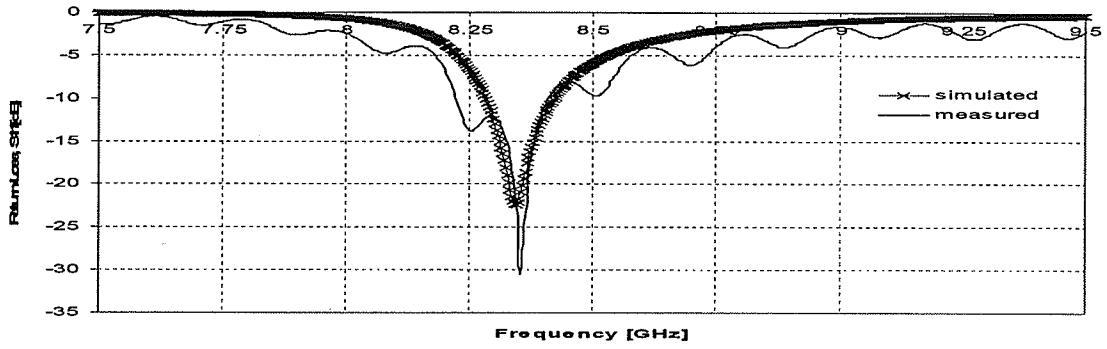

Fig.3.20. The measured and simulated return losses for single superstrate microstrip patch antenna (The parameters are listed in Table 3.18, f=8.35GHz),

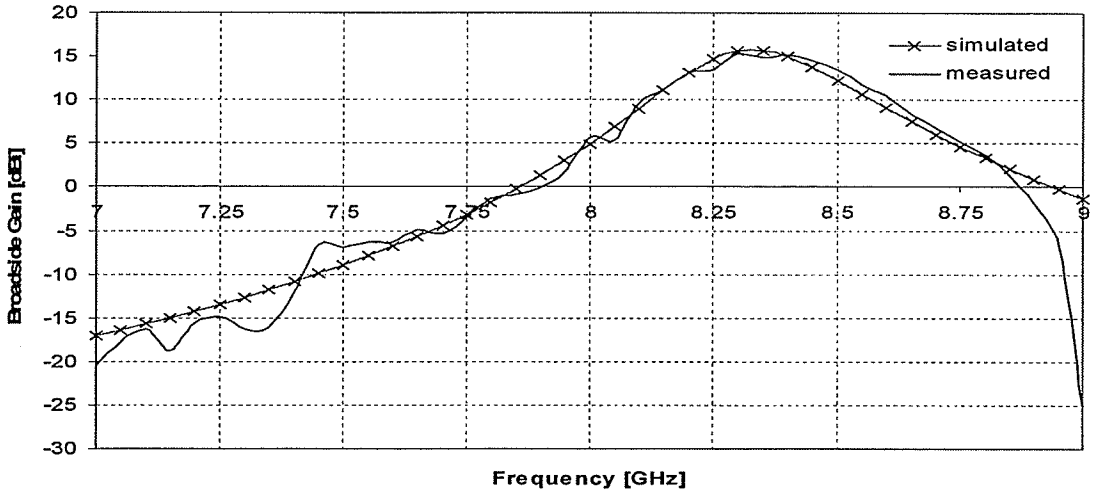

Fig.3.21 The measured and simulated gain variations with frequency for single superstrate microstrip patch antenna (The parameters are listed in Table 3.18, f=8.35GHz)

Next, the (return loss=-10dB) impedance bandwidth and (-3dB power) gain bandwidth, extracted from the measured results, are compared with simulations. These results are listed in *Table3.19*.

Table.3.19 Comparison of the measured and simulated impedance-bandwidth and gain-bandwidth for the single superstrate microstrip patch antenna (The parameters are listed in Table 3.18, f_0=8.35GHz)

Impedance-BW[GHz]		*Gain-BW[GHz]*		*D [dBi]*	
measured	***Simulated***	***measured***	***Simulated***	***measured***	***Simulated***
0.19(2.3%)	***0.14(1.7%)***	***0.36(4.3%)***	***0.29(3.5%)***	***15.25***	***15.91***

The simulated results agree well with the measured results. The measured gain is 0.66dBi less than the simulated one. The measured gain-bandwidth is wider than the simulated gain-bandwidth. This could be due to the smaller measured gain. The difference could be also due to error happens in reading from the measured results which distorted by ripples. It is interesting to note that the impedance-bandwidth can be improved, but the only way to increase the directivity-bandwidth is to lower the directivity. The radiation patterns in the two main planes are investigated next. In Fig.3.22, the comparison of the simulated and measured gain patterns of the antenna at 8.35GHz is shown. As it can be seen from *Fig.3.22(a)*, the measured and the simulated co-polarization components are quite similar, except for the nulls observed in the measured H-plane co-polarization plot at $\theta = -50^\circ$ and $+66^\circ$. This could be due to the finite transverse size of superstrate. The measured pattern also shows asymmetry compared with the simulated one. This could be mostly due to the fact that the simulator

assumes a perfect even and parallel surface for superstrate, which is not so in practice. For the cross-polarization components in *Fig.3.22(b)*, there are differences between the simulation and measurement. Some part of them is due to misalignment. However, the power level of the pattern (<-20dBi) is also about the noise level of the measuring equipments.

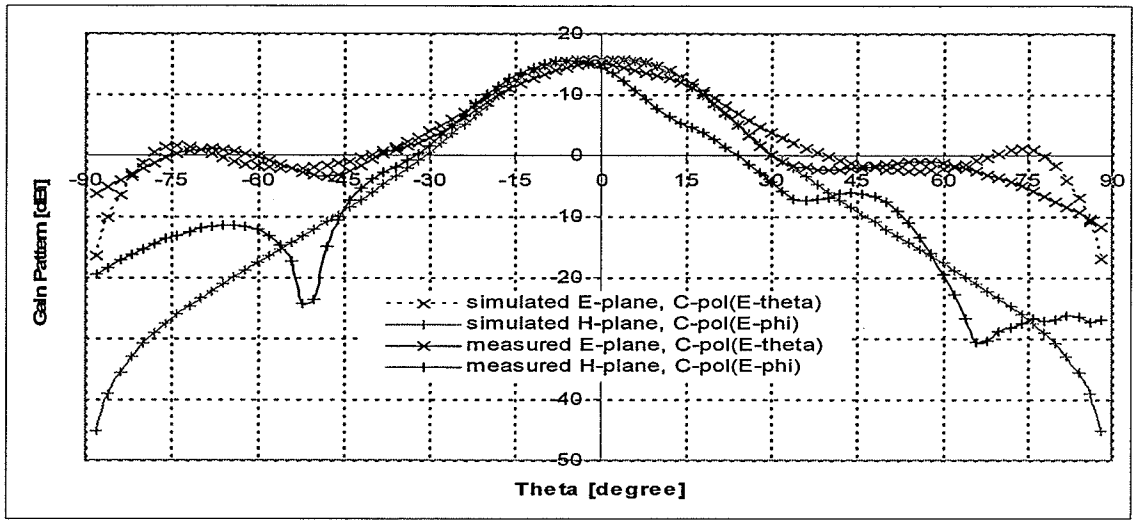

(a)

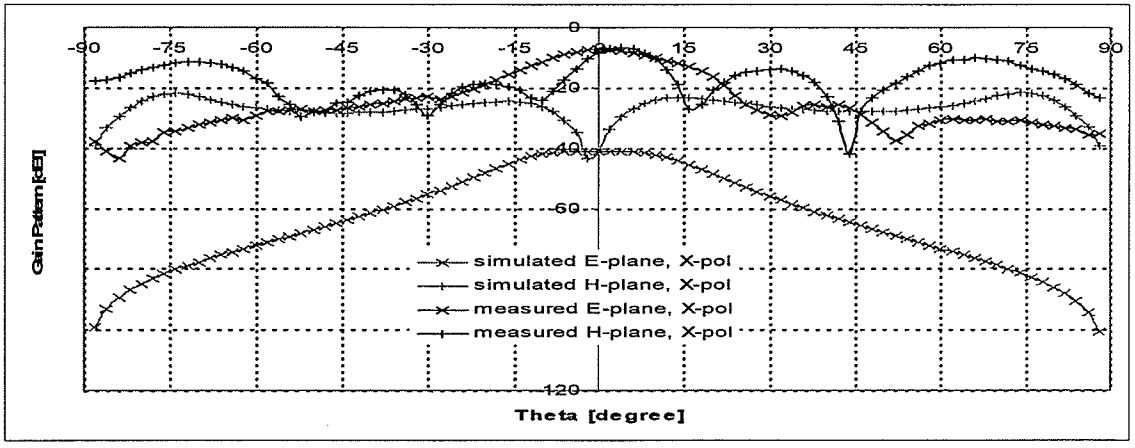

(b)

Fig.3.22 Comparison of the simulated and measured Radiation Patterns a) Co-polarization components in E- and H-plane and b) cross-polarization components in E- and H-plane (The parameters are listed in Table3.18, f=8.35 GHz)

3.7 Summary

In this chapter, the single-superstrate configuration was studied. First, the effects of superstrate parameters on the input impedance and directivity were investigated. Then, the substrate effects on input impedance and directivity were studied. Since fabrication deviation, from the design specifications and material tolerances, are inevitable, acceptable tolerances were also investigated. Besides, the radiation characteristic in both frequency- and spatial-domain was presented. For the single-superstrate microstrip patch antenna it was shown:

- The superstrate narrows the impedance bandwidth and also shifts the impedance response to lower frequencies, depending on its thickness and dielectric constant
- The directivity is optimum (D_{opt}), in the case where superstrate thickness is one quarter wavelength. The directivity is almost linearly proportional to the superstrate dielectric constant, and the air gap height offsets the substrate thickness, that is, the air gap height is a function of the substrate thickness, in order to maximize the directivity
- In case the superstrate thickness is different from one quarter wavelength, the air gap height can offset the superstrate thickness, in order to maximize the directivity (but the directivity is less than D_{opt})
- It is verified that the asymptotic formula underestimate the gain, but as superstrate dielectric constant becomes large, the asymptotic formula overestimate the gain
- The superstrate affects on the input impedance increases as the substrate thickness increases

- The deviations of the superstrate thickness and air gap height affect the directivity similarly
- There is little correlation between the return loss center frequency and the directivity center frequency
- The directivity frequency response is almost invariant, when the superstrate thickness deviation offset by the air gap height
- The radiation pattern is almost invariant when the superstrate thickness deviation is offset by the air gap height
- At lower -3dB (half power) frequency, the cross-polarization component is lower, and its side lobe level is smaller, compared to the higher -3dB frequency.
- The simulated and measured results of the antenna for its input impedance, bandwidths and radiation patterns were compared, and showed good agreements. The measured impedance bandwidth and directivity of this antenna was 2.3% and 15.25dBi, respectively at 8.35GHz.

Chapter 4

Multiple-superstrate configuration

Introduction The structure of this chapter is almost the same as the preceding chapter. It studies characteristics of multiple-superstrates over a microstrip patch antenna. Obtaining large resonant directivity with moderate dielectric constants is the main impetus for this multiple-superstrate configuration study.

As the main objective of this thesis is enhancing the directivity of microstrip patch antennas, the relation between directivity and multiple superstrates is investigated first, searching for increasing directivity. The effects on the input impedance are discussed, including different multiple-superstrate configurations with the same level of directivity. These configurations are compared with the single-superstrate configuration. After computing the tolerances due to the superstrate parameters deviations, the radiation characteristics of multiple-superstrate microstrip patch antennas, in the spatial- and frequency domains are studied. Their radiation characteristics are also compared with those of the single-superstrate configuration. A prototype antenna with double-superstrate configuration is fabricated and its characteristics are measured. The simulated and measured results of the antenna, for the impedance bandwidth, gain-bandwidth, and radiation pattern are compared. They show reasonably good agreement. The measured directivity of this antenna is 15.8 dBi, with the gain bandwidth of 7%, and the impedance bandwidth of 1.8% at 13.64GHz.

4.1. The Effects of multiple superstrates on Directivity

A double-superstrate configuration can be easily made by adding another superstrate in parallel to and above the first one, as shown in *Fig.4.1.*

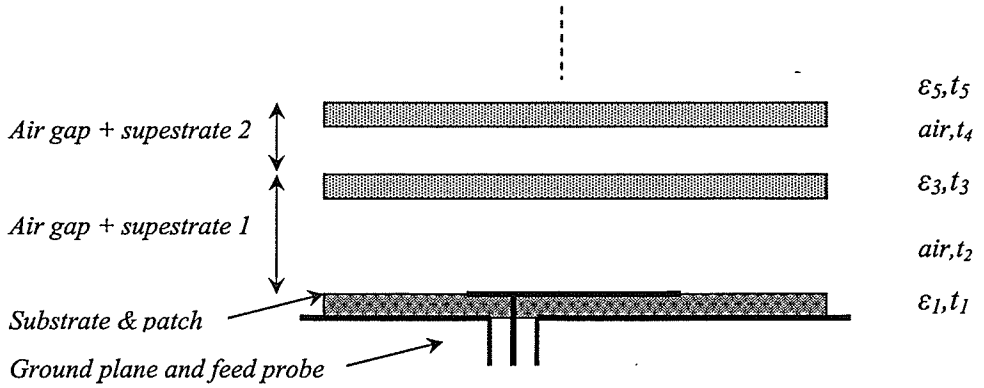

Fig.4.1. The structure of Multiple-Superstrate Microstrip Patch Antennas (ε_i, t_i is each layer dielectric constant and thickness, respectively)

This chapter is mostly devoted to the case of double-superstrate configuration. The three superstrates case is also considered in this chapter. The dielectric layers are placed above each other with odd number of indices, while the air gaps in between with even number of indices. It is expected that a higher directivity can be obtained by adding another superstrate. To investigate this, a microstrip patch antenna with a single-superstrate is considered, first. The parameters of the single-superstrate configuration are listed in *Table 4.1.* Its directivity with the superstrate relative permittivity of 3 (ε_3=3) is 11.50dBi, at 10 GHz. After adding another superstrate with a relative permittivity of 3 (ε_5=3), the broadside directivity is computed with respect to the inter-superstrate height variations (t_4), for different superstrate thicknesses (t5) of 3.46mm ($0.2\lambda_5$), 4.33mm ($0.25\lambda_5$),and 5.2mm ($0.3\lambda_5$). The results are shown in *Fig.4.2.*

Table.4.1 The parameters of the single-superstrate configuration for studying the properties of multiple-superstrate configuration

Layer	***Material***	***Geometry***
Superstrate	ε_{r5}=3	Thickness=4.33 mm ($0.25\lambda_3$)
Air gap	Air	Height=12.9 mm ($0.43\lambda_0$)
Patch	Copper	Rectangular 9.1×12 mm
Substrate	ε_r=2.2	Thickness=1.575 mm
Ground Plane	Copper	Infinite
Feed	Coaxial Probe	X_f=-2.8 mm, Y_f=0 mm (location from the center of patch)

As it is seen from Fig.4.2, the directivity rises with the inter-superstrate height t_4 and reaches its maximum at certain optimum height t_{4r}, and falls thereafter much similar to

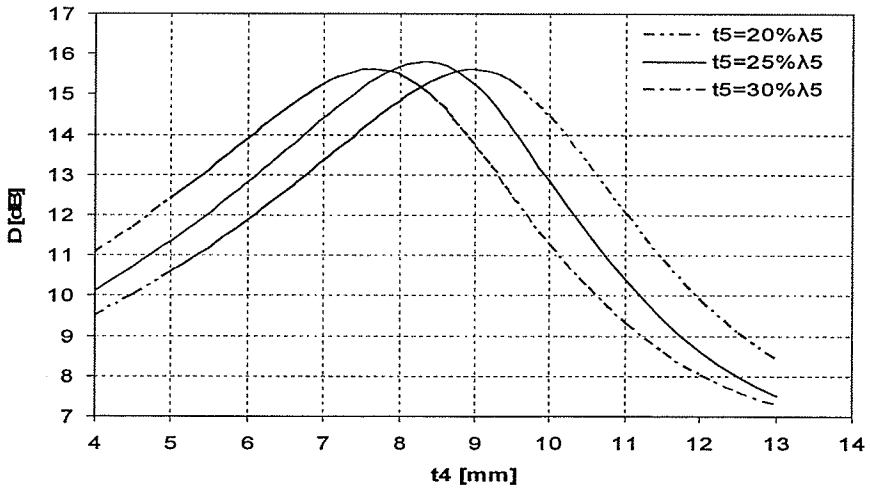

Fig.4.2. Directivity variation with inter-superstrate height t_4 for a double-superstrate configuration, with different superstrate thicknesses (ε_{5}=3, f_0=10GHz, the other parameters are listed in Table 4.1)

the single superstrate case. Again, the optimum superstrate thickness of $0.25\lambda_5$ is observed, which resembles the resonant mode in the T-line model derived in [14]. In order to verify the optimum thickness of one quarter wavelength for the superstrate further, the directivity over a range of thicknesses in steps of one hundredth of wavelength are calculated and summarized in *Table.4.2*. It should be noticed that the resonant thickness for the second superstrate agrees with the T-lines model for the embedded Herzian dipole [15], but the resonant air gap height does not agree with that model, i.e. t_{4r} is not equal to $0.25\lambda_0$.

Table 4.2 Maximum directivity for a double-superstrate configuration with different superstrate thicknesses (ε_5=3, f_0=10GHz, the other parameters are listed in Table4.1)

t_5 [mm]	t_4 [mm]	D [dBi]
3.98($0.23\lambda_5$)	8.58($0.286\lambda_0$)	15.77
4.15($0.24\ \lambda_5$)	8.49($0.283\lambda_0$)	15.79
4.33($0.25\ \lambda_5$)	*8.28($0.276\lambda_0$)*	*15.8*
4.5($0.26\ \lambda_5$)	8.19($0.273\lambda_0$)	15.79
4.68($0.27\ \lambda_5$)	8.1($0.27\lambda_0$)	15.77

Extending the asymptotic gain formula [6], the directivity of the double-superstrate configuration may also vary proportionally with the second superstrate dielectric constant. In other words, the directivity for a double-superstrate may be proportional to

ε_5, as well as ε_3. This hypothesis can be simply verified by comparing the directivity of the single-superstrate microstrip patch antenna with a double-superstrate microstrip patch antenna when,

$$\varepsilon_{3DS} \times \varepsilon_{5DS} = \varepsilon_{3SS} \tag{4.1}$$

where,

ε_{3DS}: first superstrate relative permittivity in a double-superstrate configuration

ε_{5DS}: second superstrate relative permittivity in a double-superstrate configuration

ε_{3SS}: superstrate relative permittivity in a single-superstrate configuration.

For ε_{3SS}=9 and $\varepsilon_{3DS} = \varepsilon_{3DS}$ =3, the directivity variations with respect to t_2-t_{2r} and t_4-t_{4r}, respectively, are calculated and shown in Fig.4.3.

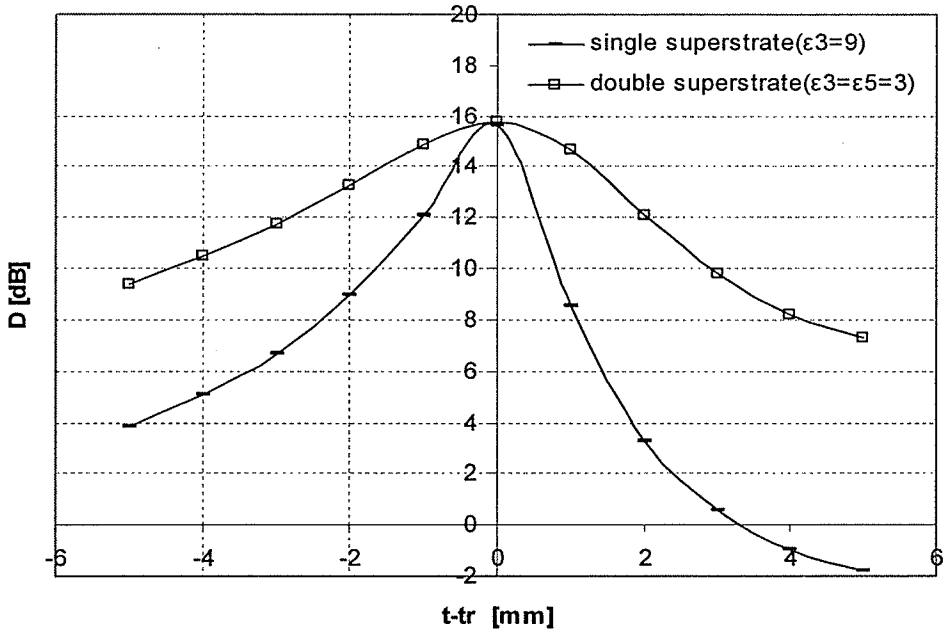

Fig.4.3. Directivity variations for single- and double-superstrate configurations with t_2-t_{2r} and t_4-t_{4r}, respectively (f_0=10GHz, the other parameters are listed in Tables 4.1 and 4.3)

As it is seen from Fig.4.3 the maximum directivities are equal, but the directivity variation is flatter in the double-superstrate configuration, since the directivity for the single-superstrate configuration has been plotted with respect to t_2, while the directivity for the double-superstrate configuration has been plotted with respect to t_4, while the lower air gap height (t_2) affects directivity more, as it will be discussed in section 4.4. The maximum directivities and the relevant parameters are summarized in Table 4.3 for comparison.

Table 4.3 Comparison of the directivities for single-superstrate (ε_3=9) and double-superstrate (ε_3= ε_5=3) configurations (f_0=10GHz, the other parameters are listed in Table 4.1)

Layer relative permittivity and thickness (mm)	***D [dBi]***
ε_2=1, t_2=13.15(0.44λ_0) ε_3= 9, t_3=2.5(0.25λ_3)	*15.63*
ε_2= ε_4=1, t_2=12.9(0.44λ_0), t_4=8.3(0.27λ_0) ε_3= ε_5=3, t_3=4.33(0.25λ_3), t_5=4.33(0.25λ_5)	*15.8*

In order to verify this hypothesis further, the directivities of a single-superstrate configuration with relative permittivity of ε_3=27 and a triple-superstrate configuration with relative permittivities of 3, i.e. ε_3= ε_5=ε_7=3, are calculated. The directivity variations with respect to the superstrate height are shown in *Fig.4.4*. As it is seen the maximum directivities are almost equal, but the directivity variation is much flatter in the triple-superstrate configuration. This is already expected, since in the single-superstrate case,

there is only one parameter, which is its thickness, but in the triple-superstrate case there are five corresponding parameters, which are the three thicknesses of superstrates and the two spacings between them.

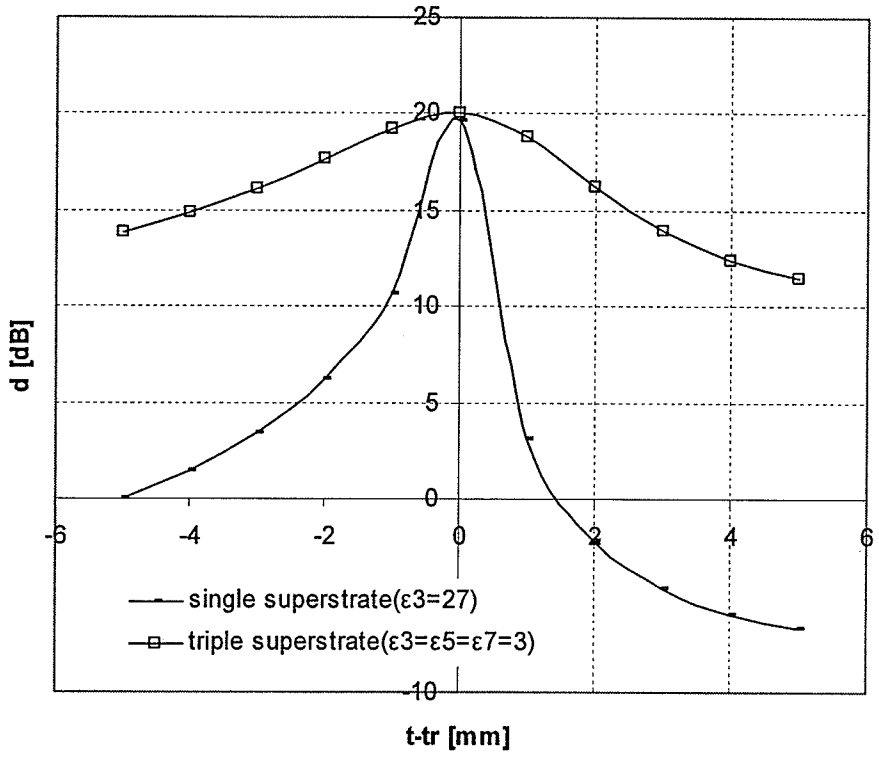

Fig.4.4. Directivity variations for single- and triple-superstrate configurations with t_2-t_{2r} and t_6-t_{6r}, respectively (f_0=10GHz, the other parameters are listed in Tables 4.1 and 4.4)

Thus, changing the height of one superstrate, and keeping the two other parameters optimum, does not affect the directivity as severely as the height of a single superstrate. The relevant parameters are summarized in *Table 4.4* for comparison. In conclusion, the results from *Tables 4.3* and *4.4* confirm the hypothesis that the directivity of multiple-

superstrate microstrip patch antennas is proportional to the relative permittivity of each superstrate layer.

Table 4.4 Comparison of the directivities between the single-superstrate (ε_3=27) and triple-superstrate (ε_3= ε_5= ε_7=3) configurations (f_0=10GHz, the other parameters are listed in Table 4.1)

Layer relative permittivity and thickness (mm)	***D [dBi]***
ε_2=1, t_2=13.28(0.44λ_0) ε_3=27, t_3=1.44(0.25λ_3)	19.89
ε_2=1, t_2=12.9(0.44λ_0) ε_3=3, t_3=4.33(0.25λ_3) ε_4=1, t_4=8.3(0.27λ_0) ε_5=3, t_5=4.33(0.25λ_5) ε_6=1, t_6=8.43(0.28λ_0) ε_7=3, t_7=4.33(0.25λ_7)	20.08

4.2. The Input Impedance of Multiple-Superstrate Configurations

In this section, the effects of higher superstrates on the input impedance will be investigated. The importance of this section is due to the fact that superstrate effects on the impedance bandwidth can be lowered in the multiple-superstrate configuration, while the directivity is maintained constant. For this purpose the examples of the previous section can be used. They are the single-superstrate cases with relative permittivities of 9 and 27, a double-superstrate case with relative permittivities of 3, and a triple-superstrate

case with relative permittivities of 3. Considering the single- and the double-superstrate configurations with similar directivities, variations of the input resistance with respect to frequency are calculated and shown in *Fig.4.5* for comparison.

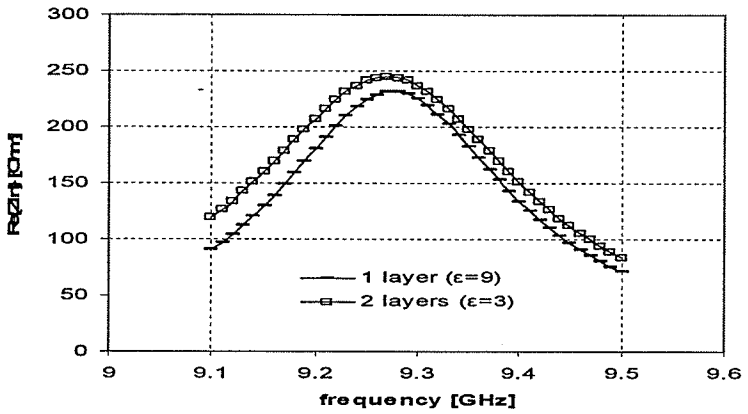

Fig.4.5. Variations of the input resistance with frequency for single- and double-superstrate configurations with similar directivities (the other parameters are listed in Tables 4.1 and 4.3)

Fig.4.6 shows the variations of the input resistance for single-superstrate (ε_3=27) and triple-superstrate (ε_3=ε_5= ε_7=3) configurations, having the same level of directivities.

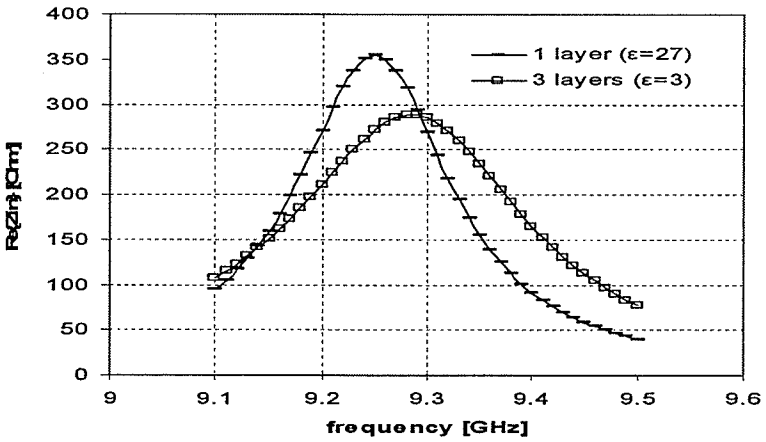

Fig. 4.6 Variations of the input resistance with frequency for single- and triple-superstrate configurations with similar directivities (the other parameters are listed in Tables 4.1 and 4.4)

Defining the impedance bandwidth as:

$$\frac{\Delta f_{0.69Rr}}{f_r} = \frac{(f_2 - f_1)|_{Rin=0.69Rr}}{f_r} \qquad (4.2)$$

the center frequencies (f_0) , peak input resistances (R_r), and the bandwidths (BW) are summarized in *Table4.5* and *4.6* ,respectively.

Tables 4.5 Comparison of the input resistance characteristics for single-superstrate (ε_3=9) and double-superstrate (ε_3= ε_5=3) configurations with similar directivities (the other parameters are listed in Table 4.1)

Layer relative permittivity and thickness (mm)	***f_0[GHz]***	***R_r[Ohm]***	***BW[GHz]***	***D[dBi]***
ε_2=1, t_2=13.15(0.44λ_0) ε_3= 9, t_3=2.5(0.25λ_3)	9.27	301	0.19(2%)	15.63
ε_2= ε_4=1, t_2=12.9(0.44λ_0), t_4=8.3(0.27λ_0) ε_3= ε_5=3, t_3=4.33(0.25λ_3), t_5=4.33(0.25λ_5)	9.27	245	0.22(2.4%)	15.8

As it can be seen the impedance bandwidth for a single-superstrate shows about 15% improvement, Table 4.5, and 50% improvement, Table 4.6, for the double- and triple-superstrate configurations, respectively, while their directivities are maintained the same.

Tables 4.6 Comparison of the input resistance characteristics for single-superstrate (ε_3=27) and triple-superstrate (ε_3= ε_5= ε_7=3) configurations with similar directivity (the other parameters are listed in Table4.1)

Layer relative permittivity and thickness (mm)	***f_0[GHz]***	***R_r[Ohm]***	***BW[GHz]***	***D [dBi]***
ε_2=1, t_2=13.28(0.44λ_0) ε_3=27, t_3=1.44(0.25λ_3)	9.25	462	0.12(1.3%)	19.89
ε_2=1, t_2=12.9(0.44λ_0) ε_3=3, t_3=4.33(0.25λ_3) ε_4=1, t_4=8.3(0.27λ_0) ε_5=3, t_5=4.33(0.25λ_5) ε_6=1, t_6=8.43(0.28λ_0) ε_7=3, t_7=4.33(0.25λ_7)	9.29	289	0.18(1.9%)	20.08

Attempting to increase the impedance bandwidth further, a modified multiple-superstrate configuration was devised. As it will be shown, deploying superstrate layers in ascending order of dielectric constants will increase the impedance bandwidth further. In order to verify this, two double-superstrate configurations are considered, while keeping their directivities are the same. For this purpose, a double-superstrate configuration with superstrate relative permittivity of 3 (ε_3=3, ε_5=3), and the modified double-superstrate configuration with the superstrates relative permittivity of 1.5 and 6 (ε_3=1.5, ε_5=6) are considered. The calculated directivity of the modified double-

superstrate configuration is 16.15dBi which is comparable to 15.8dBi of the conventional double-superstrate configuration ($\varepsilon_3=3$, $\varepsilon_5=3$). The variations of input resistance with respect to frequency are calculated and shown in *Fig.4.7*.

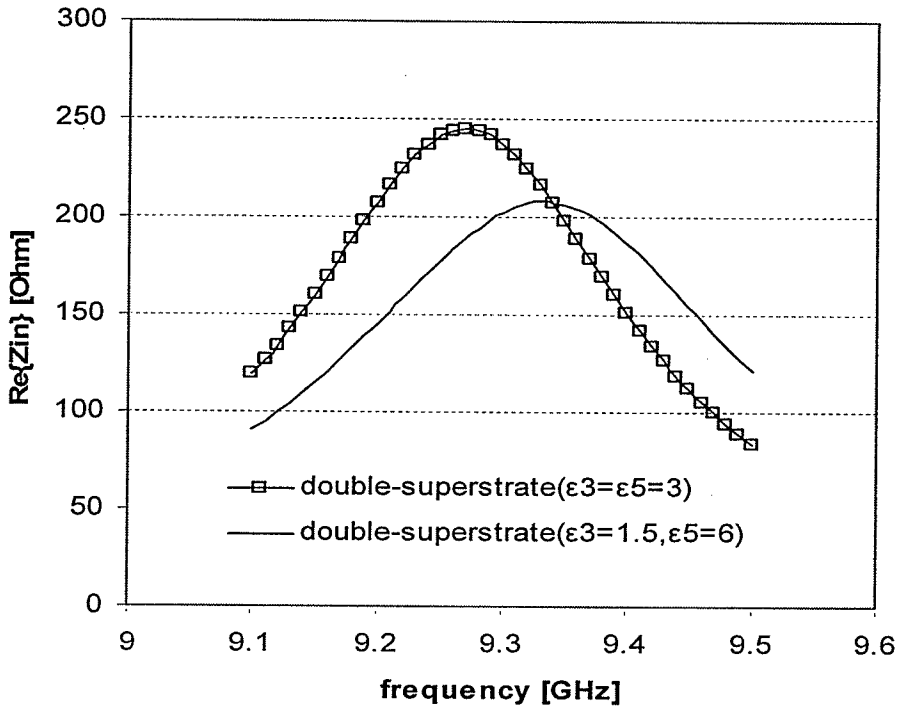

Fig.4.7 Variation of input resistance with frequency for double-superstrate and modified double-superstrate configurations with similar directivities (the other parameters are listed in Tables 4.1 and 4.7)

The center frequencies (f_0), peak input resistances (R_r), and the bandwidths ($0.69R_r$) are summarized in *Table4.7* for comparison. As it is seen, the impedance bandwidth has been improved by the modified double-superstrate configuration. This can be easily explained. Placing the layer with a low dielectric constant above the patch hardly affects the impedance bandwidth, this is equivalent to placing the high dielectric constant superstrate away from the patch, which also minimizes its effect on the impedance bandwidth little, while the resonant directivity is kept unchanged.

Tables 4.7 Bandwidth improvement by Modified multiple-superstrate(ε_3=1.5, ε_5=6) in comparison with the conventional double-superstrate(ε_3= ε_5=3) configuration (the other parameters are listed in Table 4.1)

Layer relative permittivity and thickness (mm)	*f_0[GHz]*	*R_r[Ohm]*	*BW[GHz]*	*D [dBi]*
ε_2=1, t_2=12.9(0.44λ_0) ε_3=3, t_3=4.33(0.25λ_3) ε_2=1, t_4=8.3(0.27λ_0) ε_5=3, t_5=4.33(0.25λ_5)	9.27	245	0.22(2.4%)	15.8
ε_2=1, t_2=12.6(0.42λ_0) ε_3=1.5, t_3=6.12(0.25λ_3) ε_4=1, t_4=8.4(0.28λ_0) ε_5=6, t_5=3.06(0.25λ_5)	9.33	208	0.27(2.9%)	16.15

As it can be seen from Table 4.7, about 20% bandwidth improvement has been obtained, while the directivity also shows 0.35dB increment.

4.3. Tolerance Analysis

In this section the directivity variations due to the deviation in the superstrate parameters for multiple-superstrate configurations are studied. Here, a triple-superstrate configuration is considered and its directivity variations with respect to the lower, middle, and top superstrate layer parameters deviations are investigated. For this purpose the triple-superstrate configuration considered in section 4.1 is used again. Changing the

superstrate thicknesses over the range of ±0.25 of the designed value, i.e. $\lambda_0 / 4\sqrt{\varepsilon_i}$ for each superstrate layer, the directivities are calculated and shown in *Fig. 4.8*.

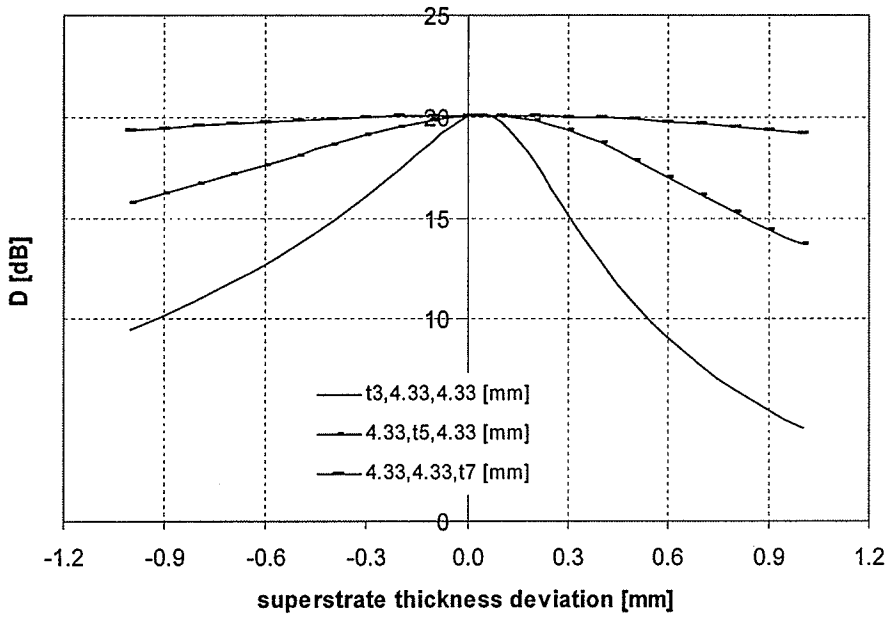

Fig. 4.8 Directivity variations due to the thickness deviations for the lower, middle, and top superstrate layers in the triple-superstrate configuration (the parameters are listed in Tables 4.1 and 4.4)

As it can be seen from *Fig. 4.8*, the directivity is least sensitive to the top superstrate thickness deviations, and is most sensitive to the lower superstrate layer thickness variations. The peak directivity differences from the optimum directivity for a ±25% thickness deviation are summarized in *Table 4.8*.

Table 4.8 Comparison of directivity differences from the optimum directivity due to superstrates thickness deviation of ±0.25 for lower, middle, and top superstrate layers in the triple-superstrate configuration(the other parameters are listed in Tables 4.1 and 4.4)

Layer thickness deviation[%]	***Directivity deviation[dB%]***
Δt_7=+0.25	-4%
Δt_7=—0.25	-4%
Δt_5=+0.25	-32%
Δt_5= —0.25	-23%
Δt_3=+0.25	-77%
Δt_3= —0.25	-56%

As it can be seen from Table 4.8, the directivity is affected the most by the thickness deviation of the lowest superstrate, and vice versa. For the positive superstrate thickness deviations, the directivity is reduced more, due to the formation of a dip at the broadside [6], i.e. the peak of the directivity is scanned off the broadside direction, and the radiation pattern becomes conical in shape.

For the superstrate dielectric constant deviation, regarding different superstrate layers, the directivity variations are also calculated, in a similar way. For this purpose, the superstrate dielectric constant deviation of ±10% is considered for a specified layer,

while the parameters of the other layers are kept unchanged. The results are listed in *Table.4.9.*

Again, it is seen that the lowest layer dielectric constant deviation has the most impact on the directivity. It is interesting to note that for a +10% deviation in ε_5 and ε_7, a higher gain is observed. These layers must be still in resonance, since their dielectric constant increment gives a higher directivity. It should be also noted that a 10% deviation is far beyond the maximum tolerances of high quality materials, which are a few percent at most.

Table 4.9 Comparison of directivity differences from the optimum directivity due to superstrates dielectric constant deviation of 10% for lower, middle, and top layers in a triple-superstrate configuration (the other parameters are listed in Tables 4.1 and 4.4)

Dielectric constant deviation[%]	*Directivity deviation[dB%]*
$\Delta\varepsilon_3 = -10\%$	-11%
$\Delta\varepsilon_5 = -10\%$	-3.6%
$\Delta\varepsilon_7 = -10\%$	-2.1%
$\Delta\varepsilon_3 = +10\%$	-11%
$\Delta\varepsilon_5 = +10\%$	$+0.4\%$
$\Delta\varepsilon_7 = +10\%$	$+1.7\%$

4.4. Radiation Characteristic of multiple-superstrate configuration

In order to investigate systematically the radiation characteristics of different multiple-superstrate configurations, the following conditions are set;

1. The air gap heights are optimum in order to maximize the directivity ($t_i=t_{ri}$, i=2,4,..)
2. The superstrates are one quarter wavelength in thickness ($t_i=\lambda_i/4$, i=3,5,..)
3. $\varepsilon_{3SS} = \varepsilon_{3DS1} \times \varepsilon_{5DS1} = \varepsilon_{3DS2} \times \varepsilon_{5DS2}$, that is the product of superstrates relative permittivities are equal, where '*SS*' stands for a single-superstrate configuration, '*DS1*' stands for the first double-superstrate configuration, and '*DS2*' stands for the second double-superstrate configuration.

By meeting these conditions, the directivity is kept almost equal among different configurations. This is accomplished by the last condition, while the two first conditions provide the optimum directivity. The multiple-superstrate configurations studied thus far can be used for this purpose. The frequency- and spatial-domain radiation characteristics are calculated and compared between multiple-superstrate configurations and the single-superstrate case, with a similar directivity. In the first part, the broadside directivity with respect to frequency is studied. The directivity bandwidths are also presented for comparison. After learning the frequency behaviour of the broadside directivity, the radiation patterns for the center frequency and -3dB (half power gain) frequencies are studied next.

The double-superstrate configurations with superstrate relative permittivities of $\varepsilon_3=\varepsilon_5=3$, and $\varepsilon_3=1.5$, $\varepsilon_5=6$, respectively for the conventional and modified one, and the

single-superstrate configuration with a relative permittivity of 9 are considered all together. The broadside directivities are calculated with respect to frequency and shown in *Fig.4.9.*

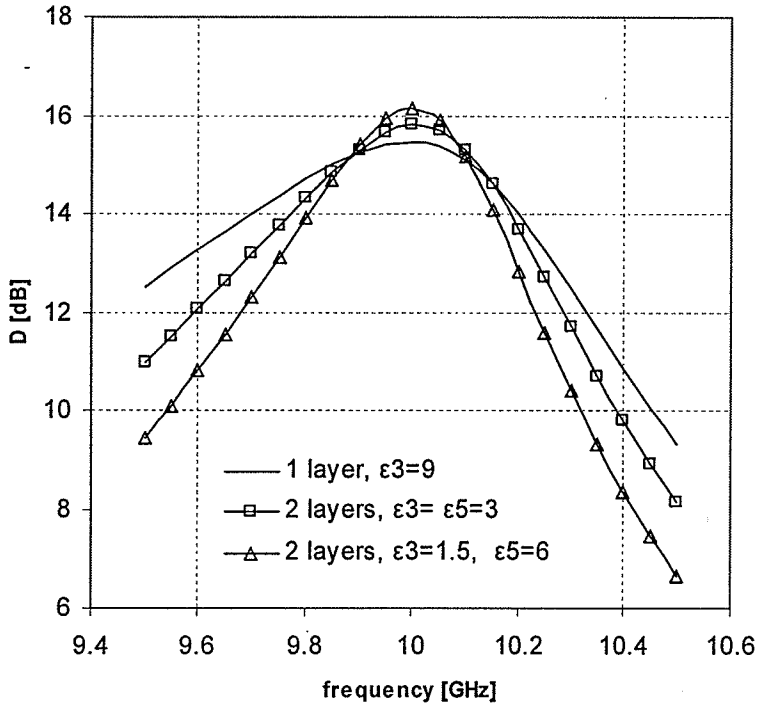

Fig.4.9 Directivity variations with frequency for single-superstrate, conventional double-superstrate, and modified double-superstrate configurations (the parameters are listed in Tables 4.1, 4.3, and 4.7)

It is seen that the single-superstrate configuration has the widest directivity bandwidth and the modified double-superstrate configuration has the narrowest. The directivity at the center frequency and the directivity bandwidth are summarized in *Table 4.10.* The directivity bandwidth of the modified double-superstrate configuration is the narrowest. However, considering both the directivity-bandwidth and impedance- bandwidth, the modified double-superstrate configuration provides a wider bandwidth compared with the

conventional double-superstrate configuration, since the impedance bandwidth is still more restrictive, Table 4.7.

Table 4.10 Comparison of the directivity bandwidth for single-superstrate (ε_3=9), conventional double-superstrate (ε_3= ε_5=3), and modified double-superstrate (ε_3=1.5, ε_5=6) configurations (f_0=10GHz, the other parameters are listed in Table 4.1)

Layer relative permittivity and thickness (mm)	*D [dB]*	*BW[GHz]*
ε_2=1, t_2=13.15(0.44λ_0) ε_3=9, t_3=2.5(0.25λ_3)	15.63	0.798(7.98%)
ε_2=1, t_2=12.9(0.44λ_0) ε_3=3, t_3=4.33(0.25λ_3) ε_2=1, t_4=8.3(0.27λ_0) ε_5=3, t_5=4.33(0.25λ_5)	15.80	0.577(5.77%)
ε_2=1, t_2=12.6(0.42λ_0) ε_3=1.5, t_3=6.12(0.25λ_3) ε_4=1, t_4=8.4(0.28λ_0) ε_5=6, t_5=3.06(0.25λ_5)	16.15	0.435(4.35%)

The directivity of these configurations in the E-plane and H-plane are calculated and shown in Fig.4.10 (a) and (b), respectively. As it can be seen, the E-plane co-polarization

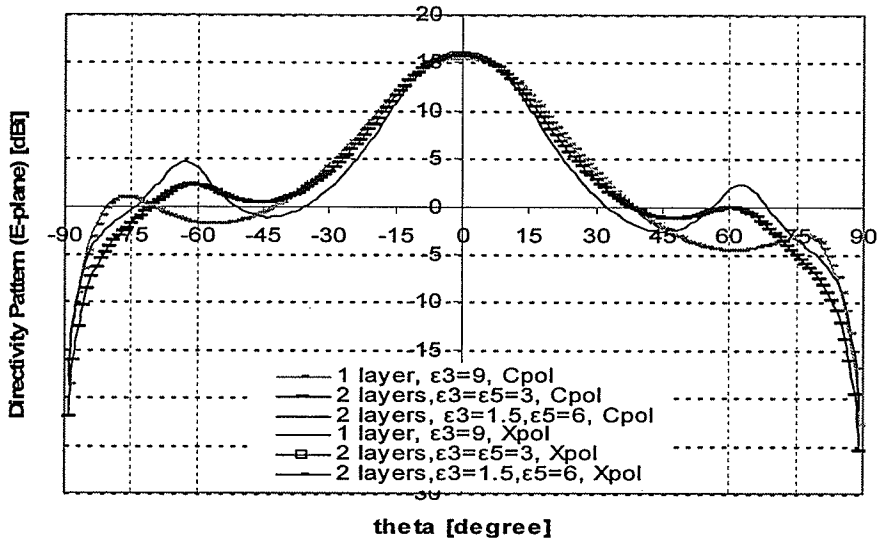

(a)

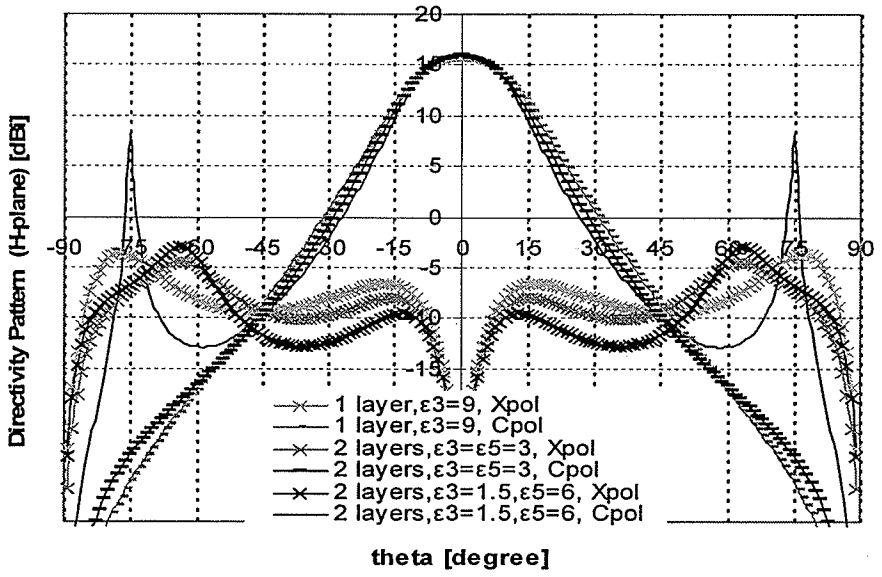

(b)

Fig.4.10 Comparison of directivity pattern for single-superstrate (ε_3=9), conventional double-superstrate (ε_3= ε_5=3), and modified double-superstrate (ε_3=1.5, ε_5=6) configurations a) E-plane and b) H-plane, (f_0=10GHz, the parameters are listed in Table 4.1 and Table 4.7)

components are almost similar, but the side lobe level is lower (*SLL≈-11.5dB*) for the modified double-superstrate configuration. The E-plane cross-polarization components are below -30dBi, so they are not seen in *Fig.4.10 (a)*. As it can be seen in *Fig.4.10(b)*, the H-plane copolarization components are quite similar for different configurations, except for a minor lobe, pencil beam in shape, for the modified double-superstrate configuration at $\theta=75^{\circ}$. The H-plane cross-polarization components are almost similar.

4.5. Experimental Verifications

In order to confirm the simulation results, a double-superstrate covered microstrip patch antenna prototype has been designed and fabricated in the Antenna Laboratory at the University of Manitoba. A superstrate with a relative permittivity of *3.2* and the thickness of *0.06 inch (≈1.52 mm)*, and loss tangent of $tan\delta=0.003$ has been chosen for this purpose. The superstrate thickness has been taken equal to 3.05 mm by using two dielectric layers, putting one layer on top of the another layer without sticking them together. So, the resonant frequency would be kept within the Ku-band (about *13.75 GHz*). The specifications of the fabricated antenna are listed in *Table 4.11*. In order to obtain the optimum directivity, the inter-superstrate heights are optimized to $t_2=10.25$ $(0.47\lambda_0)$ and $t_4=6mm$ $(0.275\lambda_0)$, respectively, by the Ansoft Designer simulator. The patch is fed by a *50 Ω* coaxial cable, using an SMA connector. The antenna return loss was computed by using Ansoft Designer, and measured by ANRITSU ME7808A Network Analyzer. The simulated and measured return loss variations with respect to frequency are shown in *Fig.4.11*.

Table.4.11. Parameters of the fabricated double-superstrate configuration

Layer	***Material***	***Geometry***
Superstrate2	ε_r=3.2	Thickness=3.05 mm ($0.25\lambda_3$)
Air gap2	Air	Height=6 mm ($0.275\lambda_0$)
Superstrate1	ε_r=3.2	Thickness=3.05 mm ($0.25\lambda_3$)
Air gap1	Air	Height =10.25 mm($0.47\lambda_0$)
Patch	Copper	Rectangular 6.5×10 mm
Substrate	ε_r=2.5	Thickness=0.38 mm
Ground Plane	Copper	48×48 mm
Feed	Probe(SMA connector)	X_f=-1.6 mm, Y_f=0 mm (origin: the center of patch)

In *Table 4.12*, the simulated and measured minimum return loss and the impedance-bandwidths are summarized. The impedance-bandwidth is defined as:

$$BW = \frac{(f_2 - f_1)|_{S_{11}=-10dB}}{f_0} \qquad (4.3)$$

As it can be seen from *Fig.4.11*, there are some differences between measured and simulated return losses. The difference between the measured and the simulated value of the center frequency is 0.145GHz (≈1.0%). This could be due to errors in fabrication, in the patch length or the feed location, since the diameter of the inner conductor of feed probe *(1.27mm)* is comparable to the patch length *(6.5mm)*. It was hard to place accurately the feed on the patch, and the difference can be ignored since, it does not affect the main objective, i.e. directivity measurements.

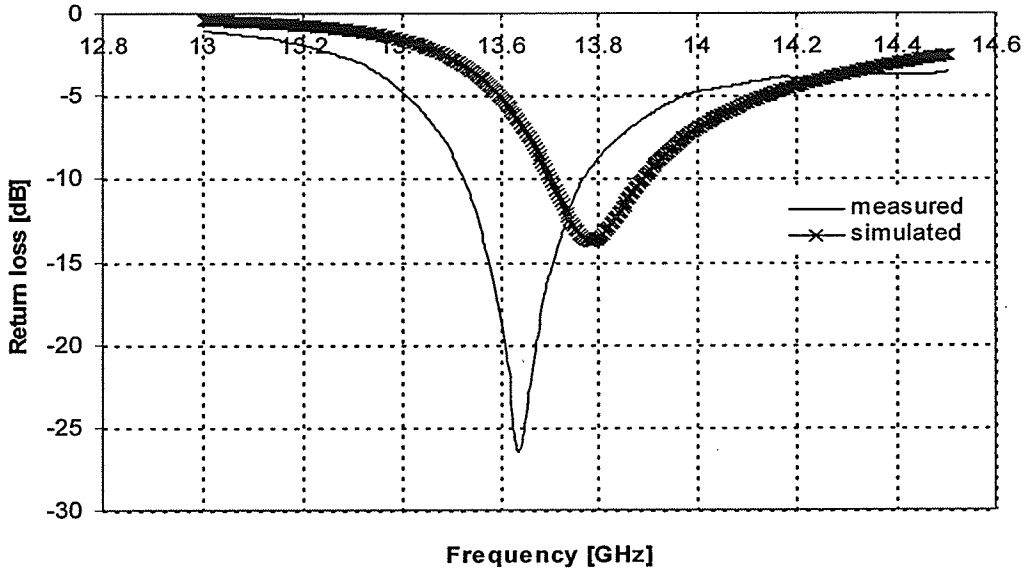

Fig.4.11 Comparison between the measured and simulated return loss with frequency for double-superstrate microstrip patch antenna (the parameters are listed in Table 4.12)

Table.4.12. Comparison of the measured and simulated return loss of the double-superstrate microstrip patch antenna (the parameters are listed in Table 4.11)

f_0 [GHz]		Return loss [dB]		Impedance BW	
Measured	**Simulated**	**Measured**	**Simulated**	**Measured**	**Simulated**
13.64	13.78	-26.5dB	-13.75dB	0.24 GHz (1.75%)	0.19 GHz (1.4%)

The radiation characteristics of the fabricated antenna were also measured in the anechoic chamber in Antenna Laboratory at the University of Manitoba. The measurement setup for measuring far-field electric field is similar to that explained in section 3.6. The broadside gain variations with frequency were measured and compared with simulated results, as it is shown in *Fig.4.12.* The measured and simulated values for gain and gain-bandwidth are summarized in Table4.13. As it can be seen from

Fig.4.12, the gain levels are almost the same, but the gain-bandwidth are different. The measured gain-bandwidth is about 2 times greater. The smaller measured gain implies a larger gain-bandwidth that is using the asymptotic formulas (2.21 and 2.22). This is not enough on its own to explain the larger gain-bandwidth. In order to explain this, more study is required.

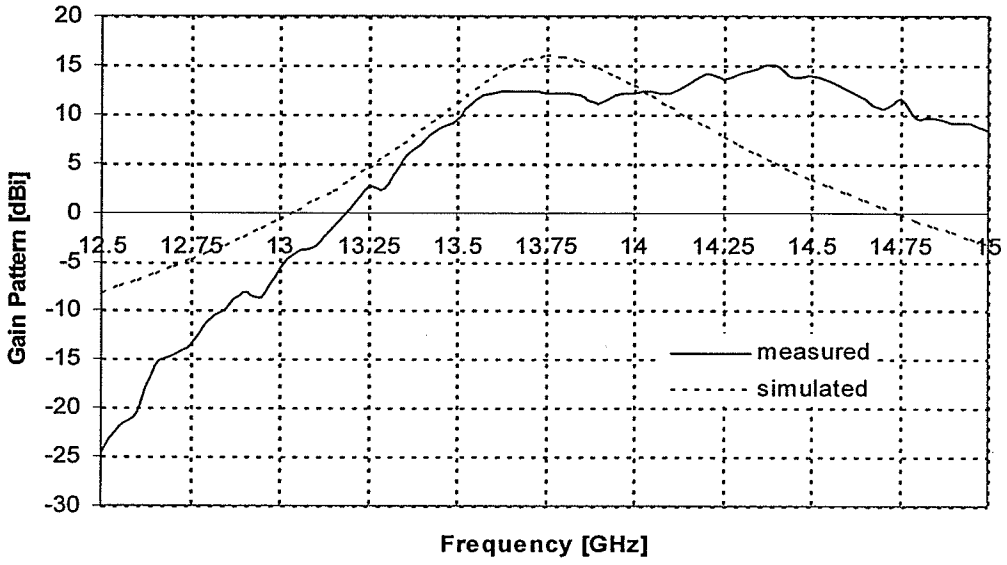

Fig. 4.12 Comparison between the measured and simulated broadside Gain with respect to frequency for double-superstrate microstrip patch antenna (the parameters are listed in Table4.11)

Table.4.13 Comparison of the measured and simulated gain characteristics with respect to frequency for double-superstrate microstrip patch antenna (parameters are listed in Table4.11)

f_0 [GHz]		Gain [dBi]		(-3dBpower) Gain-BW [GHz]	
Measured	**Simulated**	**Measured**	**Simulated**	**Measured**	**Simulated**
14.4	13.75	15.06dB	15.8dB	1.02 (7%)	0.44 (3.2%)

The radiation patterns in the two main planes (E- and H-plane) are studied next. Fig.4.13 shows the measured and simulated E-plane components. As it can be seen from Fig.4.13 (a), the simulated and measured patterns are quite similar in the range of $\theta<50°$. There is a null at about $\theta=\pm 20°$, in the measured results, and the measured E-plane co-polarization component also falls more rapidly.

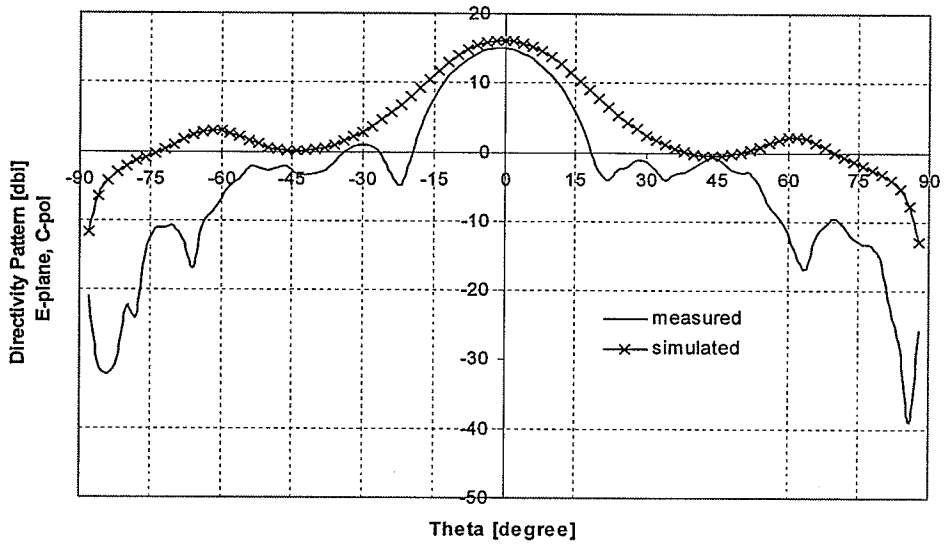

(a)

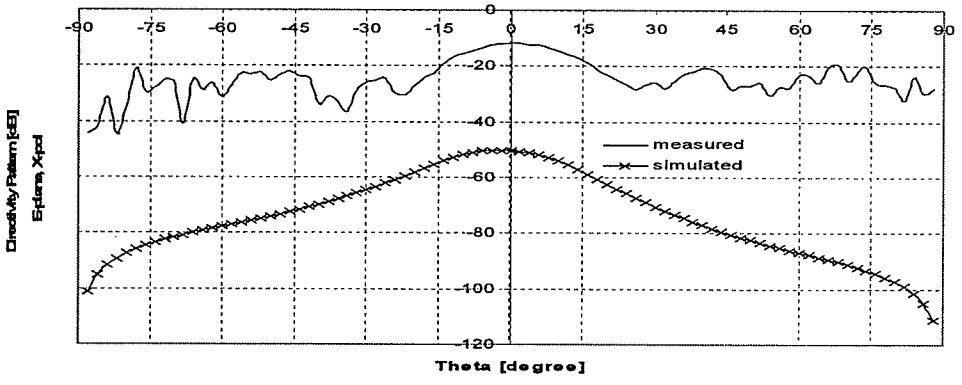

(b)

Fig.4.13 Measured and simulated Radiation pattern for double-superstrate microstrip patch antenna; a)E-plane C-pol component and b) E-plane X-pol component (the parameters are listed in Table4.11)

The simulated E-plane cross-polarization component level is below -50dBi. Fig.4.14 shows the measured and simulated H-plane components. As it can be seen from Fig.4.14 (a), the simulated and measured patterns are quite similar in the range of $\theta<15$. There are ripples in the measured H-plane co-polarization component. In Fig.4.14 (b), the measured and simulated H-plane cross-polarization components are depicted. The differences between the co-polarization components could be due to:

- The superstrate is not uniform, as there is a small air gap between its two pieces.
- The dielectric and ground plane sizes are finite.
- The deviations in the air gap height.

For the cross-polarization components, there are differences between the simulation and measurement. Some of the differences are due to misalignment and the power level of the pattern (<-20dBi) being also about the noise level of the measuring equipments. In addition, surface wave radiation from the edges of the superstrate layers or diffractions from setup (support and connecting cables) around the device under test could be the reason as well.

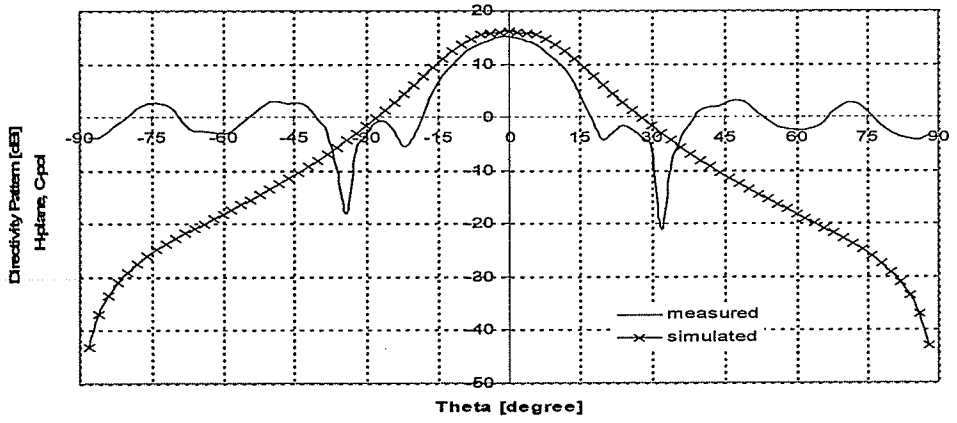

(a)

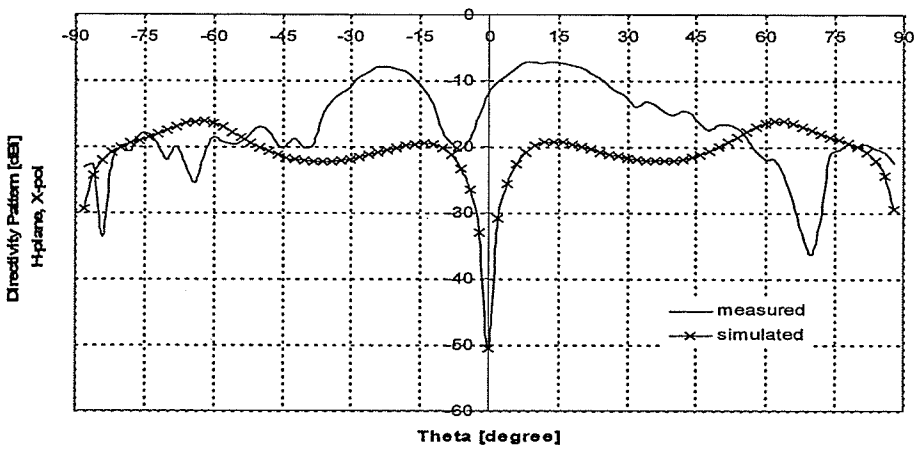

(b)

Fig.4.14 Measured and simulated Radiation pattern for double-superstrate microstrip patch antenna; a)H-plane C-pol component and b) H-plane X-pol component (the parameters are listed in Table4.11)

4.6 Summary and Conclusion

In this chapter, the multiple-superstrate microstrip patch antennas were studied. The effects of higher superstrates on the directivity were investigated, and then the input impedance of the multiple-superstrate configuration was studied. Based on the asymptotic gain formula it was verified that the directivity of the multiple-superstrate configuration at resonance is proportional to the product of superstrates relative permittivities. Different combinations of superstrate dielectric constants were studied and a modified double-superstrate configuration for improving the impedance bandwidth was proposed. Tolerance analysis was also conducted and then, the radiation characteristics in both frequency- and spatial-domain were presented. In conclusion, for the multiple-superstrate microstrip patch antenna it was shown that:

- In order to optimize the directivity, each superstrate layer thickness should be a quarter wavelength in superstrate (λ_d) and the superstrate air gap heights should be adjusted in turn from the bottom up

- For optimizing the directivity, the substrate thickness is offset by the air gap height
- Multiple-superstrate configuration generally, gives a wider impedance bandwidth than the single-superstrate configuration for a similar directivity, since the superstrate layers affect the input impedance less, due to either smaller superstrate dielectric constant or a larger superstrate height
- Lower superstrate layers have more impact on directivity
- Directivity bandwidth of a double-superstrate configuration is narrower than the single-superstrate configuration for a similar directivity
- The radiation pattern for the conventional double-superstrate configuration is almost similar to that of the single-superstrate configuration (for a similar directivity), but for the modified double-superstrate configuration, a minor lobe, pencil beam in shape, is observed in H-plane.

A prototype antenna was fabricated and measured in the Antenna Laboratory of University of Manitoba. The simulated and measured results of the antenna for its input impedance, bandwidths and radiation patterns were compared, which showed acceptable results. There was a difference between simulated and measured gain-bandwidth results which requires more study. Measured directivity of the antenna prototype with a superstrate relative permittivity of 3.2 is 15.07 dBi, with a gain-bandwidth of 7%, and an impedance-bandwidth of 1.8% at 13.64GHz.

Chapter 5

Modified single-superstrate configuration

Introduction In chapter two, it was mentioned that resonant superstrate gain enhancement method and that of the short back-fire antenna rely on the multiple reflection phenomenon. An idea that inspired by Shafai et al. is the combination of these techniques [22]. A basic feature of the short back-fire antenna which can be applied to the single-superstrate configuration is its simple subreflector that can be implemented by a parasitic patch attached to the superstrate. Adding a parasitic patch is useful when the superstrate with the desired thickness is not commercially available. For instance, the resonant superstrate at one GHz with a relative permittivity of 9 should be 25mm in thickness. It will be shown that a superstrate of thickness smaller than one quarter wave-length with a parasitic patch can give the same level of directivity obtained by the superstrate of one quarter wave-length in thickness. In this regard, the directivity variations with respect to the radius of the parasitic patch are investigated. The effects of the single-superstrate configuration (SSC) with a parasitic patch on the microstrip patch input response are studied next. Then, the radiation characteristics in frequency- and spatial-domain are investigated, and the measured results of a prototype antenna will be illustrated in order to validate the simulation results. The measured and simulated results show reasonable good agreement. The measured directivity of this antenna is 15.61 dBi, with the directivity-bandwidth of 7.3% at 4.8GHz.

5.1. The directivity of the modified SSC microstrip patch

In order to obtain the directivity of 15dBi at 5GHz, a conventional single superstrate configuration microstrip patch antenna, with a superstrate relative permittivity of 9.8 is designed. The specifications of this antenna are listed in Table5.1.

Table5.1 The specifications of the conventional single-superstrate configuration MSPA for studying the properties of the modified single-superstrate configuration

Layer	***Material***	***Geometry***
Superstrate	ε_r=9.8	Thickness=4.79 mm ($0.25\lambda_3$)
Air gap	Air	Height=29.4 mm ($0.49\lambda_0$)
Patch	Copper	Rectangular 18.5x25 mm
Substrate	ε_r=2.5	Thickness=0.38 mm
Ground Plane	Copper	Infinite
Feed	Coaxial Probe	X_f=-5 mm, Y_f=0 mm (location from the center of patch)

As it is seen from Table5.1, the required superstrate thickness should be 4.79mm. In case a superstrate of 3.175 ($0.66\lambda_3/4$) in thickness is to be used instead, the directivity is decreased to 11.36dBi. The simplest way to compensate for the directivity reduction is to optimize the air gap height (section 3.4.2). The results are shown in Table5.2. As it is seen from Table5.2, optimizing the air gap height (t_{2opt}=31mm), can not restore the directivity to the designed value of 15dBi. Then, a parasitic patch, i.e. a conducting subreflector, is added underneath the superstrate a) before optimizing t_2, Fig5.1(b), and b) after optimizing t_2, Fig5.1(c) in order to restore the directivity.

Table5.2 Directivity compensation of the single-superstrate configuration MSPA with $t3=0.66\lambda_3/4$ by the air gap height optimization (f_0 =5GHz, the other parameters are listed in Table5.1)

t2[mm]	*D[dBi]*
31.1(0.518λ_0)	*14.06813*
31.0(0.517λ_0)	*14.14128*
30.9(0.515λ_0)	*12.6148*

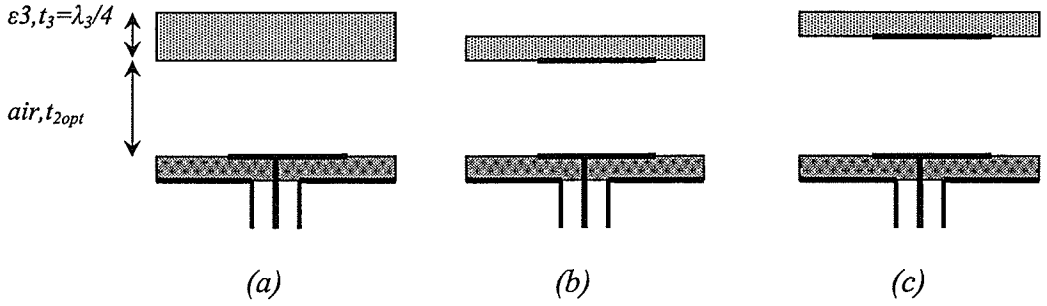

Fig.5.1. The structure of the modified single-superstrate microstrip patch antennas; a) conventional SSC, b) Parasitic patch added SSC with $t3<\lambda_3/4$, and c) Modified SSC with $t3<\lambda_3/4$ (ε_i, t_i is each layer dielectric constant and thickness)

Fig.5.1(a) shows the conventional single-superstrate configuration, that is the superstrate with one quarter wave-length thickness ($\lambda_3/4$) and its corresponding air gap height, i.e. t_{2opt} of 29.4mm. Fig.5.1(b) shows the single-superstrate configuration when the superstrate thickness is less than one quarter wave-length with an added parasitic patch underneath the superstrate in order to compensate for the directivity before re-optimizing the air gap height, i.e. t_2=29.4mm. Fig.5.1(c) shows the single-superstrate configuration when the superstrate thickness is less than one quarter wave-length with an added parasitic patch underneath the superstrate, but after re-optimizing the air gap height, i.e.

the new t_{2opt} of 31mm. Next, the directivity is computed under both conditions, i.e. without re-optimizing the air gap height or t_2= 29.4mm and with re-optimizing the air gap height or t_2=31mm, respectively. The calculated directivity with respect to the parasitic patch radius is illustrated in Fig5.2. As it can be seen, in the case of without re-optimizing, the directivity shows little increment. But, in the latter case, which will be called the modified single-superstrate configuration from now on, the directivity rises proportionally with the parasitic patch radius. The directivity variations have been also computed for t_2 of 32mm (greater than $t_{2re\text{-}opt}$), and t_2 of 30mm (smaller than $t_{2re\text{-}opt}$), while $t_{2re\text{-}opt}$ =31mm. So, it is justified that the case with t_2=31mm gives the maximum directivity and for a parasitic patch radius of 25mm, the design value of directivity is restored, that is 15.53dBi.

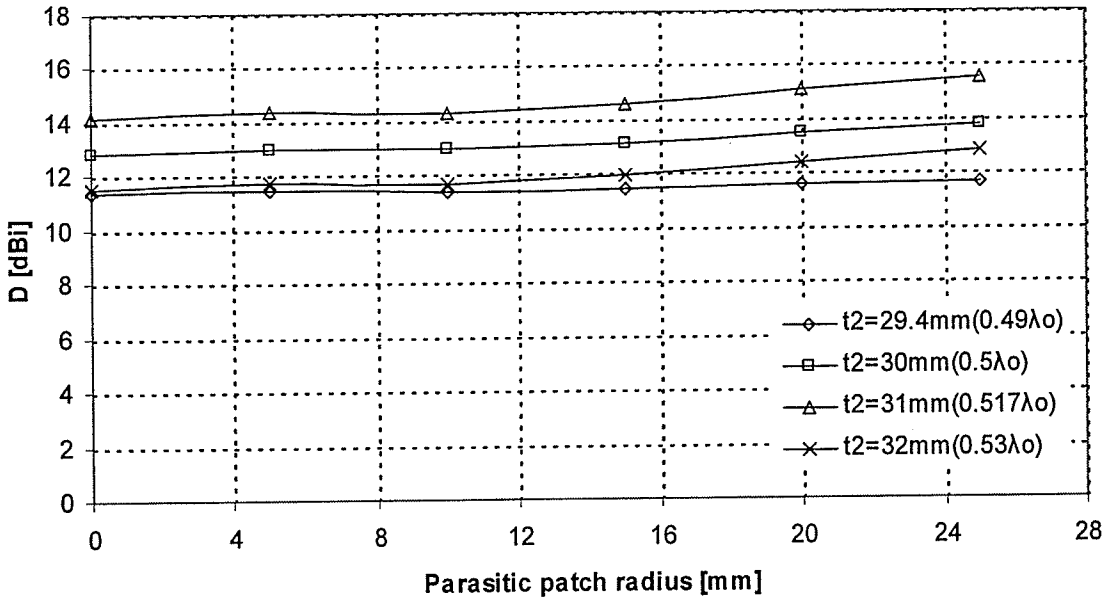

Fig.5.2. Comparison of the directivities without and with re-optimizing the air gap height for $t3=0.66\lambda_3/4$ (f_0 =5GHz, the other parameters are listed in Table5.1)

5.2. *The effects of the modified SSC on microstrip patch input resistance*

In this section, the effects of the parasitic patch size on the input resistance will be investigated. Considering the modified single-superstrate configuration with different parasitic patch radii, variations of the input resistance with respect to frequency are calculated and shown in *Fig.5.3* for comparison.

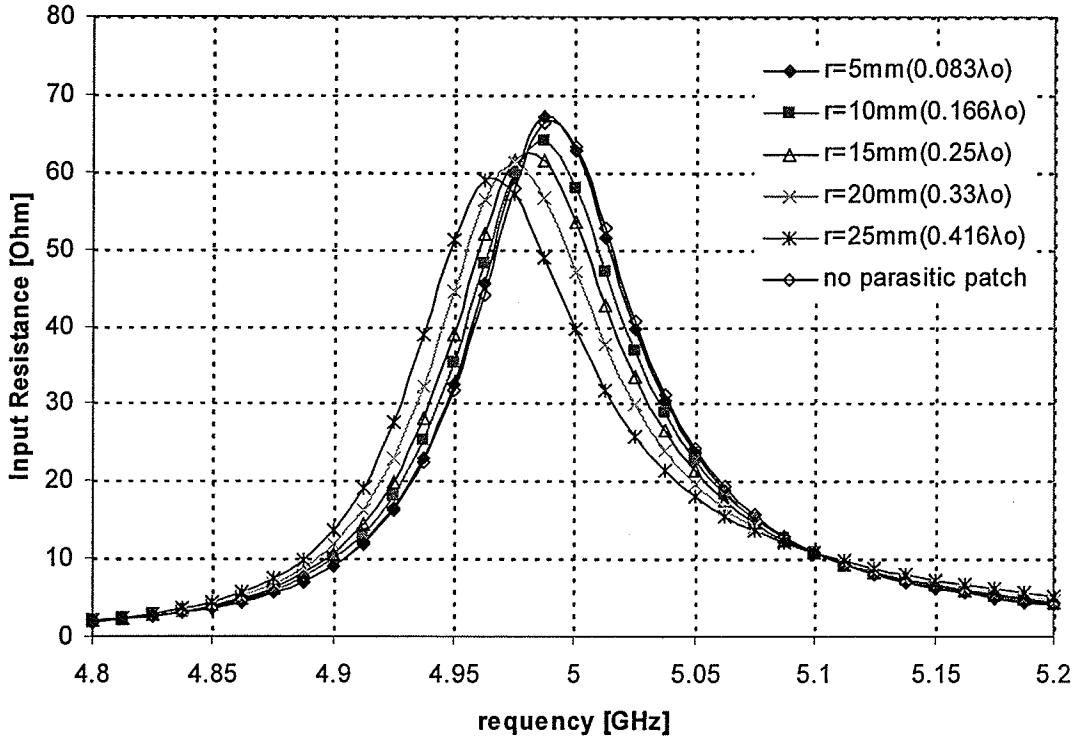

Fig.5.3. Variations of the input resistance with frequency for modified single -superstrate configuration for different parasitic patch radii (t_2=31mm(0.517 λ_0), t_3=3.175mm (0.66λ_3/4), f_0 =5GHz, the other parameters are listed in Tables 5.1)

As it is seen from Fig.5.3, the effects on the input resistance due to the single-superstrate, with an added parasitic patch, are different from those of the superstrate alone. The only

similarity is the shift of the input resistance frequency response to lower frequencies. But, its value is much smaller, i.e. the percentage of the frequency shift is much smaller than that of the conventional single-superstrate. The maximum input resistance (R_r), resonant frequency (f_r), and the percentage of frequency shift ($df_r\%$) and bandwidth (BW) for different parasitic patch radii (r's) are summarized in Table 5.3, where the bandwidth is defined as (3.1).

Table5.3. Comparison of the microstrip patch antenna input resistance characteristics for different parasitic patch radii (r) attached underneath the superstrate (t_2=31mm (0.517 λ_0), t_3=3.175mm (0.66λ_3/4), f_0 =5GHz, the other parameters are listed in Table5.1)

r [mm]	*R_r[Ohm]*	*f_r[GHz]*	*df_r [%]*	*BW [GHz]*
0	67.2	4.99	-	0.055(1.1%)
5	67.2	4.99	0	0.055(1.1%)
10	64.05	4.985	-0.1%	0.055(1.1%)
15	62.77	4.98	-0.2%	0.0575(1.2%)
20	61.29	4.975	-0.3%	0.055(1.1%)
25	59.3	4.9675	0.45%	0.0575(1.2%)

As it is seen from Table 5.3, the impedance bandwidth does not show much difference from that of a superstrate alone. The main difference is in R_r reduction, which decreases with the parasitic patch radius.

5.3. Experimental verifications

In order to confirm the simulation results for the modified single-superstrate configuration, a microstrip patch antenna prototype with an added parasitic patch superstrate has been designed and fabricated in the Antenna Laboratory at the University

of Manitoba. A superstrate with a relative permittivity of 9.8 and thickness of 0.125 inch (≈3.175 mm) has been chosen for this purpose. At the frequency of 5GHz, the superstrate thickness is equal to $0.66\lambda_3/4$, that is the directivity would not be maximum. In order to restore the resonant directivity, the radius of the parasitic patch is taken equal to r=25mm ($0.417\lambda_0$) attached underneath the superstrate after re-optimizing the superstrate height to t_2=31 mm ($0.517\lambda_0$) by the Ansoft Designer simulator. The patch is fed by a 50 Ohm coaxial cable, using an SMA connector. The specifications of the fabricated antenna are listed in *Table5.4*.

Table5.4 The specifications of the modified single-superstrate configuration MSPA for measurement

Layer	***Material***	***Geometry***
Superstrate	ε_r=9.8	Thickness=3.175 mm ($0.66\lambda_3/4$), 150×150mm^2
Parasitic Patch	Copper	Circular, radius=25 mm ($0.417\lambda_0$)
Air gap	Air	Height=31 mm ($0.517\lambda_0$)
Patch	Copper	Rectangular, 18.5×25 mm
Substrate	ε_r=2.5	Thickness=0.38 mm, 150×150mm^2
Ground Plane	Copper	250×250mm^2
Feed	Coaxial Probe	X_f=-3 mm, Y_f=0 mm (location from the center of patch)

The antenna return loss was computed by using Ansoft Designer, and also measured by ANRITSU ME7808A Network Analyzer. The simulated and measured return loss variations with respect to frequency are shown in *Fig.5.4*. As it can be seen from Fig.5.4, there are some differences between the measured and simulated return losses. The

difference between the measured and simulated center frequencies (f_0) is 0.175GHz. This is due to the error in fabrication. The difference can be ignored since it does not affect the main objective, i.e. directivity measurements, but the mismatch loss should be considered in this regard. The antenna impedance matching is not attempted here, since the same radiating patch was supposed to be used with different parasitic patches. Therefore, the mismatch loss L_m, is calculated by equation (2.32), and will be considered later on. The simulated and measured return loss, mismatch loss and the corresponding center frequencies are summarized in Table 5.5. The radiation characteristics of the fabricated antenna were also measured in the anechoic chamber in Antenna Laboratory at the University of Manitoba. The measurement set up for measuring far-electric field is similar to that explained in section 3.6. The broadside gain variations with frequency were measured and compared with simulated results, as it is shown in *Fig.5.5.* Table5.6 summarizes the measured and simulated values for directivity, corresponding center frequency, and directivity-bandwidth.

Table5.5 Comparison of the measured and simulated return loss, mismatch loss, and their corresponding center frequencies for the modified single-superstrate microstrip patch antenna (the parameters are listed in Table 5.4)

f_0 [GHz]		***Return loss [dB]***		***Mismatch loss [dB]***	
measured	simulated	measured	simulated	measured	simulated
4.825	5.0	-6.05	-10.54	-1.24	-0.4

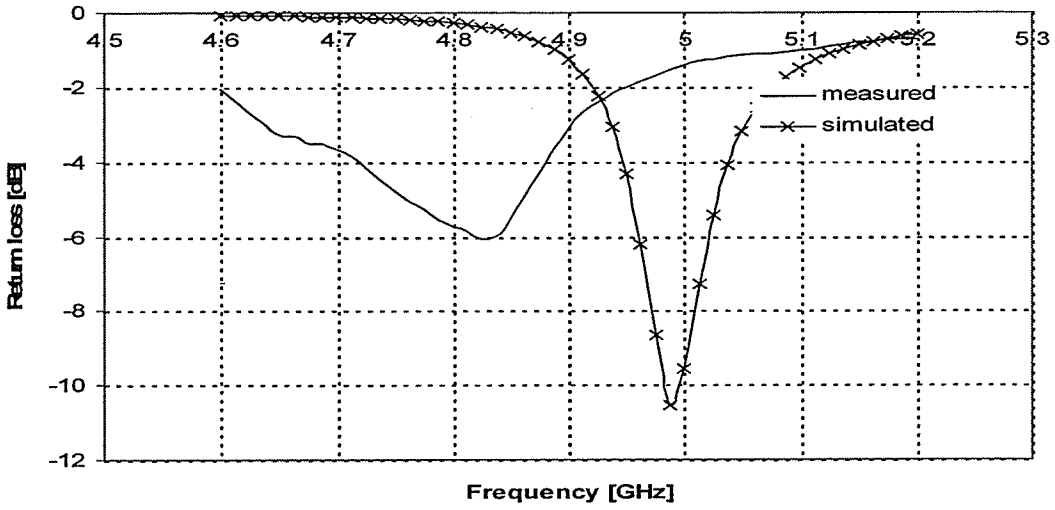

Fig.5.4. Comparison between the measured and simulated return loss variations with frequency for modified single-superstrate microstrip patch antenna (the parameters are listed in Table 5.4)

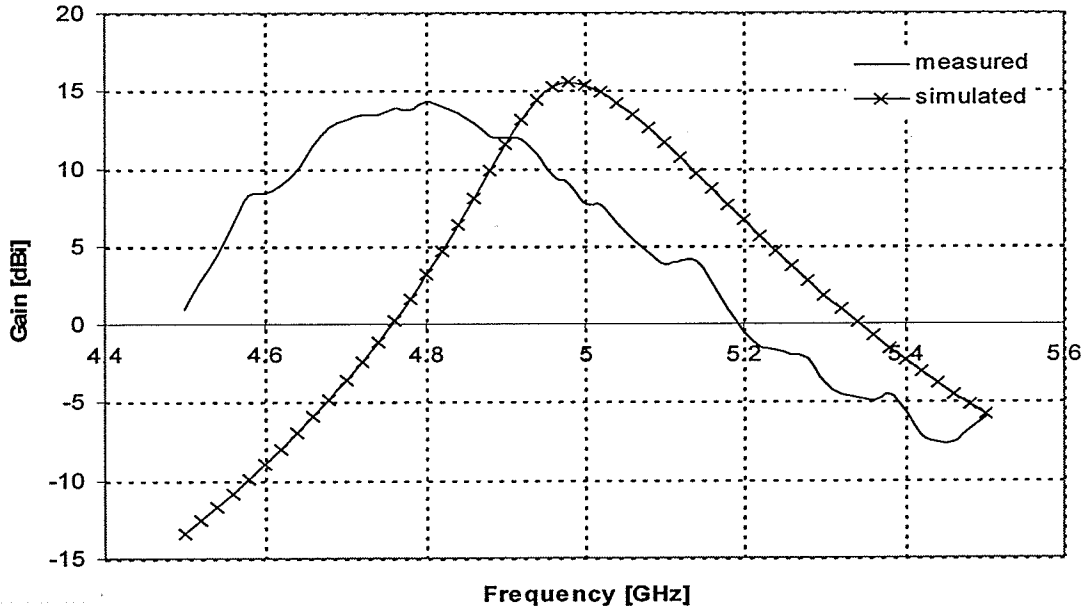

Fig.5.5. Comparison of the directivity variations with respect to frequency between the simulated and measured results (the parameters are listed in Table 5.4)

Table5.6 Comparison of the measured and simulated directivity, the corresponding center frequency , and directivity-bandwidth for the modified single-superstrate microstrip patch antenna (the parameters are listed in Table 5.4)

f_0 [GHz]		D [dB]		directivity-bandwidth [GHz]	
measured	simulated	measured	simulated	measured	simulated
4.8	5.0	15.61	15.53	0.35(7.3%)	0.40(8%)

As it can be seen from Fig.5.5, the frequencies where the maximum gains are obtained are the same frequencies at which the return loss is minimum, for both the measured and simulated results, as expected. The difference between the peak simulated and measured gains can be explained by considering the mismatch loss (L_m), that is in case of impedance matching, the measured gain would be 15.61dBi. This agrees well with the simulated result of 15.53dBi. The measured and simulated directivity-bandwidth are 7.3% and 8%, respectively. The radiation patterns in the two main planes (E-plane and H-plane) are studied next. Fig.5.6(a,b) show the measured and simulated co-polarization components in the E- and H-planes. As it can be seen from Fig.5.6(a,b), the measured and simulated E- and H-plane co-polarization patterns are quite similar. The difference in the broadside gain between the measured and simulated results can be explained by the mismatch loss which should be considered for the measured result. There is a null at about $\theta=40°$, in the measured patterns, which should be due to the finite extent of the superstrate transverse to the broadside direction. The measured H-plane co-polarization component is different from the simulated result for the $\theta>40°$, this should be due to the

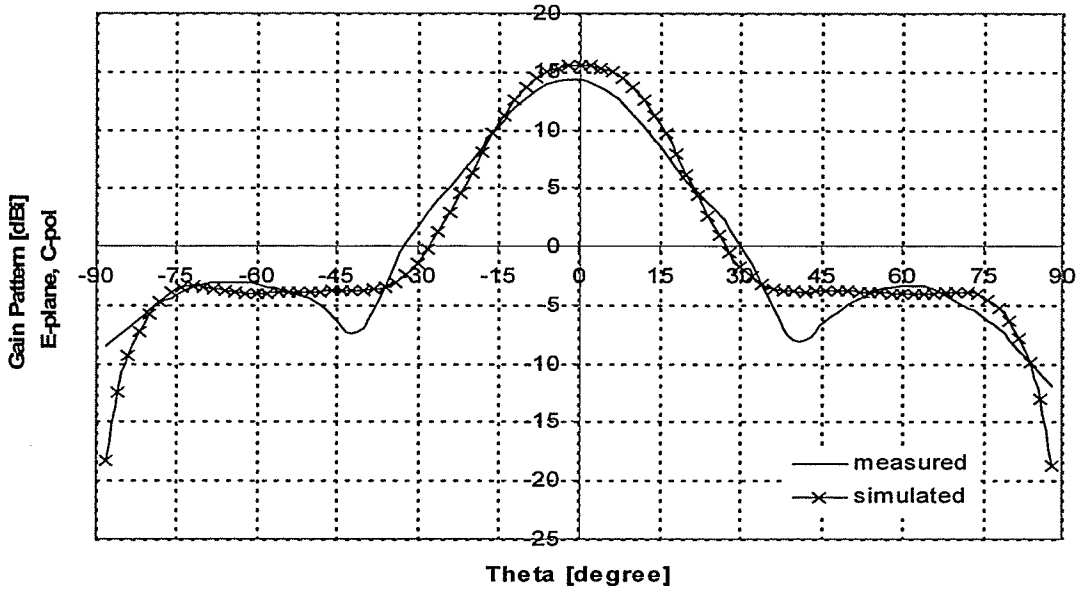

(a)

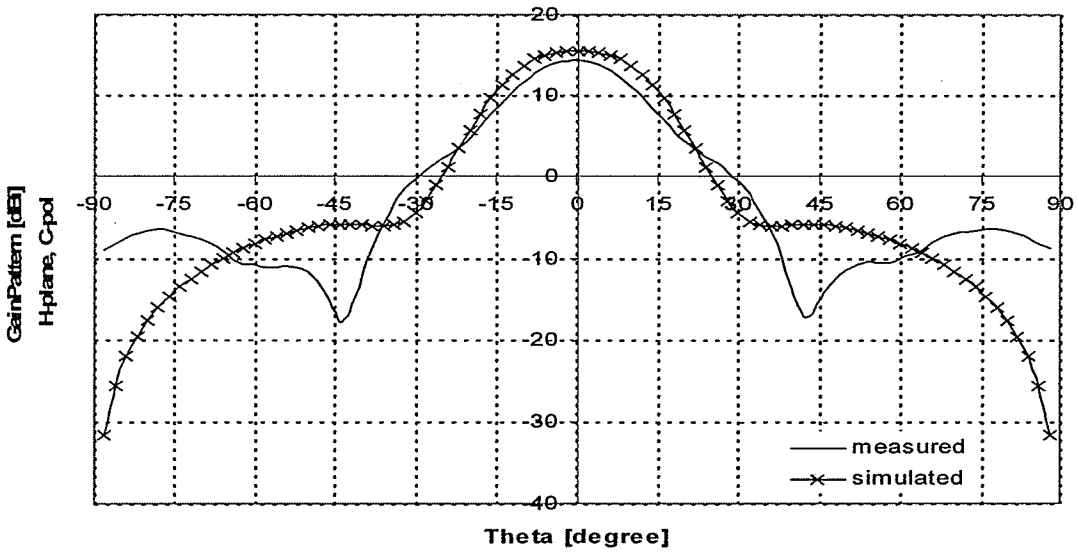

(b)

Fig.5.6. Comparison of the directivity patterns between the simulated and the measured results for a) E-plane co-polarization components, and b) H-plane co-polarization components (the parameters are listed in Table 5.4)

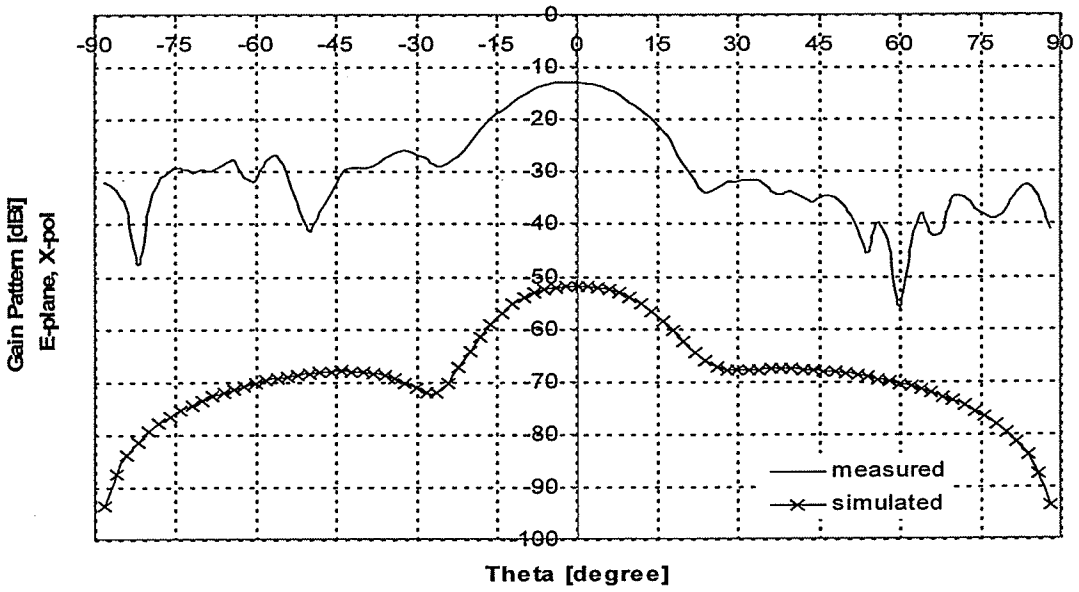

(a)

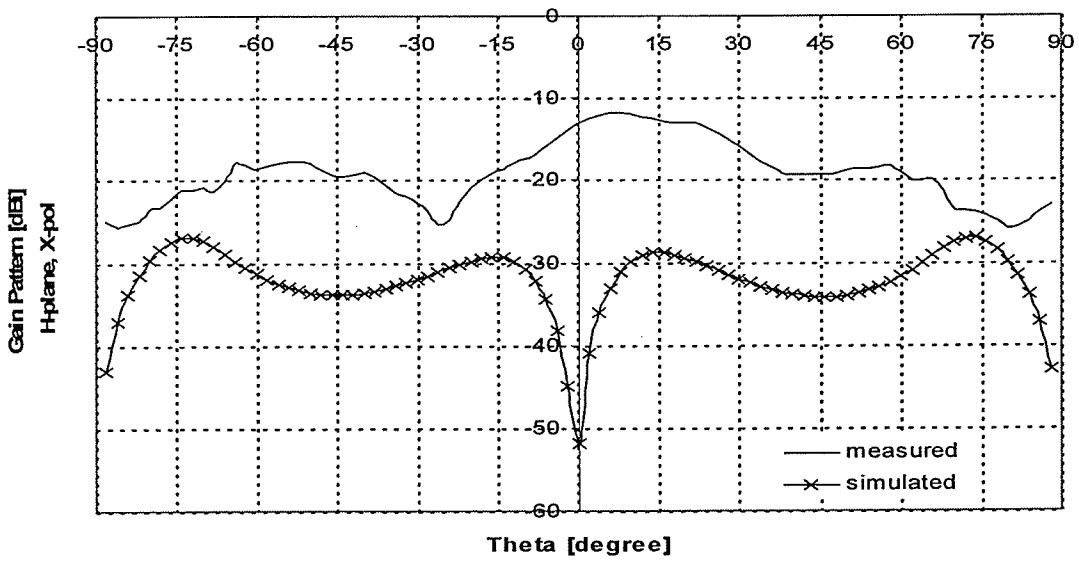

(b)

Fig.5.7 Comparison of the directivity patterns between the simulated and the measured results for a) E-plane cross-polarization components, and b) H-plane cross-polarization components (the parameters are listed in Table 5.4)

surface waves or diffractions radiated from the edges of superstrate. Fig.5.7(a,b) show the measured and simulated cross-polarization components in the E- and H-planes. For the cross-polarization components, there are differences between the simulation and measurement. Some of the differences are due to misalignment and the power level of the pattern (<-20dBi) being also about the noise level of the measuring equipments. In addition, surface wave radiation from the edges of the superstrate layers or diffractions from other set up support and connecting cables around the device under test could be the reason as well.

5.4. Summary and Conclusion

In this chapter, the modified single-superstrate configuration for the microstrip patch antennas was studied. The effects of the added parasitic patch underneath the superstrate on the directivity were investigated, and then the input resistance of the modified single-superstrate configuration was studied. It was verified that the directivity of the modified single-superstrate configuration increases proportionally with the radius of parasitic patch. Different radii of parasitic patch were studied, in order to restore the directivity while the superstrate thickness is smaller than one quarter wave-length. The radiation characteristic in both frequency- and spatial-domain was presented. In conclusion, for the modified single-superstrate microstrip patch antenna it was shown that:

- In order to restore the directivity when the superstrate thickness is much smaller than one quarter wave-length, compensation by re-optimizing the air gap height would not be sufficient

- For restoring the directivity of the conventional single-superstrate configuration when the superstrate thickness is smaller than one quarter wave-length, a parasitic patch with a proper radius underneath the superstrate is added after re-optimizing the air gap height which called "modified single-superstrate configuration"
- The directivity of the modified single-superstrate configuration increases with the parasitic patch radius proportionally
- The modified single-superstrate decreases the peak resonant input resistance and shifts the input resistance frequency response toward the lower frequencies, but the bandwidth remains almost constant
- The directivity-bandwidth for the modified single-superstrate remains almost unchanged, that is about 8%, compared with the conventional single-superstrate configuration.

A prototype antenna was fabricated and measured in the Antenna Laboratory of University of Manitoba. The simulated and measured results of the antenna for its input impedance, bandwidths and radiation patterns were compared, which shows acceptable results. There was a difference between simulated and measured gain which was due to the mismatch loss. The measured directivity of the antenna prototype with superstrate relative permittivity of 9.8 is 15.61 dBi with a superstrate thickness of $0.66\lambda_3/4$, with directivity-bandwidth of 7.3% at 4.8GHz.

CHAPTER 6

Conclusions

This thesis has provided a comprehensive study of the dielectric covered microstrip patch antennas as a resonant gain enhancement method. In this method, one or more dielectric layers (superstrate), with proper permittivities, thicknesses, and heights are placed above the patch. Under these conditions, the resonance is created for the field inside the layered structure of the antenna, which results in a high directivity. The structures used for the designs and simulations in this thesis can be categorized into two groups, namely the single-superstrate configuration (SSC) and multiple-superstrate configuration (MSC). The former group consists of a conventional SSC and a modified SSC (MSSC). The conclusions arising from this study are outlined below.

For the SSC of microstrip patch antenna:

- The directivity maximizes at a particular superstrate height near half wavelength, while its thickness is one quarter wave-length
- The input resistance peak value moves to lower frequencies and increases, and its bandwidth becomes narrower, all in proportion to the superstrate thickness or permittivity
- The substrate and superstrate thicknesses can be offset with their air gap height
- The superstrate thickness deviations can be tolerated by directivity compensation
- The directivity×bandwidth as predicted by the asymptotic formulas, is justified
- The measured and simulated results are in good agreement. The measured directivity of the fabricated antenna with the superstrate relative permittivity of 9.8 and thickness of 3.175mm is 15.25dBi with the directivity-bandwidth of 4.3% at 8.35GHz

For the MSC of microstrip patch antenna:

- The directivity maximizes at a particular inter-superstrate height, while the superstrate thicknesses are all one quarter wave-length
- A large resonant directivity can be obtained even with moderate superstrate dielectric constants, in contrast to the single-superstrate configuration
- The asymptotic formulas for directivity can be extended for MSC, that is the directivity varies rather linearly proportional to each superstrate relative permittivity
- The input impedance variations with frequency is less affected compared to SSC, and that would be reduced even further by deploying superstrate layers in ascending order of permittivities
- The lowest (superstrate) layer parameters has the most impact on the directivity and vice versa
- The directivity-bandwidth is narrower compared to SSC with a similar directivity
- The measured and simulated radiation patterns are almost in agreement, but the measured directivity-bandwidth is much wider which needs to be studied further. The measured directivity of the fabricated double-superstrate microstrip antenna with the superstrates relative permittivity of 3.2 and thickness of 3.05mm is 15.06dBi, with an impedance-bandwidth of 7% at 13.64GHz
- Using moderate dielectric constant superstrates requires thicker layers, which can be made by placing two layers on top of one another (dual dielectric layer)

For the MSSC of microstrip patch antenna:

- Resonant gain can be obtained even with superstrate layers thinner than one quarter wave-length (in contrast to single-superstrate configuration)

• The directivity increases with the parasitic patch radius after re-optimizing the superstrate height, while its thickness is smaller than one quarter wave-length

• The input impedance peak value moves to lower frequencies and decreases, in proportion with the parasitic patch radius

• The measured and simulated radiation characteristics are in good agreement. The measured directivity of the fabricated modified single-superstrate microstrip antenna with the superstrate relative permittivity of 9.8, thickness of 3.175mm ($0.66\lambda_3$), and the circular parasitic patch radius of 25mm is 15.61dBi with a directivity-bandwidth of 7.3% at 4.8GHz. The thesis is ended with some notes for the future research scope.

Future work

This work still has several scopes for future research, while improving the directivity bandwidth still remains as the main challenge. They can be summarized as follows:

- A detailed study of the effect of finite ground plane and superstrate size and shape
- A detailed study from the aperture antenna point of view
- More experimental verifications to confirm the accuracy of the simulations
- More studies on single-superstrate-patch configuration
- Studies on EBG materials, in regard to realizing wide-band directive MSAs

APPENDIX

A. Terminology

In this section some terms or definitions are reviewed briefly which are either unclear or inconsistent in the literature. It includes "Directivity", "Gain" and their Bandwidth. These terms are defined in a way that is intended here.

A.1 Directivity and Gain

The directivity shows how much an antenna concentrates energy in one direction in preference to radiation in other directions and is equal to its power gain if the antenna is 100% efficient. Here, power gain is expressed relative to an isotropic radiator as the reference [20].

Toward the definition of directivity, the definition of radiation intensity is needed. Radiation intensity is the power radiated in a given direction per unit solid angle and has the units of watts per square radian (or steradian) and is calculated by:

$$U(\theta,\varphi) = S(\theta,\varphi).r^2 \qquad (A.1)$$

where,

S : pointing vector [watts per squared meter]

r , θ and φ : spherical coordinates

Directivity is defined as the ratio of the radiation intensity in a certain direction to the average radiation intensity, or:

$$D(\theta,\varphi) = \frac{U(\theta,\varphi)}{U_{ave}} = \frac{4\pi U(\theta,\varphi)}{P_{rad}} \qquad (A.2)$$

where,

P_{rad} : total radiated power [watts]

When the directivity is quoted as a single number without reference to a direction, maximum directivity is usually intended. Maximum directivity follows from (*A.2*) as:

$$D = \frac{U_{\max}}{U_{ave}} = \frac{4\pi U_{\max}}{P_{rad}} \tag{A.3}$$

Directivity is solely determined by the radiation pattern of an antenna. When an antenna is used in a system we are actually interested in how efficiently the antenna transforms available power at its input terminals (P_{in}) to radiated power, together with its directive properties, so power gain (or simply gain) is defined:

$$G(\theta,\varphi) = \frac{4\pi U(\theta,\varphi)}{P_{in}} \tag{A.4}$$

The portion of input power (P_{in}) that does not appear as the radiated power is absorbed on the antenna or reflected back. This prompts us to define the radiation efficiency e_r as

$$e_r = \frac{P_{rad}}{P_{in}} \tag{A.5}$$

Using (*A.5*) in (*A.4*) and (*A.3*) gives:

$$G(\theta,\varphi) = e_r \frac{4\pi U(\theta,\varphi)}{P_{rad}} = e_r D(\theta,\varphi) \tag{A.6}$$

Similarly, for maximum gain:

$$G = e_r D \tag{A.7}$$

"e_r" can be written as:

$$e_r = e_c e_d (1 - |\Gamma^2|) \tag{A.8}$$

where

e_c : conduction efficiency (implying the conduction losses)

e_d : dielectric efficiency (implying the dielectric losses)

Γ : reflection coefficient at the input terminals of the antenna.

Since the gain is a power ratio, it can be calculated in decibels as follows:

$$G_{dBi} = 10 \log_{10} G \qquad (A.9)$$

Similarly for directivity:

$$D_{dBi} = 10 \log_{10} D \qquad (A.10)$$

'i' in dBi stands for isotropic, since in their definitions, average power (isotropic radiator) is used.

If the conduction and dielectric losses can be ignored, by using high quality materials, the radiation efficiency in decibels is:

$$10 \log_{10} e_r = 10 \log_{10}(1-|\Gamma|^2) = L_m \qquad (A.11)$$

where Lm is the mismatch loss. That is the loss due to reflection or mismatch losses between the antenna and the transmission line. Finally, the relation between gain and directivity in its simplest form is:

$$G_{dBi} = D_{dBi} + L_m \qquad (A.12)$$

A.2 Directivity Bandwidth

The bandwidth of an antenna is defined as "the range of frequencies within which the performance of the antenna, with respect to some characteristic, conforms to a specified standard" [21]. The bandwidth can be considered to be the range of frequencies, on either side of a center frequency (usually the resonance frequency), where the antenna characteristics (such as input impedance, pattern, beamwidth, polarization, side lobe

level, gain, beam direction, radiation efficiency, etc.) are within an acceptable value of those at the center frequency.

For the directivity, the center frequency is that frequency where the directivity is maximum. The -3dB (or half power) frequencies are the frequencies on either side of center frequency where the directivity falls -3db below its maximum value. Therefore the "-3dB directivity bandwidth" is the range of frequencies between -3dB frequencies. The "-3dB gain bandwidth" definition is defined in the same way.

REFERENCES

[1] G.V. Trintini, "Partially Reflecting Sheet Arrays", Antennas and Propagation, IRE Trans., Vol. 4, Apr.1956, pp.666-671.

[2] R.G. Immell and, B.H.Sasser, "A Highly thinned Array using the Image Element Antenna", Proceeding of 1979 Antenna Application Symposium, held at Robert Allerton Park University of Illinois, USA, Sep 1979.

[3] Y. Sugio, T. Makimoto, S . Nishimura, and H. Nakanishi, "Analysis for Gain Enhancement of multiple-reflection Line Antenna with Dielectric Plates," Trans. IECE, Jan. 1981, pp. 80-112.

[4] N.G.Alexopoulos and D.R. Jackson "Fundamental Superstrate (cover) effects on Printed Circuit Antennas" Antennas and Propagation, IEEE Transactions on, Vol. 32, NO.8, Aug. 1984, pp.807–816.

[5] Y. Sugio, T. Makimoto, S. Nishimura, and H. Nakanishi, "Gain Enhancement of Dielectric Covered Antennas with a Ground Plane", IEE ICAP 83, April 1983, pp.289-293.

[6] D.R. Jackson and N.G.Alexopoulos, "Gain Enhancement Methods for Printed Circuit Antennas" Antennas and Propagation, IEEE Transactions on, Vol. 33, No. 9 , Sep. 1985 pp.976 – 987.

[7] H. W. Ehrenspeck, "The Backfire Antenna, a New Type of Directional Line Source," Proc. IRE (Correspondence), Vol. 48, January 1960, pp. 109-110.

[8] E. Nielsen and K. Pontoppidan, "Backfire Antennas with Dipole Elements", Antennas and Propagation, IEEE Transactions on, Vol.18, No.3, May 1970, pp.367 – 374.

[9] H. W. Ehrenspeck, "The Short Backfire Antenna" Proc. IEEE (Correspondence), Vol. 53, August 1960, pp. 1138-1140.

[10] M. Rayner and A.D. Olver, A.D. Monk, "FD-TD Design of Short Backfire Antennas" Microwaves, Antennas and Propagation, IEE Proceedings - , Vol. 144, No.1, Feb.1997, pp.1 – 6.

[11] D.P.Gray and L. Shafai, "Parametric Study of Short Backfire Antennas with different Cavity Profiles", Antennas and Propagation Society International Symposium, 2000 IEEE , Vol. 3 , 16-21 July 2000, pp.1314 - 1317.

[12] Y. Sugio, T. Makimoto, and T. Tsugawa, "Variational Analysis for Gain Enhancement and Input Characteristics of Dielectric loaded Antennas ", Antennas and Propagation Society International Symposium, 1989. AP-S. Digest Vol.3, 26-30 June 1989, pp.1364 – 1367.

[13] S. Ramo, J.R. Whinnery, and T. VanDuzer, "Field and Waves in Communication Electronics", 3rd edition, New York: Wiley, 1965, ch.5,6.

[14] Chi-Sen Lin, Shun-Shi Zhong, Jian-Hui Shi, and Yuan Wang, "Gain Enhancement Technique for Microstrip Antennas", Antennas and Propagation Society International Symposium, 1989. AP-S. Digest , 26-30 June 1989, Vol.1, pp. 454 – 457.

[15] H.Y.Yang and N.G. Alexopoulos, "Gain Enhancement Method for Printed Circuit Antennas through Multiple Superstrate" Antennas and Propagation, IEEE Transactions on, Vol. 35, No. 7 , July 1987, pp.860–863.

[16] A.A. Kishk, L. Shafai, "Gain Enhancement of Antennas over Finite Ground Plane Covered by a Dielectric Seet", IEE Proceedings, Vol.134, Pt.H, No.1, Feb 1992,pp.60–64.

[17] G. Qasim and S. Zhong, "Radiation Characteristics of Microstrip Patch Antennas with Dielectric Covers", Antennas and Propagation Society International Symposium, 1992. AP-S. 1992 Digest IEEE, Vol.4, 18-25 July 1992, pp.2208 – 2211.

[18] Xiao-Hai Shen, G.A.E. Vandenbosch, and A. Van de Capelle, "Study of Gain Enhancement Method for Microstrip Antennas using Moment Method", Antennas and Propagation, IEEE Transactions on , Vol. 43, No. 3, March 1995, pp.227 – 231.

[19] G.A.E. Vandenbosch and A. Van de Capelle, "Mixed-Potential Integral Expression Formulation of the Electric Field in a Stratified Dielectric Medium-Application to the case of a Probe Current Source", Antennas and Propagation, IEEE Transactions on , Vol. 40, No. 7, July 1992, pp.806 – 817.

[20] W.L. Stutzman and G.A. Thiele, "Antenna Theory and Design", 2nd edition, New York: Wiley, 1998.

[21] C.A. Balanis, "Antenna Theory: analysis and design", 2nd edition, New York: Wiley, 1997.

[22] L. Shafai, D.J. Roscoe, M. Barakat, "Simulation and Experimental Study of Microstrip fed Cavity Antennas", ANTEM'96 Proceedings, 1996, pp.549-554.

[23] Ansoft Corporation, USA, Ansoft Designer 1.0., 2003.